

Development of a twin screw extruder with an integrated cooling roller system

J.S.Oosthuizen

12574139

Dissertation submitted in partial fulfillment of the requirements for the degree Master of Engineering at the Potchefstroom campus of the North-West University

Supervisor: Prof. LJ Grobler

Month and year: November 2011

ABSTRACT

The Center for Advanced Manufacturing at the Potchefstroom campus of the North West University aims to develop a twin screw extruder that is able to process powder coating resin. The facility has thus far produced various components and sub systems for local and international manufacturers of extrusion products.

The research presented in this thesis aims to both develop a twin screw extruder with an integrated cooling roller system and to investigate the performance of a twin screw extruder.

The development of a twin screw extruder consists of the selection of the drive section of the extruder, the complete design of a twin screw extruder gearbox, the investigation and design of a suitable barrel for the manufacturing of powder coatings as well as the development of a unique cooling roller unit for the forming of the processed product when exiting the extruder.

The extruder was manufactured from the designed components and systems. It was found on further testing that it was capable of producing a powder coating resin of good quality.

In order to evaluate the performance of an extruder, the transfer of energy through the extruder needs to be understood. Furthermore it is necessary to understand the theory behind each type of energy being consumed by the extruder, as well as the factors influencing the usage of that energy.

The theories investigated were verified in practice by measuring the energy consumption of a twin screw extruder operated under various conditions. These tests provided a correlation between the consumption of mechanical and electrical energy. The results gave an indication of the effectiveness of the screw configuration of the processing section of the extruder, making it possible to determine how the configuration should be amended in order to improve the performance of the extruder.

The two aims of the thesis were satisfactorily completed. The developed twin screw extruder is able to manufacture powder coatings of good quality and the performance evaluation of a twin screw extruder was also successfully completed. It enables the manufacturer to measure and evaluate the energy consumption of the process in order to improve the performance of the extruder.

TABLE OF CONTENTS

1	<i>Introduction</i>	<i>1</i>
1.1	Background.....	2
1.2	Problem statement	3
1.3	Aspects to be addressed	4
1.3.1	Twin screw extruder development.....	4
1.3.2	Cooling roller unit development	4
1.3.3	Performance evaluation of a twin screw extruder.....	4
1.4	Thesis outline	5
2	<i>Needs and Barriers for the development of a twin screw extruder with an integrated cooling roller system.....</i>	<i>6</i>
2.1	Introduction.....	7
2.2	What is powder coating?	7
2.3	How is powder coating powder produced?	7
2.4	What is extrusion?	9
2.5	Choice between viable extruder types	10
2.6	Needs and Barriers for developing a twin screw extruder	12
2.6.1	Drive unit.....	13
2.6.2	Extrusion processing	25
2.7	Post extrusion processes.....	38
2.8	Cooling of the extruded powder coating powder	38
2.9	Traditional cooling units.....	38
2.10	Needs and barriers in developing a cooling roller unit.....	39
2.10.1	Cooling mechanisms	39
2.10.2	Forming mechanism.....	41
2.10.3	Transporting mechanism.....	41
2.11	Conclusion	42
3	<i>Functionality and Detail Design</i>	<i>44</i>
3.1	Introduction.....	45
3.2	Technical specification	45
3.3	Extruder Development	46

3.3.1	Drive Unit	46
3.3.2	Process section.....	65
3.3.3	Final design of twin screw extruder	73
3.3.4	Cooling unit design	74
3.4	Conclusion	83
4	<i>Manufacturing and Assembly.....</i>	85
4.1	Introduction.....	86
4.2	Manufacture and assembly	86
4.3	Conclusions	92
5	<i>Testing of the Performance of a Twin Screw Extruder.....</i>	93
5.1	Introduction.....	94
5.2	The energy balance of an extruder	94
5.3	Specific mechanical energy	97
5.4	Specific thermal energy	99
5.5	Measurement of energy consumption of an extrusion system.....	100
5.5.1	Measurement of energy consumed by the drive system.....	100
5.5.2	Measurement of the energy consumed by the process temperature control zones	100
5.6	Conclusion	102
6	<i>Testing and evaluation.....</i>	103
6.1	Introduction.....	104
6.2	Setup of test equipment.....	104
6.3	Test procedure.....	106
6.4	Test results	109
6.4.1	Introduction	109
6.4.2	Detail results	110
6.5	Interpretation of results.....	114
6.6	Conclusion	117
7	<i>Conclusions and recommendations</i>	119
7.1	Conclusions	120
7.2	Recommendations	121

LIST OF FIGURES

Figure 2-1: Continuous powder coating manufacturing process (KG, TIGER Coatings GmbH & Co., 2010).....	9
Figure 2-2: Twin screw extruder with post process product cooling. Courtesy of (CFAM Technologies (Pty) Ltd, 2011)	12
Figure 2-3: Drive unit of a twin screw extruder (CFAM Technologies (Pty) Ltd, 2011).	13
Figure 2-4: Torsion shaft gearbox design (KOHLGRUBER, Klemens, 2007).	16
Figure 2-5: Example of a cluster gearbox (CFAM Technologies (Pty) Ltd, 2011).	17
Figure 2-6: Pressure angle α (Courtesy of MITCalc, mechanical design software).	20
Figure 2-7: Tooth forces of loaded gearing (Courtesy of MITCalc, mechanical design software).	23
Figure 2-8: Twin screw extruder processing section (CFAM Technologies (Pty) Ltd, 2011).	25
Figure 2-9: Opened clam shell barrel (PERKINS, Baker, 2006).	26
Figure 2-10: Solid twin screw extruder barrel (CFAM Technologies (Pty) Ltd, 2011). ...	26
Figure 2-11: Geometry of fully wiped twin flight twin screw extruder	30
Figure 2-12: Movement of a fully wiped twin flight profile.	31
Figure 2-13: 1DL screw elements, one with a 2D pitch and one with a 1D pitch	32
Figure 2-14: Geometric variables of a double-flighted screw profile. Green: fully wiped contour, Red: actual contour, Blue: barrel wall. (KOHLGRUBER, Klemens, 2007).	33

Figure 2-15: Feed screw and kneading elements (CFAM Technologies (Pty) Ltd, 2011).	35
Figure 2-16: Polymer strand dies (CFAM Technologies (Pty) Ltd, 2011).	36
Figure 2-17: Food processing die (VAN NIEKERK, Werner, 2008).	37
Figure 2-18: Barrel knife plate (CFAM Technologies (Pty) Ltd, 2011).	37
Figure 2-19: Post extrusion processes (CFAM Technologies (Pty) Ltd, 2011).	38
Figure 2-20: Chill rolls and chill roll conveyor unit (Micro Powder Tech, 2005), (Spectra Consultech).	39
Figure 2-21: Cooling mechanism of a typical chill roller.	40
Figure 2-22: Double passage rotary union (Deublin, 2010), (Talco Inc.).	40
Figure 2-23: Forming of molten extrudate into a crushable ribbon.	41
Figure 3-1: Screw dimensions and center distance	49
Figure 3-2: Splitter gearbox. Courtesy of (CFAM Technologies (Pty) Ltd, 2011).	57
Figure 3-3: Forces developed on the gearbox shaft.	57
Figure 3-4: Shear Force Diagram	58
Figure 3-5: Bending Moment Diagram.....	59
Figure 3-6: Deflection of the shaft.....	59
Figure 3-7: Bending angle of the shaft.....	60
Figure 3-8: Location of maximum bending stress in shaft	61
Figure 3-9: Bending Stress of the shaft	61
Figure 3-10: Effective diameter of the shaft at the keyway	62
Figure 3-11: Torsional moment and stress in torsion of the shaft	62
Figure 3-12: Basic geometry of the clam shell barrel (CFAM Technologies (Pty) Ltd, 2011).	65

Figure 3-13: Processing zones on the screw configuration.	66
Figure 3-14: Bottom and top barrel temperature control zones (CFAM Technologies (Pty) Ltd, 2011).....	67
Figure 3-15: Barrel permanent cooling ports (CFAM Technologies (Pty) Ltd, 2011).	68
Figure 3-16: Clam shell barrel assembly (CFAM Technologies (Pty) Ltd, 2011).	68
Figure 3-17: Interfacing components of the barrel with the rest of the extruder (CFAM Technologies (Pty) Ltd, 2011).	69
Figure 3-18: Liner bore dimensions (CFAM Technologies (Pty) Ltd, 2011).....	71
Figure 3-19: Liner inserts geometry (CFAM Technologies (Pty) Ltd, 2011).....	71
Figure 3-20: Knife plate cooling (CFAM Technologies (Pty) Ltd, 2011).....	72
Figure 3-21: Final design of knife plate (CFAM Technologies (Pty) Ltd, 2011).....	72
Figure 3-22: Exploded view of 28mm twin screw extruder (CFAM Technologies (Pty) Ltd, 2011).....	73
Figure 3-23: Twin screw extruder 28mm (CFAM Technologies (Pty) Ltd, 2011).	73
Figure 3-24: Traditional product cooling method.	74
Figure 3-25: Wrapping belt concept.....	75
Figure 3-26: Extrudate film on chilled roller.	78
Figure 3-27: Temperature against time plot for the cooling of the extrudate.	78
Figure 3-28: Contact angle of product with the chilled roller	80
Figure 3-29: Belt wrapped around cooling roller (CFAM Technologies (Pty) Ltd, 2011).	81
Figure 3-30: Cooling roller system (CFAM Technologies (Pty) Ltd, 2011).....	82
Figure 4-1: Extruder frame (CFAM Technologies (Pty) Ltd, 2011).	86

Figure 4-2: Machining of splitter gearbox housing (CFAM Technologies (Pty) Ltd, 2011).	87
Figure 4-3: Splitter gearbox and Barrel backing plate (CFAM Technologies (Pty) Ltd, 2011).	88
Figure 4-4: Extruder barrel or processing section fitted to the frame (CFAM Technologies (Pty) Ltd, 2011).	88
Figure 4-5: Processing section and drive unit of the extruder (CFAM Technologies (Pty) Ltd, 2011).	89
Figure 4-6: Cooling roller unit components (CFAM Technologies (Pty) Ltd, 2011).	90
Figure 4-7: Chilled roller unit with installed conveyor belt (CFAM Technologies (Pty) Ltd, 2011).	91
Figure 4-8: Twin screw extruder with integrated cooling unit (CFAM Technologies (Pty) Ltd, 2011).	92
Figure 5-1: System boundary for energy balance Courtesy of (COPERION, 2010).	94
Figure 6-1: Instrumentation for measuring of energy consumption of extruder	104
Figure 6-2: Test facility and test equipment.	105
Figure 6-3: Current transformers and data loggers.	106
Figure 6-4: Mechanical configuration (screw configuration) 1, 2 and 3.	107
Figure 6-5: Temperature profile over barrel.	108
Figure 6-6: Test procedure	108
Figure 6-7: Extruded product. Overcooked left, undercooked right.	109
Figure 6-8: Extruded product from mechanical configuration 1.	110
Figure 6-9: Extruded product from mechanical configuration 2.	110
Figure 6-10: Comparison of configurations 1 and 2 at 400rpm.	111

Figure 6-11: Comparison of configurations 1 and 2 at 500rpm.....	111
Figure 6-12: Comparison of configurations 1 and 2 at 600rpm.....	112
Figure 6-13: Comparison of STE of configurations 1 and 2.....	112
Figure 6-14: Comparison of SME of configurations 1 and 2	113
Figure 6-15: Comparison of the total energy usage (TEU) of configurations 1 and 2. .	113

LIST OF TABLES

Table 2-1 Comparison of single and twin screw extruders (RAUWENDAAL, Chris, 2001).	11
Table 3-1 Standard 28mm Laboratory Twin Extruder specifications	46
Table 3-2 Fixed design parameters of the gearbox	50
Table 3-3 Chosen design parameters of gearbox.....	50
Table 3-4: Gear tooth parameters	52
Table 3-5: Summary of the deflections, angular bending and safety factors of the input and two output shafts of the gearbox.	64
Table 3-6: Cooling roller design specifications	76
Table 3-7: Thermo Physical properties of extrudate	76
Table 6-1: Barrel temperature set values	107

ACKNOWLEDGEMENTS

I would first like to thank my heavenly Father for the power He has bestowed on me to complete this thesis.

I would like to acknowledge the following people for their contributions during the course of this project:

- Peet and Janette Oosthuizen for their love and support.
- Jan and Louise Oosthuizen for their prayers and support.
- Prof. LJ Grobler and Danie Vorster for their guidance, time and effort.
- Dr. Barend Botha for his guidance and motivation.
- Bartus Bondesio and Andre Schutte for their motivation and valuable help with the manufacturing.
- All my colleagues at the Centre for Advanced Manufacturing for their help and support.
- Anton Dednam, Andries Buys and René Coetzee for their help and the rest of my friends and family for their support.
- Dr. Danie Burger for his guidance and help with this dissertation.

CHAPTER 1

INTRODUCTION

This chapter starts with a brief introduction on the research topic that leads to the problem statement being formulated. This is followed by a discussion of the issues that need to be addressed. A chapter outline is also supplied to provide the reader with an overview of the dissertation.

1.1 Background

All multiple screw extruders originate from the single screw extruder. The first single screw extruder was invented approximately 2250 years ago by Archimedes. It was used to transfer water to different elevations, and is still used for that purpose today in countries such as Egypt, Holland and in many water purification plants.

The single screw used as an extrusion apparatus was developed in the second half of the 19th century for the industrial and heavy engineering industry. It was mainly used in the production of ceramic compounds, natural rubber, oily fruits and oil seeds.

The extruder is indisputably the most important piece of machinery in the polymer processing industry, making it one of the most innovative processes of the last few decades. Extrusion technology was later transferred to the food industry, and ultimately to the processing of wood pulp and cellulose. Extruders are used to pump, mix, carry out chemical reactions, homogenize, hydrate, dehydrate, melt, cook, shear, expand and texturize¹ different products.

Screw extrusion machines often contain multiple (normally two) screws rather than a single screw, which may rotate in the same or opposite direction. Closely intermeshing twin screw extruders occupy a dominant position among extruders and are used in a wide variety of applications. They are used extensively in the production, compounding, and processing of plastics, and the processing of rubber.

The technology transfer from the plastics industry to the food industry created a true processing breakthrough and initiated the development of many new products. Food extrusion products include pasta products, sausages, ice cream, confectionaries, expanded snacks and cereals, baby foods, dry and semi-moist pet food, fish feed and more (Potente, J.L., 2003; Kohlgruber, K., 2007; Corre, J.B. & Le, A., 2008).

¹ Texturize: To give a desired texture by a special process.

1.2 Problem statement

Extruders are used for the manufacturing of a large variety of food and polymer products in South Africa. However, extruders are also extensively used in the processing of powder coating products. Furthermore, the local coating powder producers use imported extruders for processing. The main problem local manufacturers have with imported machines is that they are quite expensive, as well as expensive to maintain. An inherent property of extruders is that the components are subjected to extreme conditions and undergo severe wear and tear. Consequently, in the event of a component failure, long lead times are inevitable, because these components must be sourced from international companies, causing extensive production down time.

Therefore, the need exists for a locally developed cost-effective twin screw extruder that can be used by the local powder coating industry.

Extruders are big energy consumers, unnecessary high energy consumption is caused by the use of incorrect equipment, unsuitable screw configurations and poor operating parameters and conditions, e.g. the incorrect temperature profiles for a certain product.

The basic principal of extrusion is that the product is processed by the transfer of mechanical energy to thermal energy. Incorrect mechanical configurations and operating parameters cause insufficient transfer of energy to the product, leading to a large energy input from external sources such as electrical heating elements, which increases the total energy consumption of the extruder. Therefore, the need exists for a process by which the energy efficiency of an extruder can be evaluated.

1.3 Aspects to be addressed

The aspects requiring attention in order to address the problem statement formulated in Section 1.2, are discussed in the following section.

1.3.1 Twin screw extruder development

The specific aspects concerning the development of a twin screw extruder are as follows:

Extruder drive section

The first aspect to be addressed is the drive section of an extruder. As a starting point, the motor selection for a small scale extruder is investigated. Secondly, the gearbox of an extruder is investigated, taking into account different types and design considerations, from which a gearbox was designed and built.

Extruder processing section

For the processing section the various aspects regarding the different barrel and liner design for different applications are addressed.

1.3.2 Cooling roller unit development

The development of the cooling unit addresses the concepts and evaluation of traditional cooling units, in an attempt to develop an improved cooling unit.

1.3.3 Performance evaluation of a twin screw extruder

In this section of the project the energy consumption of an extruder is closely investigated. The aspects addressed include the understanding of the energy transfer through the extruder processing section, and the measuring and evaluation of energy consumption.

1.4 Thesis outline

The thesis consists of two parts. Part 1 is the development of a twin screw extruder and cooling roller unit. Part 2 consists of the evaluation of the performance of a twin screw extruder.

Part 1

Chapter 2 consists of the relevant literature pertaining to the design of a twin screw extruder and relevant issues. This chapter concludes with a critical overview of the literature used in the design of the extruder and cooling system.

Chapter 3 presents the detail design of the extruder and cooling roller system.

Chapter 4 presents the manufacturing of the extruder, as illustrated by a series of photos. A discussion accompanying each photo aids the reader to visualize the assembly of the machine from the design stage to the finished product.

Part 2

Chapter 5 contains the theory regarding the energy consumption of an extruder, and investigates the energy balance of an extruder. Specific mechanical energy and specific electrical energy are also evaluated. The chapter concludes with a method to measure an extruder's energy consumption.

Chapter 6 presents the integration of measuring equipment into an extruder. It describes the procedure followed for measuring the energy consumption. The chapter includes the interpretation of results and concludes with the test results obtained from the measurements.

Chapter 7 concludes the thesis by stating how each of the issues mentioned in Section 1.3 is answered.

CHAPTER 2

NEEDS AND BARRIERS FOR THE DEVELOPMENT OF A TWIN SCREW EXTRUDER WITH AN INTEGRATED COOLING ROLLER SYSTEM

Part 1

In Chapter 1 the background regarding extrusion was sketched, as well as the purpose and motivation for this dissertation. This chapter focuses on the requirements and the challenges involved in the development and manufacturing of a twin screw extruder with an integrated cooling roller system.

It is important to understand the manufacturing industry in which this extruder operates in order to understand the requirements for developing a twin screw extruder for that specific application.

It is furthermore important to understand the different systems comprising an extruder, and why certain concepts are used in the design of twin screw extruders.

2.1 Introduction

This chapter describes the requirements and challenges for the development of a twin screw extruder with an integrated cooling roller system.

As stated in the Problem Statement in Chapter 1, the final deliverable of this study is to be used in the powder coating industry. It is therefore necessary to understand the concept of powder coating and the process of manufacturing the raw products for these coatings.

Finally the requirements and challenges involved in the development of a twin screw extruder are investigated.

2.2 What is powder coating?

Powder coating is a surface treatment for metallic products with powder of mixed composition applied by various methods to a subsurface. It is used when a hard finish which is tougher than conventional paint, is required (<http://www.akzonobel.com>).

Examples of the instances where powder coatings are used:

- Architectural aluminum cladding found on window and door sections.
- Products such as fridges, stoves, washing machines, security doors, patio furniture, etc.
- Industrial goods such as shelves, brackets and covers.
- In the automotive industry for a wide variety of car parts.
- Alloy components providing excellent protection against elements and high quality surface finish.

2.3 How is powder coating powder produced?

Ingredients

Powder coating powder consist of a mixture of resins, curing agents, additives, post additives, pigments and extenders or fillers (<http://www.akzonobel.com>). Resin is always present in the mixture and is usually either thermoplastic or thermosetting polyesters or thermosetting epoxies. In order to bind the coating, curing agents such as primid² and dicyandiamide are added. A wide range of additives and post additives are used to provide properties such as a matt effect or a

²Primid: Substances or mixtures of substances added to a polymer composition to promote or control the curing reaction.

hardened finish of the coated surface. Post additives are added after the powder is cured, to prevent surface cracks. Powder coatings also add colour to a surface. There are basically two types of colouring pigments used in powder coatings, these are (<http://www.akzonobel.com>):

- Inorganic pigments that provide a pale or dull effect to the surface.
- Organic pigments providing bright finishes.

Extenders are added to reduce glossiness and supply the coating with extra durability (<http://www.akzonobel.com>).

Powder coatings can be divided into two main categories, namely thermoplastic and thermosetting coatings:

- The thermosetting coatings have a cross linker in the formulation. When the powder is cured it reacts with other chemicals in the powder polymer which increases the molecular weight and improves the performance properties.
- The thermoplastic coatings do not undergo any additional reactions in the backing process. The most common polymers used, are polyester, polyurethane, polyester-epoxy (hybrid), straight epoxy and acrylics (<http://www.p2pays.org/ref/10/09793.pdf>).

Manufacturing process

In the manufacturing process the above-mentioned ingredients are weighed into batches and premixed using different types of batch mixers and blenders.

Thereafter the mixture is fed into a compounding twin screw extruder where it is melt-mixed. During extrusion the resinous mixture is heated to above its melting point and made homogeneous by means of mechanical shear. The temperature/shear plays a key role in achieving optimal dispersion of the coating's components, and the activation of the resins and hardeners.

After extrusion the molten product is formed to a crushable ribbon and cooled with chilled rolls, before it is laid onto a conveyor belt for further cooling.

The ribbon is then pulverized and classified to the desired particle size for specified applications.

Figure 2-1 shows a graphical representation of the continuous powder coating powder manufacturing process.

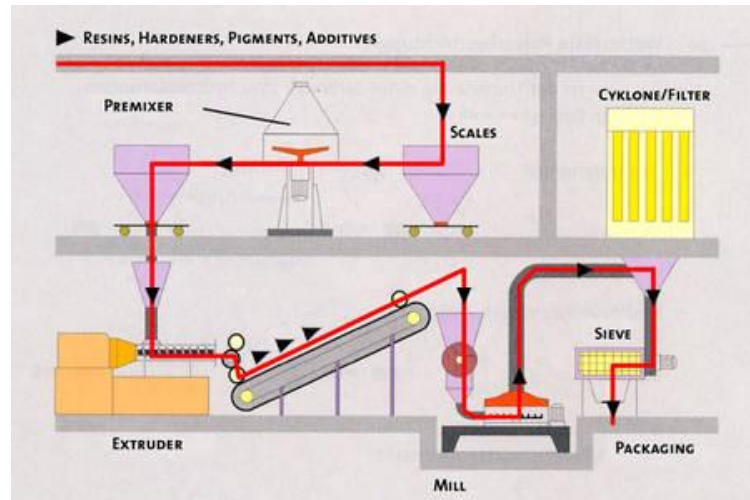


Figure 2-1: Continuous powder coating manufacturing process (KG, TIGER Coatings GmbH & Co., 2010).

2.4 What is extrusion?

Extrusion is the process in which material is drawn into a barrel by a rotating conveying shaft. Inside the barrel the material is plastified³ by mechanical shear. The material is then thoroughly mixed and homogenised⁴. Depending on the manner in which the product should exit the extruder, the material can either be pumped out of the barrel with low pressure, typically for powder coating applications, or by the addition of pressure, the product can be extruded into a desired shape, such as polymer compounding and composite profile extrusions.

Various products are produced by making use of extrusion, for example foods and feeds, polymers, pharmaceutical products, wood composite profile extrusion and the manufacturing powder coating powder.

Extrusion is used in the manufacturing of powder coating powder due to its excellent dispersive and distributive mixing capability.

³Plastified: To soften a material by heating or kneading.

⁴Homogenised: to become equal or homogeneous by mixing

2.5 Choice between viable extruder types

The characteristics of extruders may better be appreciated by considering the fundamental differences between single and twin screw extruders. A major difference is the type of transport that takes place in the extruder. Single screw extruders rely on drag in order to transport the material. Friction drag is necessary for solid conveying and viscose drag for the conveyance of molten material. Therefore, the conveying behaviour is to a large extent dependent on the friction properties of solid material and the viscous properties of molten material. There are many materials that cannot be extruded by single screw extruders due to unfavourable frictional properties.

The transport in an intermeshing twin screw extruder is to some extent a positive displacement type of transport. The degree of positive displacement is determined by how well the flight of one screw closes the channel of the other screw. The most effective positive displacement extruder is the fully wiped intermeshing counter rotating twin screw extruder. No extruder can be a pure positive displacement device, because the machine cannot be built in practice without any clearances. Thus leakage flows will reduce the degree of positive displacement in any twin screw extruder. Table 2-1 provides a comparison of single and twin screw extruders.

Table 2-1 Comparison of single and twin screw extruders (Rauwendaal, C., 2001).

Twin screw extruder (TSE)	Single screw extruder (SSE)
Used in profile, compounding and reactive extrusion	Used in simple profile extrusion and co-extrusion
Often used in modular design of screw and barrel-great flexibility	Modular design of screw and barrel is rarely used - less flexibility
Prediction of extruder production is difficult	Prediction of extruder performance is less difficult than for a twin screw extruder
Good feeding can handle pellets, powder and liquids	Fair feeding; slippery additives tend to give problems
Good melting; dispersed solids melting mechanism	Fair melting; contiguous solids melting mechanism.
Good distributive mixing with effective mixing elements	Good distributive mixing with effective mixing elements
Good dispersive mixing with effective mixing elements	Good dispersive mixing with effective mixing elements
Good degassing	Fair degassing
Intermeshing TSE can have completely self-wiping characteristics	Non self-wiping: barrel is wiped but screw root and flight flanks are not
Modular TSE is very expensive	SSE is relatively inexpensive
Co-rotating TSE can run at very high screw speed, up to 1400 rpm	SSE usually between 10-150 rpm; high screw speeds possible but not often used

Table 2-1 clearly shows the significant differences between single and twin screw extruders. As stated in Section 2.3, for the manufacturing of powder coatings, the raw material is fed into a compounding extruder where it is melted and mixed thoroughly by mechanical shear to obtain proper dispersion of the coating components. The comparison of the two types of extruders in Table 2-1, makes it clear that the twin screw extruder is the better extruder to use in this application. It is a compounding extruder that is modular and provides good melting, distributive mixing, and dispersive mixing. It is self-wiping which will play a major role with the additives and pigments added to the mixture, and it can operate at higher screw speeds, providing higher production capacity (Rauwendaal, C., 2001).

2.6 Needs and Barriers for developing a twin screw extruder

Now that it is clear which type of extruder needs to be developed, it is necessary to identify the different systems comprising a twin screw extruder. It is also necessary to determine what the needs are for each system as well as the pro's and con's for the different methods and processes for the manufacturing of each system, so that a thorough decision can be made for the manufacturing and integration of each component and system.

A twin screw extruder can be broken up into the following sections: the drive section, the processing section, the die section and, included in this study, a post processing system, namely the product cooling section. Figure 2-2 shows a graphical illustration of each section or system comprising the extruder.

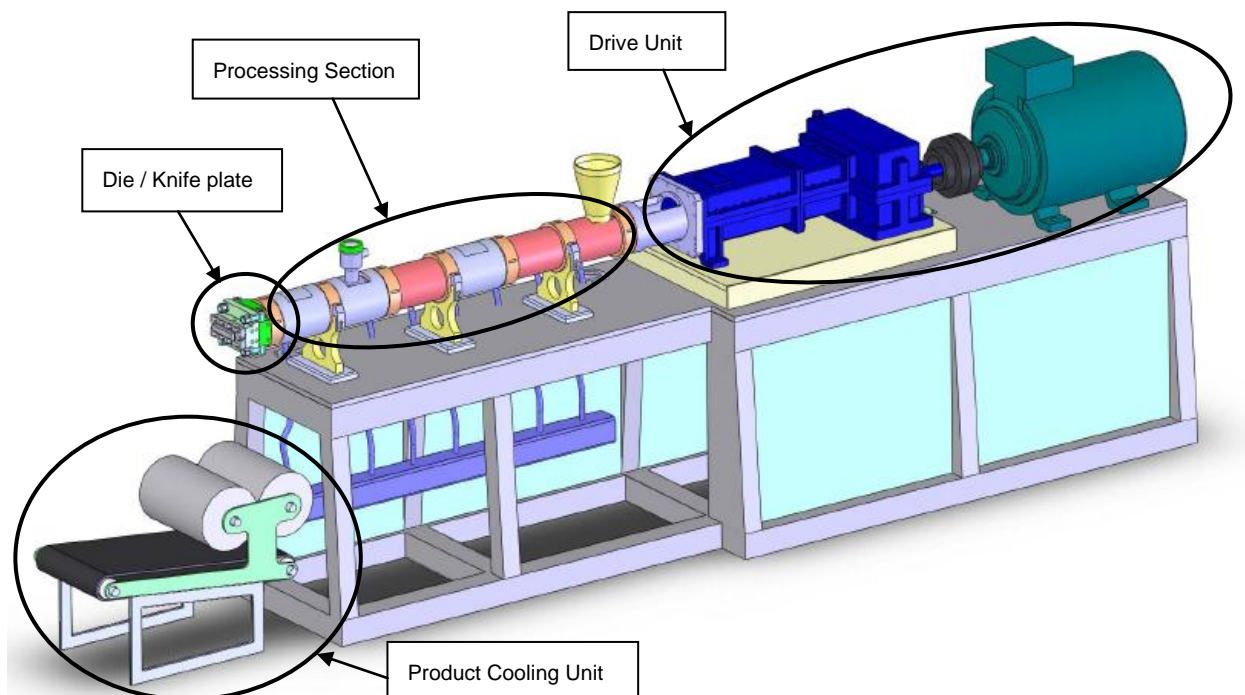


Figure 2-2: Twin screw extruder with post process product cooling. (CFAM Technologies (Pty) Ltd, 2011)

Each of these systems plays an important role in the function of the machine. At first, the drive system provides power to the processing section. The processing section is the heart of the extruder. The die section determines the manner in which the product exits the machine.

The cooling section cools and shapes the product so that post extrusion processes can handle the product.

Each of the mentioned systems is now investigated in order to understand its purpose within the whole and to provide the necessary information to choose the best possible method and concept for the design of each component.

2.6.1 Drive unit

The drive unit of a co-rotating twin-screw extruder is, second to the processing section, the most important component in the system. The drive unit consists of a motor, speed control, torque limiting mechanism and gearbox.

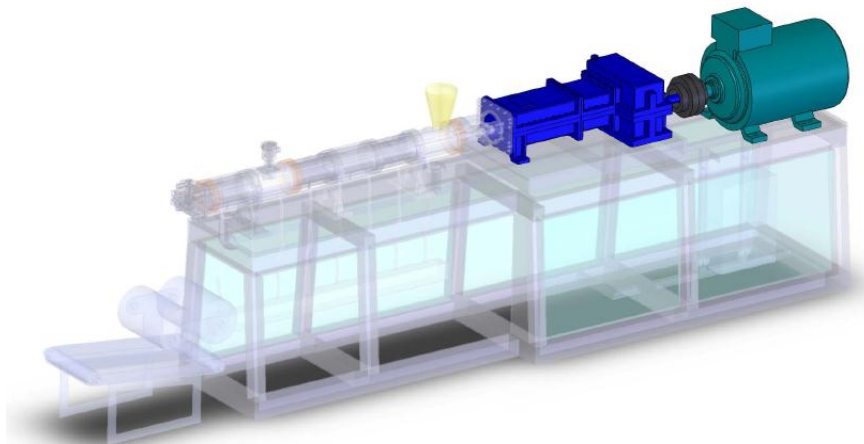


Figure 2-3: Drive unit of a twin screw extruder (CFAM Technologies (Pty) Ltd, 2011).

As discussed in Section 1.1, extruders are used for the processing of food products, polymers and pharmaceutical products. The basic materials are melted, mixed, homogenized, and discharged from the extruder in the form of pellets, films, sheets, or profiles depending on the required form. The energy required for the processing of products within an extruder is generated from mechanical shear by a modular screw. Thus the greatest amount of energy required to process the product is provided by the drive system.

2.6.1.1 Electric motor

The electric motor supplies torque to the gearbox which in its turn provide power to the processing section which will be discussed later. The torque required to process a given product depends on the throughput (production rate), product viscosity, screw speed, etc. For this reason, an extruder drive requires a motor torque characteristic that provides a high torque from a low speed range up to nominal speed.

The cooling of self-cooled motors is achieved by a fan blowing air over the length of the motor. The fan is powered by the shaft of the motor, causing the volume flow of air, to be a function of the rotational speed. During extrusion the motor often operates at low speeds, reducing the volume flow, which can result in overheating of the motor. Therefore, forced cooling on the motor is often required. This can either be achieved by installing a separate motor, powering the cooling fan, or cooling the motor by circulating water through a water jacket situated around the motor. In practice forced cooling by external air cooling is more often used, due to the lower cost and simplicity.

2.6.1.2 Speed control

The energy required for driving all high-capacity electric motors is obtained from the AC network. AC motors can be supplied directly from the AC network as long as it operates at nominal speeds. If variable speed is required, AC motors are equipped with a frequency converter. DC motors are also powered from the AC network. The DC motor gets its power from a power converter, which has the capability to vary the motor speed.

Adjustable frequency drives use an AC induction motor connected to a solid state power supply capable of providing an adjustable frequency to the motor. AC motors have certain advantages such as low price, ruggedness, simplicity, no commutators⁵ or brushes, etc. The solid state power supply on the other hand is a costly item. The power supply converts AC power to DC power. It then inverts the DC by making use of two sets of solid state devices into AC with a required frequency.

A power converter generates from the 3-phase main supply a pulsating DC voltage for a DC motor. The motor speed is determined by the amount of DC voltage generated. This can be altered via the thyristor control of the power converter. The smaller number of solid state devices tends to give the DC drive a better reliability than the AC drive system, but the brushes and commutator maintenance is the principal drawback of this system (Kohlgruber, K., 2007).

2.6.1.3 Extruder gearbox

The twin screw extruder gearbox has two main tasks, namely reducing motor speed to the operating speed of the extruder (reduction gearbox) and to distribute the torque to the two adjacent output shafts (splitter gearbox).

⁵Commutator: A cylindrical arrangement of insulated metal bars connected to the coils of a direct-current electric motor or generator, providing a unidirectional current from the generator or a reversal of current into the coils of the motor

Reduction gearbox

As mentioned above, the reduction gearbox reduces the high rotational speed of the drive to the low speed of the extruder screws. Typical reduction ratios of gearboxes range largely from 3: 1 to 5: 1 in order to adapt to the process requirements. Helical spur gears are typically used in the reduction gearbox. These gears have a low noise level and a high efficiency and long working life.

The heat generated in the gearbox is generally 2 to 4% of the transmitted power of the gearbox. The gears are usually lubricated by splash or force lubrication by an oil pump system. Cooling of the oil generally takes place by means of an integrated heat exchanger in the gearbox or, in case of heavy loaded gearboxes, by water-cooled systems (Potente, J.L., 2003).

Splitter gearbox

The splitter gearbox is essential to a twin screw extruder. The torque must be evenly distributed between two output shafts. The two shafts have a fixed center distance (extruder screw design parameter), which causes a couple of challenges to address during the gearbox design.

High axial force in the extruder screws is caused by the melting pressure in the die, and must be absorbed by thrust bearings on the output shafts of the gearbox. The challenge is to accommodate a strong enough thrust bearing next to a closely adjacent shaft. Extruder gearboxes are generally designed with one large spherical roller thrust bearing on one output shaft and a tandem axial thrust bearing on the other. Some gearboxes are built with two sets of tandem axial thrust bearings. The drawback for the use of these bearings is high cost and availability.

Torsion shaft gearbox concept

In order to get the two output shafts adjacent to one another, one shaft is driven directly by the reduction gearbox and the other by a few sets of gears (torsion shafts), giving the second shaft the same speed/torque as the first one. Because of the small clearances between the two extruder screws and the importance of timing for closely intermeshing screw profiles, care must be taken in the design of the gears, where the build-up of back lash on the torsion shafts is at a minimum, in order to keep the screws from rubbing against one another. For the same reason the torsion shafts must be designed in such a manner that the angular deflection of the shafts, caused by the transfer of torque, does not cause a timing difference on the output shafts. Figure 2-4 shows a typical torsion shaft gearbox arrangement.

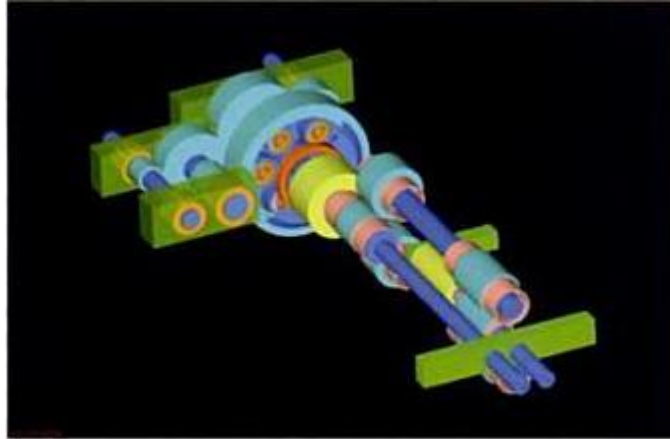


Figure 2-4: Torsion shaft gearbox design (KOHLGRUBER, Klemens, 2007).

Generally, in these types of gearboxes the reduction gearbox and splitter gearbox is one unit and its housing is manufactured from a casting. This is advantageous when the amount of gearboxes being manufactured, are enough to justify the building of casting moulds. For small quantities, the housings can be manufactured from a mild steel fabricated construction. This requires a lot of machining and becomes very expensive for larger housings.

Cluster gear gearbox concept

There is another twin screw gearbox design concept that eliminates the torsion shafts and thus also the teeth clearance (backlash) build-up. In this design both output shafts are driven by one gear (cluster gears). On the negative side, due to the size limitation of the driven gears on the output shafts, the driving gear must be larger in diameter. This causes the gear set to increase the output speed, which in return means that the reduction gearbox must have a larger reduction in order to get the required final ratio.

With these types of gearboxes, the reduction gearbox is either integrated in the splitter gearbox, or intermitted between the motor and splitter gearbox, or a geared motor is used for the reduction and then directly connected to the splitter gearbox. This is advantageous, because a geared motor is less expensive than a separate motor and reduction gearbox. Furthermore, spare parts are less expensive and are readily available. An example of a cluster type gearbox is presented in Figure 2-5.

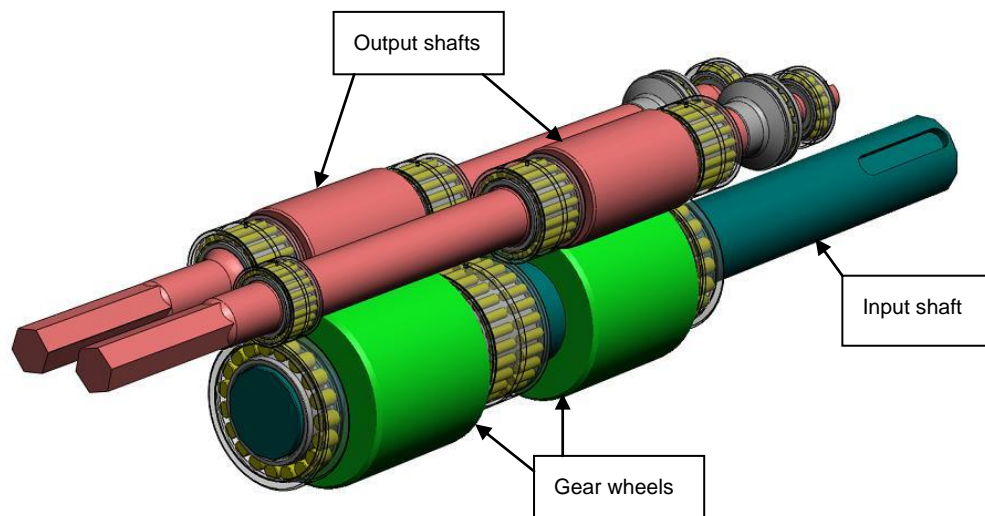


Figure 2-5: Example of a cluster gearbox (CFAM Technologies (Pty) Ltd, 2011).

The input shaft (blue) drives two gear wheels (green gears) with the same number of teeth. Each of these gears mates with its corresponding mating gear on the output shafts (two pink shafts). In heavily loaded gearboxes, such as the one shown in Figure 2-5, the helix angle of the two gear sets are opposite to one another. This causes the axial forces generated by the gears to eliminate each other, in order to improve bearing life.

In smaller lightly loaded gearboxes, the driving gear can be a single gear, driving both output shafts. In these gearboxes spur gears can be used due to smaller tooth forces. This enables the designer to use one driving gear, simplifying the design.

The center distance required by the extruder screw profile governs the shaft diameter and size of the gear on the adjacent shaft, due to the fact that as the one increases, the other decreases. This results in the driven gear having a size limit. In order for the driving gear to mesh with the driven gear, it should have a larger number of teeth. This means that this gearbox design increases the output shaft speed. The reduction gearbox used for driving must thus compensate for the increase in speed.

Another challenge especially with heavily loaded gearboxes is to find bearings that fit within the center distances of the extruder, as well as the gear sets, and are capable of withstanding the forces developed by the gears.

If these engineering challenges can be overcome, the gearbox design is easy and it is then cost-effective to manufacture this gearbox.

2.6.1.4 Extruder gearbox design

In designing a gearbox there are basic theories that can be used. Considering the function and key components of a gearbox, it is possible to determine which theories are applicable.

The function of a gearbox is to transform the power from one rotating shaft to another, while either increasing or reducing the speed and torque of the rotating shafts by means of intermeshing gears. Rotating shafts are supported by bearings or bushes that act as the connection between the rotating shaft and the fixed gearbox housing. Thus all the resultant forces developed by the gears are absorbed by the bearings.

In order for a shaft to transfer power, it must be able to withstand the torque produced by the power. Torque and rotational speed go hand in hand with power, as expressed in Equation 2-1.

$$P = T \times \omega \quad [2-1]$$

Power (P) is always constant. If torque (T) is increased the speed (omega ω) will decrease. This expresses the basic functioning of a gearbox. For example in a reduction gearbox, the shaft will be subjected to torque but also undergoes bending caused by radial and tangential forces produced by the gearing. The nature of the mentioned forces will be discussed later. Torque will induce shear stress and bending loads will induce normal stress in the shaft. Shear stress is calculated with:

$$\tau = \frac{T \times \rho}{J} \quad [2-2]$$

Where:

- τ is the shear stress [Pa]
- T the torque [T]
- ρ is the die distance from the center line of the shaft to the point where maximum stress occurs [m]
- J is the polar moment of inertia of the cross section of the shaft [m^3]

Normal stress can be calculated for σ_{max} by the following equation:

$$\sigma_{max} = \frac{M \times c}{I} \quad [2-3]$$

Where:

- M is the maximum bending moment in the shaft [Nm]
- c is the distance from the shaft center line to a point farthest away from the center line [m]
- I is the second moment of inertia [m^4]

In gear design the following parameters play a role. Equation 2-4 represents the variation in rotational speed from one gear to another and Equation 2-5 represents the gear ratio.

$$Z_1 \times N_1 = Z_2 \times N_2 \text{ and } N_2 \times T_1 = N_1 \times T_2 \quad [2-4]$$

$$i = \frac{Z_1}{Z_2} \text{ and } i = \frac{T_2}{T_1} \quad [2-5]$$

Where:

- Z_1 is the number of teeth of the driving gear
- N_1 is the rotational speed of the driving gear [rpm]
- Z_2 is the number of teeth of the driven gear
- N_2 is the rotational speed of the driven gear [rpm]
- T_1 is the torque in the shaft of the driving gear [Nm]
- T_2 is the torque in the shaft of the driven gear [Nm]
- i the gear ratio

The following principles are important to understand the designing of gears.

The module m is the ratio of the pitch diameter to the number of teeth. The module is the index of tooth size and can be calculated as follows:

$$m = \frac{d}{N} \quad [2-6]$$

Where:

- m is the module
- d the pitch diameter [mm]
- N the number of teeth

The pressure angle (α) is the angle at which two meshing gear teeth come into contact with one another. Figure 2-6 presents a graphical illustration.

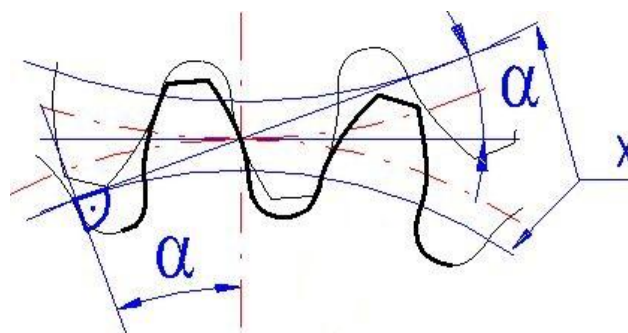


Figure 2-6: Pressure angle α (Courtesy of MITCalc, mechanical design software).

Tooth⁶ing with a helix angle of 0° (straight tooth⁶ing) is used with slow speed and where increased noise doesn't cause any problems. The advantage of teeth with a zero slope is that the force acting on the teeth does not produce any axial forces, which means that less expensive bearing arrangements can be used for supporting the shaft. Tooth⁶ing with a slope larger than 0° (helical gears) is used in high speed applications. It has higher loading capacity which means the same amount of power can be transferred with less number of teeth, decreasing gearbox size and weight. Helical gears also produce less noise and vibrations. The downside, however, is that axial forces are produced which reduce bearing life.

⁶Tooth⁶ing: Gear teeth.

Another important parameter for designing gearboxes is the center line distance. This is the distance between two intermeshing gears. The center distances for gears need to be machined very accurately, because it has a great effect on the manner in which the teeth of the two gears come in contact with one-another. This is called meshing. Inaccurate center distances can have a negative effect on tooth surface life, tooth load distribution and, backlash. The value is dependent on the module, number of teeth, pressure angle, and helix angle.

Gear strength

Two fundamental principles are used in the strength calculation of gears. One for bending and the other one for surface durability of gear teeth. The AGMA (American Gear Manufacturing Association, 1988) methodology for stress calculation calls it stress numbers.

For bending stress (σ_b) of the gear tooth the equation is:

$$\sigma_b = W^t K_o K_v K_s \frac{1}{b m_t} \frac{K_H K_B}{Y_J} \quad [2-7]$$

Where for SI units:

- W^t is the tangential transmitted load [N]
- K_o is the overload factor
- K_v is the dynamic factor
- K_s is the size factor
- b is the face width of the gear teeth [mm]
- m_t is the normal module of the teeth
- K_H is the load distribution factor
- K_B the rim-thickness factor
- Y_J is the geometry factor for bending strength (which includes root fillet stress-concentration factor K_f)

The AGMA concerning items includes aspects such as:

- Transmitted load magnitude
- Overload
- Dynamic augmentation of transmitted load
- Size
- Geometry, pitch and face width
- Distribution of load across the teeth
- Rim support of the tooth
- Lewis form factor and root fillet stress concentration

The calculation for the allowable bending stress is expressed in Equation 2-8.

$$\sigma_{all} = \frac{\sigma_{FP} Y_N}{Y_\theta Y_Z} \quad [2-8]$$

Where:

- σ_{FP} is the allowable bending stress number for the material used [MPa]
- Y_N is the stress cycle factor for bending strength
- S_F is the safety factor for bending strength

The equation for calculating contact stress (σ_c) is

$$\sigma_c = Z_E \sqrt{W^t K_o K_v K_s \frac{K_H}{d_{w1} b} \frac{Z_R}{Z_I}} \quad [2-9]$$

Where W^t , K_o , K_v , K_s and b are the same terms as defined for Equation 2-7, the additional terms are:

- Z_E is an elastic coefficient [$\sqrt{N/mm^2}$]
- Z_R is the surface condition factor

- d_{w1} is the pitch diameter of the pinion [mm]
- Z_I is the geometry factor for pitting resistance

The relation of calculated contact stress number to the allowable contact stress number is:

$$\sigma_{all,c} \leq \frac{\sigma_{HP}}{S_H} \frac{Z_N}{Y_\theta} \frac{Z_W}{Y_Z} \quad [2-10]$$

Where:

- $\sigma_{all,c}$ is the allowable contact stress number for the material used [MPa]
- Z_N is the stress cycle for pitting resistance
- C_H is the hardness ratio factor for pitting resistance
- S_H is the safety factor for pitting
- K_T is the temperature factor
- K_R is the reliability factor

Gear forces

In order to transfer power from one gear to another, the gear teeth come in contact at the pitch circle diameter (PCD) with the angle α (pressure angle) to a line tangential to the PCD at the point of contact. This causes a normal force (F_n) to that surface. The normal force can be broken into 3 vectors, tangential force (F_t), radial force (F_r) and an axial force (F_a) (only for helical gearing where $\beta \neq 0$). Figure 2-7 presents a graphical illustration of the force vectors.

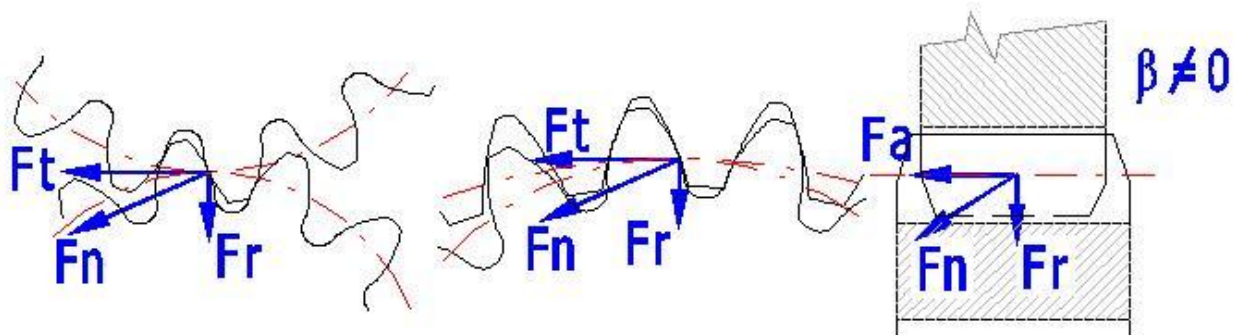


Figure 2-7: Tooth forces of loaded gearing (Courtesy of MITCalc, mechanical design software).

The forces can be calculated using Equations 2-11 to 2-13:

$$F_t = \frac{T}{PCD/2} \quad [2-11]$$

$$F_n = F_t / \cos(\theta) \quad [2-12]$$

$$F_r = F_n \times \sin(\theta) \quad [2-13]$$

Where:

- T is the torque transferred by the gear [Nm]
- PCD the pitch circle diameter of the gear [m]

Each of the mentioned forces is transferred to the gearbox housing through the shaft carrying the gear as well as the bearings supporting the shaft. Shaft design and bearing selection can be done based on these values.

2.6.2 Extrusion processing

The processing section forms the heart of the extruder. The raw product is fed into the processing section at the feed port of the barrel. The product is then conveyed with a set of screws through a chamber called the barrel. Through the length of the barrel work is done on the product which is discussed later. Certain process parameters, e.g. temperature, are carefully set at specified locations throughout the barrel for the correct processing of the product. The product exits the barrel through a die or knife plate depending on the product being manufactured.

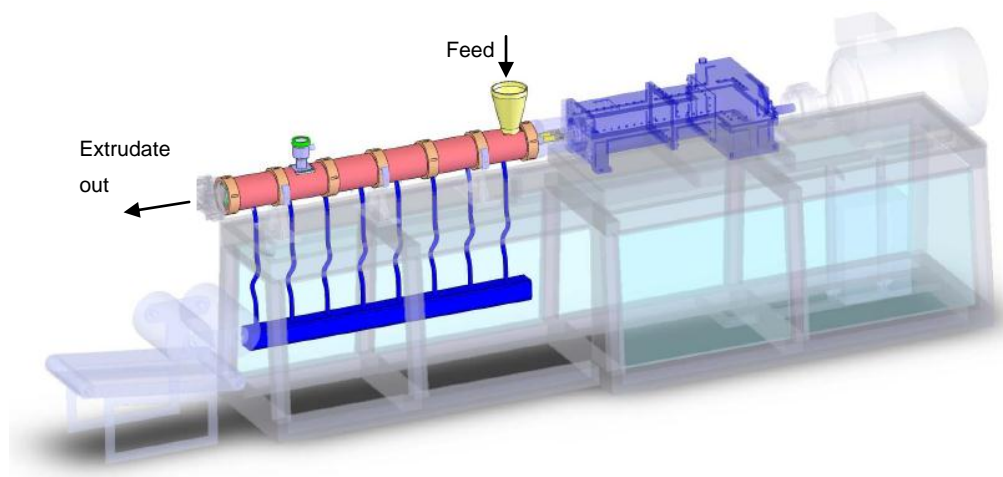


Figure 2-8: Twin screw extruder processing section (CFAM Technologies (Pty) Ltd, 2011).

2.6.2.1 Extruder barrel and process control

Function

The function of the barrel is to act as a mechanical structure connecting the processing section to the frame of the extruder. The barrel's main function is to host the liners that form the chamber wherein the screws operate. It also forms a cooling jacket around the liners and hosts the heating elements that in conjunction with the cooling jackets, carefully fine-tunes the processing temperatures.

Different barrel types

There are two types of barrels, namely clamshell barrel and solid barrels. The advantage of the clamshell barrel is that it gives easy access to the screws. The barrel can be loosened and

opened for inspection and cleaning. Figure 2-9 shows an opened clam shell barrel. The disadvantage of the clamshell barrel is that it is limited by the amount of pressure that can be applied in the process.



Figure 2-9: Opened clam shell barrel (PERKINS, Baker, 2006).

The solid barrel is mainly used in the production of polymers where large Length to Diameter (L/D) ratios are required. Here very high pressures are achieved. The advantage of a solid barrel is that it is easy to achieve a secure seal between the different barrel sections, resulting in a barrel that can withstand very high pressures. The disadvantage is that the only way to clean the screws is to remove them from the barrel. This has to be done by pulling the screws out of the barrel or by pulling the barrel over the screws, which is a difficult task. Figure 2-10 shows an example of a twin screw solid barrel segment.



Figure 2-10: Solid twin screw extruder barrel (CFAM Technologies (Pty) Ltd, 2011).

Temperature control zones

The temperature inside the barrel is controlled in order to achieve the desired processing conditions for the production of a specific product. The barrel is divided into a number of independent process temperature control zones, providing the flexibility to get a temperature profile throughout the process. Depending on the product manufactured the temperature profile can be increasing, decreasing, flat or in combinations.

Temperature control is achieved by the application or extraction of heat. Heat is applied through either electric heating, fluid heating or steam. Electric heating has significant advantages over liquid and steam heating. It can cover a much larger temperature range, it is easier to maintain, clean, is cost-effective and efficient. Electric heating has thus replaced liquid and steam heating in most applications.

Electric heaters can be divided into two types: resistance heaters and induction heaters. Resistance heaters are commonly used, because they are easy to replace, widely available and relatively inexpensive. The service life and efficiency, however, depend on the quality of surface contact of the entire heater and the barrel material. Improper contact can cause local overheating which can lead to premature failure.

Induction heating is done by an alternating current that passes through a coil surrounding the extruder barrel. The alternating current causes an alternating magnetic field inside the barrel with the same frequency. This in return induces an electromotive force in the barrel, causing eddy currents. The losses of the circulating current are responsible for the heating effect. The advantage of this type of heating is much reduced temperature gradients in the extruder barrel, because the heat is generated evenly through the depth of the barrel as opposed to resistance heating. Power consumption is low because of efficient heating and reduced heat losses. It is also possible to have a cooling system directly in the barrel surface allowing accurate temperature control. The disadvantage of inductive heating is the high cost involved (Kohlgruber, K., 2007).

In order to maintain the desired temperature profile over the barrel, heat also needs to be extracted. Extraction of heat is usually accomplished by the running of compressed air or chilled water through a number of ports in each zone or by blowing air over the barrel. Each method has a particular advantage, namely:

- Blowing air over the barrel is by far the least expensive method, no auxiliary equipment is required. It is however less effective and hot spots inside the barrel can easily be formed, degrading the quality of the extruded product.

- Usage of chilled water or compressed air through a cooling jacket can eliminate hot spots, but require expensive equipment, such as chiller plants. The advantage of compressed air over water is the achievement of a much smoother temperature profile due to the lower heat transfer capability of air. This is usually used in polymer compounding where large length to diameter ratio extruders are used (Kohlgruber, K., 2007).

2.6.2.2 The barrel cavity

Wear can be a significant problem in an extruder barrel, particularly when the polymer contains abrasive components. Many extruder barrels are made with a wear resistant inner surface to increase the service life. The most common types of hardening to achieve wear resistance (or degree of) are nitriding⁷, bi-metallic alloying and liner inserts.

Nitriding can be done by plasma, gas, ion or liquid nitriding techniques. Generally ion-nitriding gives the best results. The barrel must be prepared properly in order to achieve good results. Usually the barrel is hardened and tempered to obtain the desired core properties. By conducting the ion-nitriding process a total nitriding depth of about 0.4mm can be achieved.

Bimetallic barrels are made by centrifugal casting. The melting point of the bimetallic alloy is lower than the melting point of the barrel material. The process is started by charging the barrel with the bimetallic alloy. The barrel is then slowly rotated while heat is applied. When the required temperature is reached, the barrel is rotated at very high speeds, forcing the molten alloy to form a uniform layer with a strong bond to the barrel surface. The final step is to hone the barrel to achieve a smooth surface and accurate size. The depth of a bimetallic liner usually ranges between 1.5mm to 2mm .

Another method is by inserting a metallic liner into the barrel. The inside of the barrel is carefully machined and ground to achieve very accurate sizes. In order to attain a hard, wear resistant liner, the liner is manufactured from heat-treatable tool steel. The liner is machined to pre-grinding sizes with no bore. It is then through-hardened to about 54 HRC; thereafter it is ground to obtain a very accurate fit in the prepared barrel. Before it is inserted into the barrel, the extruder bore is cut into the liner by means of electric discharge machining. The advantage of this type of liner is that the liner insert can easily be replaced when it is worn. It also gives much design freedom to facilitate cooling ports in the barrel and extending the liner beyond the length

⁷Nitriding: is a process which introduces nitrogen in the surface of a material. It is used in metallurgy for surface-hardening treatment of the steel surface

of the barrel in order to provide better secured sealing between the barrel segments (Kohlgruber, K., 2007).

2.6.2.3 Closely intermeshing screws

The basic concept of extrusion is to process material by viscous dissipation, in other words, the transfer of mechanical energy to heat energy. This is done by a single screw, a pair of screws or two or more segmented screw shafts called multiple screw extruders. Thus screws form the heart of the extruder. Everything revolves around the screw. The rotation of the screw conveys the material, it provides the largest amount of heating energy to the product and causes homogenization, mixing and dispersion of the material (Rauwendaal, C., 2001).

Geometry and screw design of twin screw extruders

The geometry of closely intermeshing twin screw extruders is characterized by the fact that both the adjacent screw profiles have identical geometry, are symmetrical and rotate at the same speed.

A screw profile consists of 3 parts, namely the tip, flank and root. The tip consists of an arc whose diameter is the same as the external diameter of the extruder screw profile and whose center point is the center of the profile. The edge of the tip passes over to the adjacent flank area. For screws that wipe the inside of the barrel tightly, the flank area consists of an arc with radius equal to the center distance. The flank passes tangentially over to the root areas, which has the diameter of the screw core, whose circle center is the center of the profile. The tip cleans the root of the opposite screw and vice versa, and the corner of the profile between the tip and flank cleans the opposing flank (Kohlgruber, K., 2007).

Figure 2-11 shows the geometry of a fully wiped twin flight profile, where DE is the outer diameter of the screw or, in other words, the inner diameter of the extruder bore. A is the center line distance of the two adjacent screws. The flank area has the same radius as the center distance and the root diameter DI , and can be calculated with the following equation:

$$\frac{DE}{2} + \frac{DI}{2} = A \quad [2-14]$$

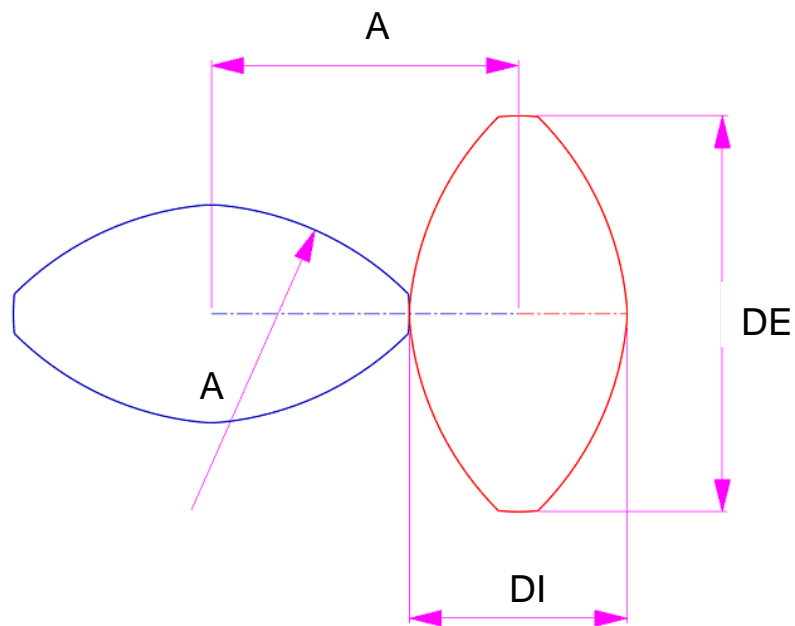


Figure 2-11: Geometry of fully wiped twin flight twin screw extruder

The basis of the closely intermeshing screw profile is the fully wiped profile. As presented in figure 2-11, the basis of the fully wiped profile is based on arcs. This can be explained by replacing the rotation of the two profiles by holding one profile in a fixed position and rotating the other at a distance equal to the center distance around the fixed profile. Figures 2-12 illustrate this motion.

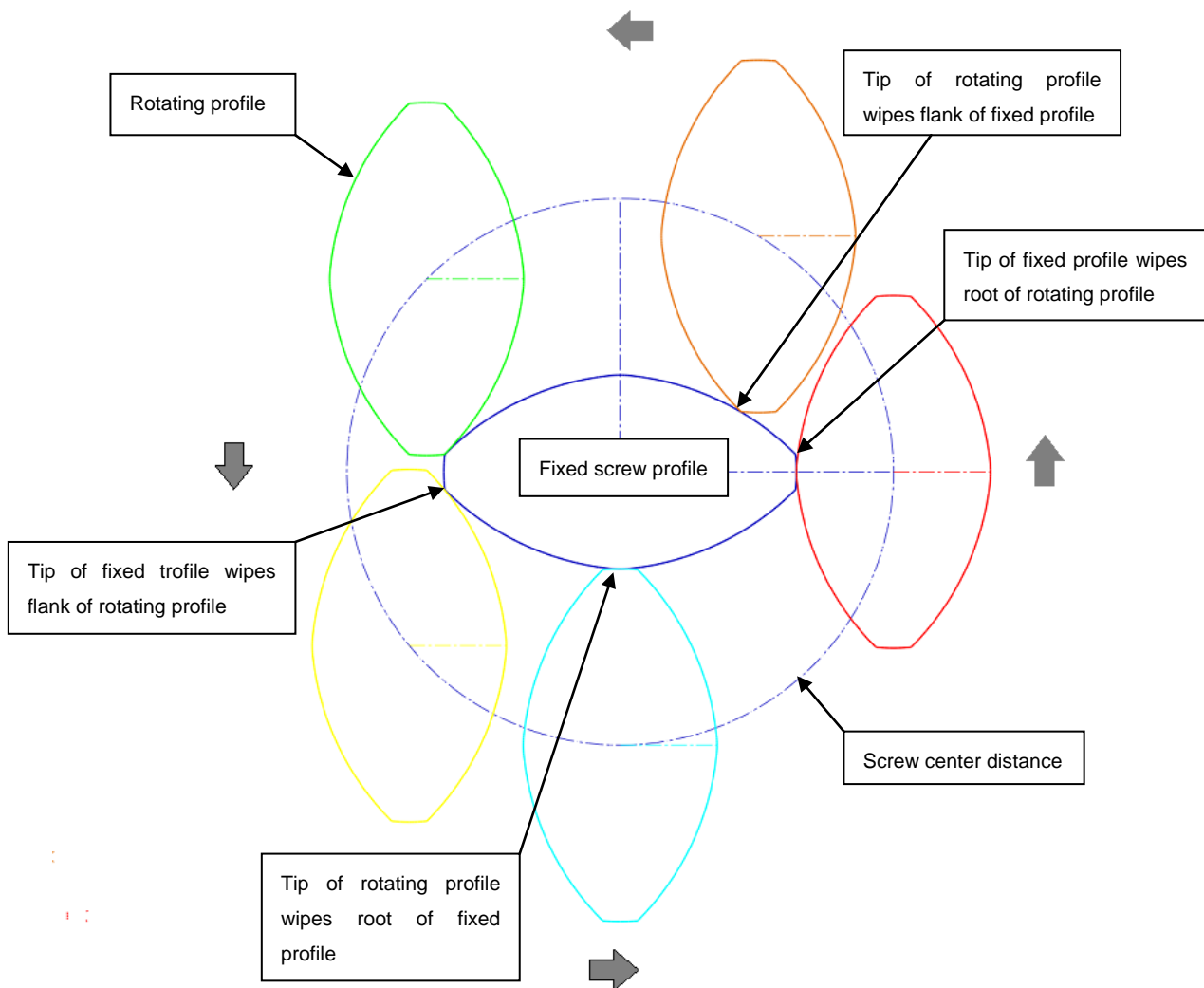


Figure 2-12: Movement of a fully wiped twin flight profile.

Figure 2-12 shows that the edge of the tip wipes the flank of the opposing screw profile and the tip wipes the screw core.

Conveying of the material is done by extending the screw into a third dimension through helical rotation. Each screw element has a constant pitch, and variations in pitches through the entire screw are achieved by using different types of elements. Figure 2-13 shows two screw elements, both have a length of $1DL$ ($1 \times$ screw nominal diameter), where one has a pitch of $2D$ and the second a pitch of $1D$.

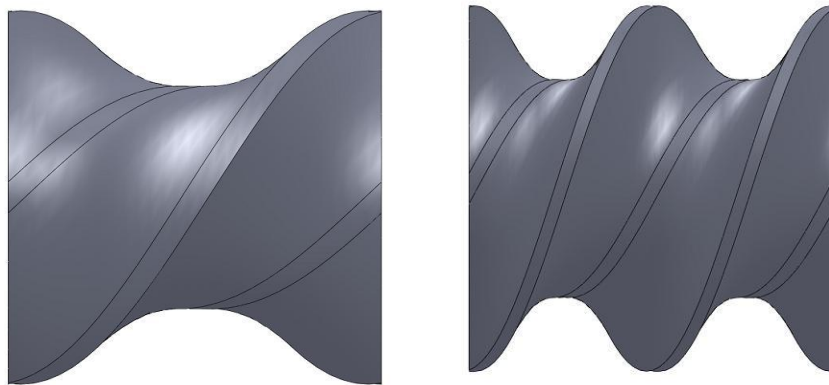


Figure 2-13: 1DL screw elements, one with a 2D pitch and one with a 1D pitch

In practice the screw profiles cannot be manufactured to the exact dimensions as previously described. There must be clearances between the opposing flanks, as well as between the screw tips and core diameter in order to:

- prevent metallic erosion,
- compensate for manufacturing tolerances and unevenness,
- compensate for angle discrepancies,
- compensate for uneven heat expansion, and
- avoid excessive product stress due to insignificantly wide gaps.

Screw clearance is achieved by adding two dimensions to the screw profile, s for clearance between the two screws, and δ for clearance between the screw tip and barrel wall. Figure 2-14 shows the fully wiped profile in green and the actual profile in red. The offset of the screw flank is $s/2$ and is kept constant throughout the whole flight. The bore diameter of the barrel is represented by D and the screw center distance is A .

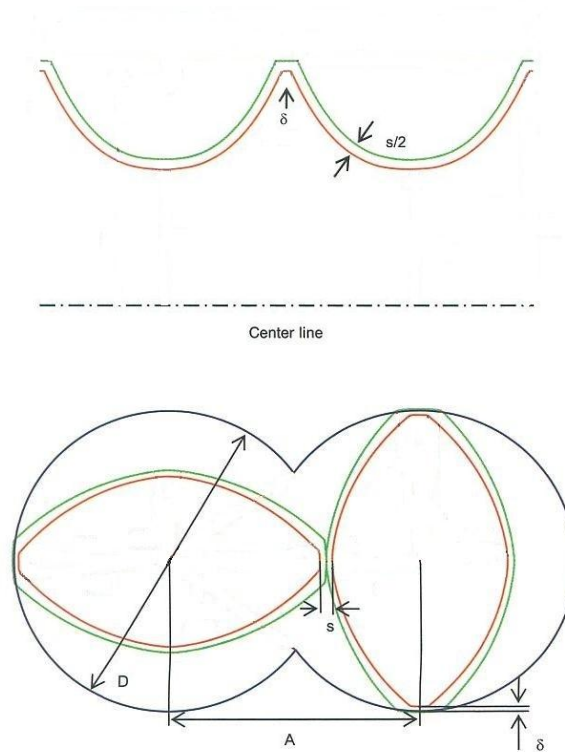


Figure 2-14: Geometric variables of a double-flighted screw profile. Green: fully wiped contour, Red: actual contour, Blue: barrel wall. (KOHLEGRUBER, Klemens, 2007).

A modular extruder screw comprises of a set of screw elements. The basic elements present on a screw are:

- feed screws,
- kneading elements, and
- compression elements.

Each element has a function, and in different combinations and sequences it enables the whole screw to perform its processing task.

Feed screws

A conveying or feed screw element (Figure 2-15) usually has a large pitch and length. Normally it has a length of 1.5 times the diameter of the screw; the pitches can vary but a pitch of 1.5 times the diameter is the norm. The characteristic of screws with a large pitch is that it has a fast conveying action and exerts low pressure to the product. These elements are generally used in the feeding section of the barrel where it transports the product into the barrel up to the first processing section. Depending on the product needs, a large pitch screw can be used later in the process where pressure drops may be required for the degassing of the product.

Kneading elements

Kneading elements (Figure 2-15) are used for the plastification of polymers, dispersion of fillers and mixing of materials. These elements normally consist of a number of kneading disks which have the same profile as the self-wipe profile of the screw elements. Kneading elements can be conveying, natural or reversing, depending on the angle of each consecutive kneading disk. Elements with wide disks provide a large amount of shear to the product where thinner disk elements contribute to the mixing characteristic of kneading elements. These elements transfer most of the mechanical energy from the rotation of the screw to the product through mechanical shear.

Compression elements

Compression elements (Figure 2-15) are elements with pitches shorter than their length. The characteristic of such an element is that it decreases the rate of flow and increases the pressure on the product. These elements are thus used to slow down the product in order to provide a better fill of the barrel over the processing sections, which in turn increase the efficiency of that particular section. The pressurizing capability of the element is used at the end of the barrel where high pressures are required. Figure 2-15 shows an example of each of the mentioned basic screw elements.

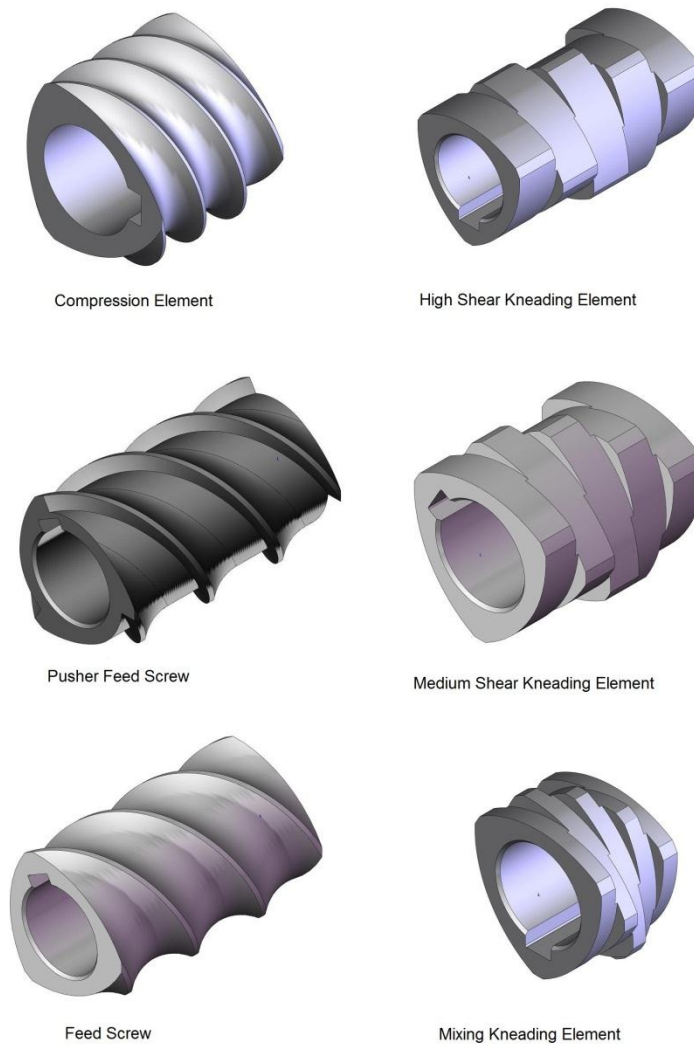


Figure 2-15: Feed screw and kneading elements (CFAM Technologies (Pty) Ltd, 2011).

The elements described above are the basic elements that comprise an extruder screw. There are however more types of elements such as mixer elements, cut flight elements, blister disks, eccentric discs and single flight kneading disks. These elements are not discussed in this study due to the fact that they are rarely used, especially in the processing of powder coatings powder.

2.6.2.4 Functionality of the die and knife plate

The extruder die is the final component or processing apparatus within the processing section. There are two major functions of the extruder die. Firstly, the die provides a restriction to the flow of the product, causing a build-up of product in the direction of the feed port. This provides the required pressure and shear inside the barrel for effective processing of the material. Secondly, the die shapes the final product.

Die design and its effect on expansion, uniformity and appearance of the product are often overlooked. Die shear rates may be altered dramatically by changing from a single die opening to multiple die openings.

Extruder strand dies are used in the compounding of polymers where product shape is required. The die provides a round shape to the product before it is cooled and cut into little cylinders (approximately 3x3mm) as the final product depending on the customers need. Figure 2-16 shows examples of polymer strand dies.

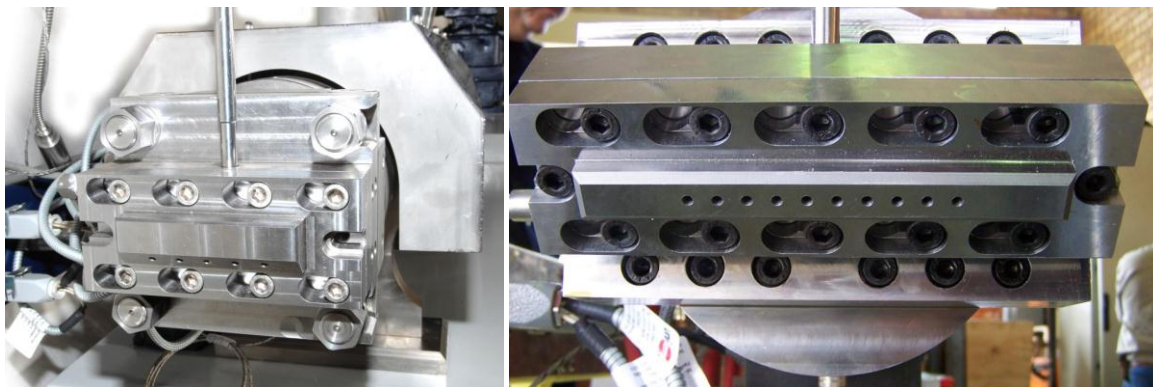


Figure 2-16: Polymer strand dies (CFAM Technologies (Pty) Ltd, 2011).

For the manufacturing of foods and feeds, the design of the die opening determines the manner in which the product expands. A decrease in diameter causes the product to expand in the radial direction and the land length (in other words the depth of the constant diameter just mentioned) contributes to the overall expansion. After expansion the product is cut to the desired length with a cutter running perpendicular to the direction of extrusion on the surface of the die. Figure 2-17 shows a graphical illustration of a food processing die with a die face cutter.

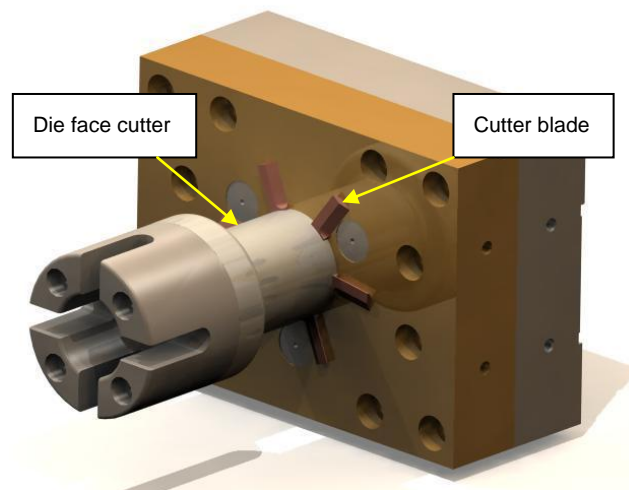


Figure 2-17: Food processing die (VAN NIEKERK, Werner, 2008).

With the manufacture of powder coating powder, a shape-giving die is not required because the desired shape is given to the product after the material has exited the extruder. The die used for this application is called a knife plate. The function of the knife plate is to have a slight increase in pressure for filling the barrel and an angled edge to push the product going upwards by the rotation of the screws away from the barrel. Figure 2-18 presents a graphical illustration of a knife plate.

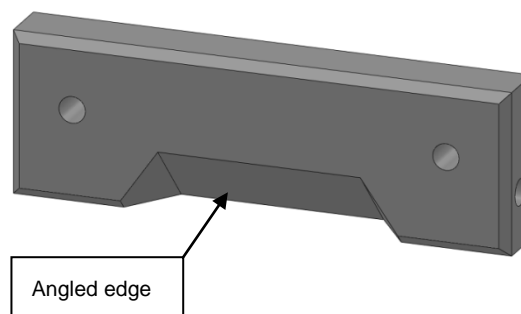


Figure 2-18: Barrel knife plate (CFAM Technologies (Pty) Ltd, 2011).

Note that the knife plate only covers the top half of screws, causing a very low pressure build-up.

2.7 Post extrusion processes

Extrusion, depending on the product being manufactured, is a cooking, texturizing, plastification or forming process. After the product exits the extruder it usually goes through a couple of processes such as cooling, drying, flavouring, forming, packaging, bagging, etc., until it is ready to leave the factory. In the manufacture of powder coating powder, the molten resin needs to be cooled and shaped after extrusion before it can go through subsequent processes.

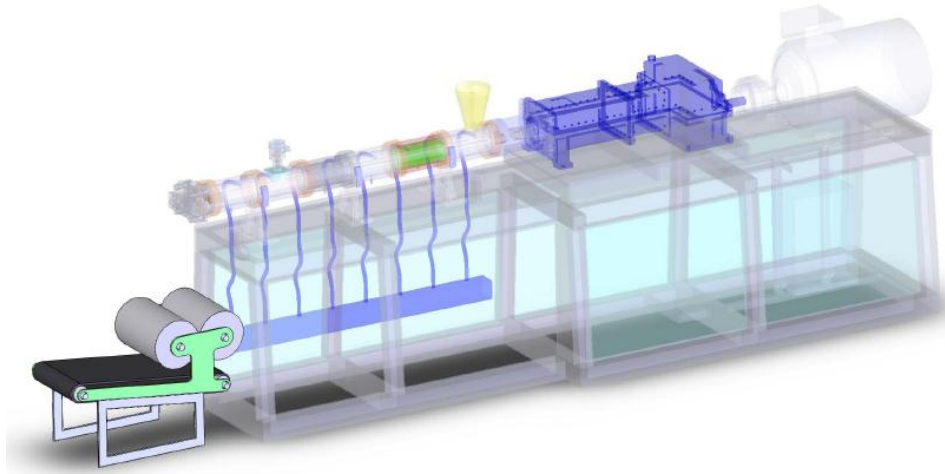


Figure 2-19: Post extrusion processes (CFAM Technologies (Pty) Ltd, 2011).

2.8 Cooling of the extruded powder coating powder

With the manufacture of powder coating powder, the temperature of the molten extrudate (product exiting the extruder) is at approximately 180°C . Thus, in order for the product to proceed to the rest of the process the melted extrudate needs to be solidified before it can be processed further. This is usually done by making use of chill rolls or a cooling belt, whereby the extrudate is converted into a crushable ribbon. After the ribbon is cooled, it is pulverized into a very fine powder. The powder is then classified by particle size before final packaging occurs (<http://www.p2pays.orgt/ref/10/09793.pdf>).

2.9 Traditional cooling units

There are basically two types of cooling units used for the cooling of powder coatings. The first is a unit consisting of a pair of adjustable, cooled rollers. The extrudate is fed through the set rollers which squeeze the molten material into a thin continuous ribbon. The cooled extrudate then passes through a flaker, reducing it to small sized chips suitable for feeding into a grinding machine. A major drawback with this type of cooling unit is the short contact time of the molten

product with the roller, which does not cause the material to reach the desired solidification temperature.

The second type of cooling unit consists of a set of similarly chilled rollers followed by a conveyor belt. The conveyor, usually metal, stretches for a couple of meters and is cooled from underneath with spray nozzles, spraying chilled water onto the conveyor. Exiting the extruder the extrudate passes through the pair of rollers, forming it to a continuous thin ribbon. It is then laid onto the conveyor where it is cooled before it goes through a flaker at the end of the conveyor belt. The advantage of this type of cooling unit is that the product easily reaches the desired temperature. On the other hand, this machine takes up a large amount of space, is labour intensive and costly to maintain.

Figure 2-20 shows an example of both the chill roll type machine and the chill roll-conveyor cooling machine.



Figure 2-20: Chill rolls and chill roll conveyor unit (Micro Powder Tech, 2005), (Spectra Consultech).

2.10 Needs and barriers in developing a cooling roller unit

Now that the different types of product cooling machines have been evaluated, a closer look can be taken at the major components in order to determine the requirements and challenges in the development of a cooling unit.

2.10.1 Cooling mechanisms

The product is cooled via the conduction of the heat through the metallic wall of the roller by continuously circulating water that is externally cooled by a chiller. The low temperature of the water in the roller causes it to be continuously covered with condensate and chilled rollers are

therefore manufactured from stainless steels or are coated to guard against corrosion which contaminates the product. Figure 2-21 shows the cooling mechanism of a typical chill roller.

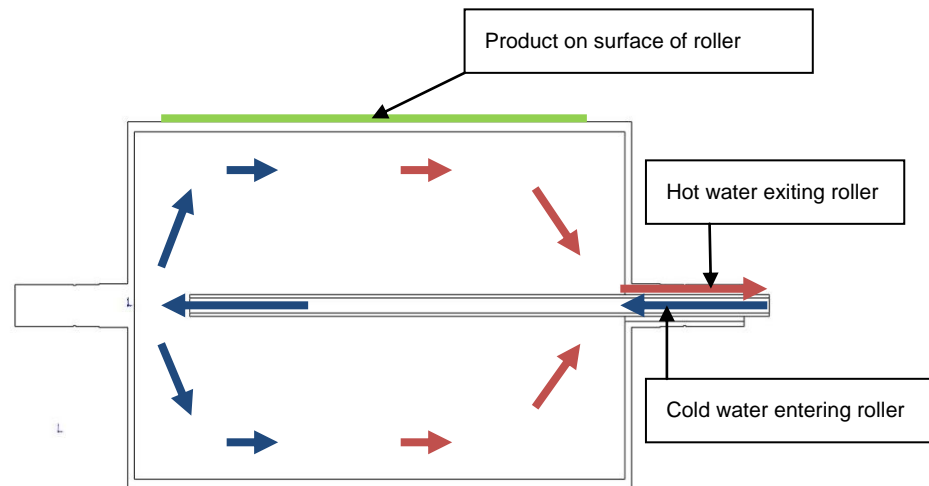


Figure 2-21: Cooling mechanism of a typical chill roller.

The product comes in contact with the cooling surface of the roller. Heat is transferred through the surface of the roller to cold water inside the roller. The water inside the roller is circulated by chilled water.

Because the roller has a continuous rotation, the circulation of the water is done by an apparatus called a double passage rotary union (Figure 2-22).

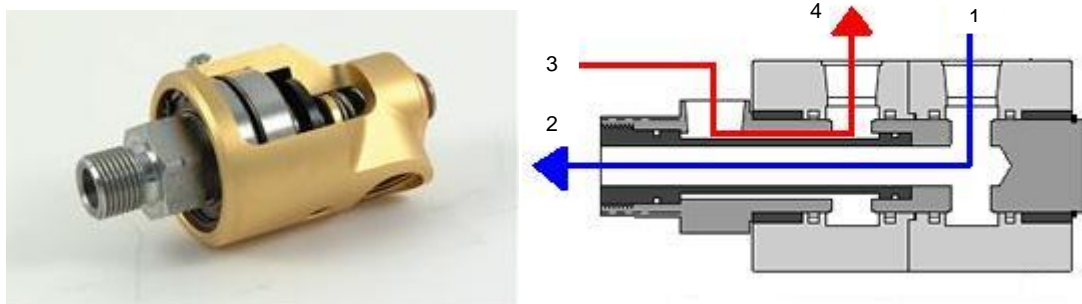


Figure 2-22: Double passage rotary union (Deublin, 2010), (Talco Inc.).

Cold water enters the stationary part of the union at point 1, then flows to point 2 which is the rotary part connected directly to the roller. After heat is transferred to the water, it re-enters the union at point 3 and exits the chilled roller at point 4 for circulation through the chiller plant.

2.10.2 Forming mechanism

In order to be able to pulverize the product after extrusion, the molten extrudate needs to be formed into a continuous strip or ribbon. This is achieved by two adjustable chilled rollers running close to each other, where the gap provides a product with the desired thickness. Figure 2-23 shows a graphical illustration of the process.

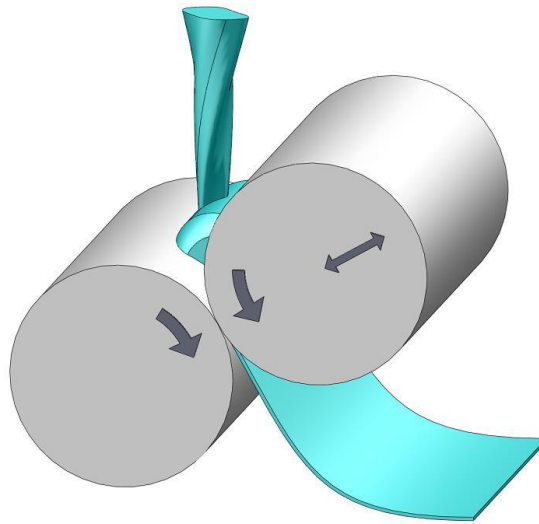


Figure 2-23: Forming of molten extrudate into a crushable ribbon.

2.10.3 Transporting mechanism

The transporting mechanism described here is the conveyor belt mentioned in Section 2.9. The conveyor is usually manufactured from a continuous stainless steel sheet with a thickness ranging from 0.3 to 0.6 *mm*.

2.11 Conclusion

Drive system

After examining the possibilities for a drive system, it was found that using a solid state power supply with a 3-phase AC motor will be the most cost-effective option. Not only is it widely available, but it requires low maintenance.

Extruder gearbox

Considering what has been presented in Section 2.6.1.3., the following needs to be taken into account in the development of a small extruder:

- A geared motor unit is easier and cheaper to buy off-the-shelf than to buy or to manufacture a complete integrated reduction and splitter gearbox.
- The design and manufacture of a splitter gearbox can easily be done in a general manufacturing facility. No castings are necessary and the manufacturing of the gears can be done by any gear cutter manufacturer.

Barrel

For the manufacturing of powder coating powder, the best barrel design concept to use is a clam shell barrel due to the following reasons:

- Powder coating powder consists of polyesters or epoxies with added hardeners. In the event of operational failures in the production of powder coatings, these resins cure inside the barrel and cannot be re-melted; therefore, clam shell barrel are required, which can be opened and cleaned.
- The advantage of using clam shell barrels is that it is much easier and cost-effective to replace liner segments when they become worn.

Screws

The ability to design and generate screw profiles, provide the capability to design and manufacture different types of processing elements. This enables the powder coating manufacturer to change the screw configuration in order to optimize the process capability of the equipment.

Knife plate

The exiting of the product after processing is mostly determined by the form in which the material is required. For the manufacturing of powder coating powder the forming of the product takes place after the product has exited the extruder. Therefore, a knife plate is required to provide a slight pressure build-up inside the barrel and allow the product to flow freely to the cooling unit in the manufacturing process.

Cooling unit

There are two different product cooling apparatus that are traditionally used: the paired roller type and the conveyor type. The paired roller unit has the advantage that it is compact, but has little contact time with the product resulting in poor cooling of the product. The conveyor belt unit is able to cool the product to the desired temperature. The drawback is however that these units are large and bulky machinery that takes up a lot of room and requires frequent and expensive maintenance. Therefore, a cooling unit is necessary which makes use of the advantages of both types of cooling units.

CHAPTER 3

FUNCTIONALITY AND DETAIL DESIGN

*In **Chapter 2** an overview is given regarding the product manufactured by the extruder. It also provides information on different design considerations for different aspects of the machine.*

This chapter focuses on the design and functionality of the extruder's critical systems and components that are specifically built for the powder coating manufacturing industry.

3.1 Introduction

This chapter focuses on the design of key components/systems of an extruder for the powder coating manufacturing industry.

The chapter contains information regarding the technical specifications according to which the extruder was designed. This is followed by the drive system design, which comprises the geared motor selection and the splitter gearbox design.

The design of the processing section consists of the barrel design, liner design and knife plate design.

Lastly the cooling unit design is presented.

3.2 Technical specification

Extrusion has a unique capability called extrusion scale up. Scale up is where the process parameters on one extruder (and size extruder) are captured and scaled to another extruder, obtaining the same result (product).

For the extruder to be amenable to accurate scale up it has to be designed as close as possible to the industry standard extruder for that specific size. There are some essential components that have been designed and specified according to the industry standard such as the extruder drive motor size, screw center distance, screw diameter, screw length to diameter ratio and number of heating-cooling zones.

The design specifications are based on an industry standard 28mm laboratory extruder. Table 3-1 provides these design specifications.

Table 3-1 Standard 28mm Laboratory Twin Extruder specifications

Motor size	5.5kW
Gear ratio	3:1
Max extruder speed	500rpm
Product mass flow	70 kg/h
Barrel length	19 L/D
Barrel type	Clam
Screw diameter	28mm
Center distance	26.2mm
Screw profile	Triple – flighted profile
Extruder die	Knife plate
Number of heating zones	3

3.3 Extruder Development

3.3.1 Drive Unit

As stated in Section 2.6.1, the drive unit provides the mechanical power to the processing section. It is essential that the drive section is able to provide the necessary power to the processing section for maximum capacity. The power is limited by geometric constraints such as maximum shaft diameters, screw center distances, bearing sizes, etc.

3.3.1.1 Motor selection

From the design specifications, the specified motor is a 5.5kW motor. As stated in Section 2.11, the use of an AC motor has much more advantages than a DC drive; Thus the specification of

the 5.5kW, 50Hz, 4 pole 3-phase induction motor. The motor is powered by a frequency converter which enables the extruder to operate at speeds from 0rpm to 500rpm, which is the maximum operating speed of the extruder (Table 3-1).

Section 2.11 states that it is advantageous in the manufacturing of a small extruder to make use of a geared motor for the drive unit, because of the lowered cost and accessibility. Thus a geared motor is used in conjunction with a splitter gearbox.

The splitter gearbox is designed according to the configuration of a cluster gearbox, where the torque from the reduction gearbox splits into two adjacent shafts. This design has a negative effect on the reduction ratio because of geometric constraints. It is thus necessary to compensate for that during the selection of the geared motor.

The rotational speed of the electric motor is calculated by the following equation:

$$\omega = \frac{F \times 120}{U}$$

where F is the frequency of the alternating current, and U the number of poles of the motor. Thus for a 4 pole motor running at 50Hz the speed is:

$$\begin{aligned}\omega &= \frac{50 \times 120}{4} \\ &= 1500rpm\end{aligned}$$

Due to motor slip the actual speed is 1450rpm.

By making use of Equation 2-4 and 2-5 the gear and speed ratios of the two gearboxes are calculated iteratively. Equation 3-1 and 3-2 represents the reduction gearbox and Equation 3-3 and 3-4 the splitter gearbox.

$$Z_1 \times N_1 = Z_2 \times N_2 \quad [3-1]$$

$$i_1 = Z_1 / Z_2 \quad [3-2]$$

$$Z_2 \times N_2 = Z_3 \times N_3 \quad [3-3]$$

$$i_2 = Z_2 / Z_3 \quad [3-4]$$

By manipulation, the speed ratios can be written as:

$$i_1 = \frac{N_1}{N_3} \times i_2 \quad [3-5]$$

For the calculation, a gear ratio for the splitter gearbox is necessary. A typical ratio for a cluster splitter gearbox is 1: 1.6; using this value as a base for the iterative process.

If the splitter gearbox is 1: 1.6 then the ratio of the geared motor must be:

$$\begin{aligned} i_1 &= \frac{500}{1450} \times 1.6 \\ &= 0.55 \end{aligned}$$

It results that the ratio of the geared motor is 5:1.

The ratio of 1: 1.6 of the splitter gearbox has a large effect on the geometry of the gearbox. The two adjacent shafts that are a distance of 26.2mm from each other, (screw center distance Figure 3-1), limit the diameter of the gears on the two adjacent shafts. Thus, the pinion gear must be large enough to mesh with the other two gears and must leave enough space for the bearings of the three closely spaced shafts.

The triple flight fully intermeshing twin screw profiles of a standard 28mm laboratory extruder (Table 3-1) operate at a center distance of 26.2mm from one another. The fully wiped profile has a major diameter of 28mm and minor diameter of 24.4mm. Figure 3-1 is a graphical illustration of the profile meshing at a distance of 26.2mm.

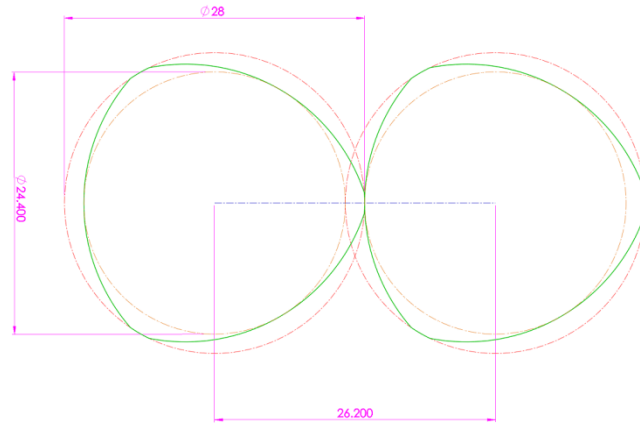


Figure 3-1: Screw dimensions and center distance

3.3.1.2 Extruder gearbox design

The design of an extruder gearbox is an iterative process, starting at the gear teeth design, and followed by shaft design.

Design of the gear teeth is the best starting point in gearbox design. It not only provides the geometry of the gearing but also the force conditions, which are essential in the design of shafts and bearings. During the shaft design certain parameters become clear, such as loading on support points (bearings), bending of the shaft at the support points and importantly, the shaft sizes at the support points for a reference diameter for selection of the bearings.

Gear design

In the design of the gearbox there are certain fixed parameters. These parameters are usually gear ratios, service life and rated power. Further, there are parameters essential to the design, but not fixed. Some of these parameters are chosen within a range or taken as fixed values according to manufacturing capabilities or functionality. Table 3-2 shows the fixed parameters to which the gearbox is designed.

Table 3-2 Fixed design parameters of the gearbox

Parameter	Symbol	Value
Gear ratio	i	1: 1.6
Distance between output shafts	A	26.2mm
Minimum safety factor for shafts	n	2
Minimum safety factor for gear teeth bending	S_F	1.4
Minimum safety factor for gear teeth surface durability	S_H	1.1
Design Life requirement	h_L	20 000 <i>hours</i> or 1×10^6 <i>Cycles</i>
Reliability	%	99

Table 3-3 provides parameters that are not fixed, but are chosen as fixed values.

Table 3-3 Chosen design parameters of gearbox

Parameter	Symbol	Value
Pressure angle	α	20°

The pressure angle is the angle of contact of two intermeshing gear teeth. This value is chosen as 20° because it is an industry standard for gear cutters, thus eliminating the need for the purchasing of a special gear cutter.

The design can be started by first determining the number of teeth for the driving and driven gears. According to Table 3-2 the gearbox must have a gear ratio of 1: 1.6. This is achieved by choosing the number of teeth of the driving gear as 25 *teeth* and the driven gear as 15 *teeth*. The calculation is done as follows:

$$i = \frac{Z_1}{Z_2} = \frac{25}{15} = 1.667$$

which is considered close enough to the desired gear ratio.

The pitch center diameter (PCD) and pitch center distance for the two intermeshing gears are calculated by choosing the normal module as 2 and substituting it into Equation 2-6, where, m is the normal module, N the number of teeth and d the PCD of the gear.

$$m = \frac{d}{N}$$

$$d_{driving} = 2 \times 25 = 50mm \text{ and } d_{driven} = 2 \times 15 = 30mm$$

providing a pitch center distance of:

$$aw = \frac{d_{driving}}{2} + \frac{d_{driven}}{2}$$

$$aw = \frac{50}{2} + \frac{30}{2} = 40mm$$

A summary of the tooth geometry is presented in Table 3-4.

Table 3-4: Gear tooth parameters

Parameter	Symbol	Value
Gear ratio	i	1: 1.6
Pinion number of teeth	Z_1	25
Gear number of teeth	Z_2	15
Normal module	mt	2
Pressure angle	α	20°
Helix angle	β	0°
Center line distance (Working center distance)	aw	40mm

Other very important parameters obtained from the gear calculations are the forces developed by the gears. These forces are the external forces acting on the shafts and gear teeth. The forces can be calculated using Equations 2-11, 2-12 and 2-13.

From Table 3-1 the drive power is 5.5kW resulting in 2.75kW for each output shaft and a maximum shaft speed of 500rpm. This generates a torque of 54 Nm in the shaft. With a PCD of the driven gear as 30mm, and a gear contact angle of 20°, the external forces were calculated as follows:

$$F_t = \frac{T}{PCD/2} = \frac{54}{0.03/2} = 3600 \text{ N}$$

$$F_n = F_t / \cos(\theta) = 3600 / \cos(20^\circ) = 3831 \text{ N}$$

$$F_r = F_n \times \sin(\theta) = 3600 \times \sin(20^\circ) = 1231 \text{ N}$$

Due to the fact that the helix angle is 0°, there are no axial forces developed by the gears, thus the value of $F_a = 0\text{N}$.

After the calculation of the external gear forces had been completed, the next step was to determine the safety factor for both bending, as well as the factor of safety for surface durability

for the gear teeth. These calculations were done based on the AGMA gear strength methodology discussed in Section 2.6.1.4. The bending stress for the gear teeth is calculated from Equation 2-7 as follows:

$$s_t = W^t K_o K_v K_s \frac{1}{bm_t} \frac{K_H K_B}{Y_J}$$

The tangential force F_t for the AGMA notation is W_{gear}^t and is calculated as $3600N$ on the gear. For the calculation of the bending strength all the related factors as well as the geometry factor were calculated in Annexure C, the values of the factors are as follows:

- $K_o = 1$
- $K_v = 1.1$
- $K_H = 1.123$
- $K_B = 1$
- $Y_J = 0.25$

The normal module (m_t) is 2 (Table 3-4) and the face width b was chosen as $24mm$ as a starting point because the gear strength calculation are an iterative process. The bending stress is thus calculated as:

$$s_t = 3600 \times 1 \times 1.1 \frac{1}{0.024 \times 2} \frac{1.123 \times 1}{0.25}$$

$$s_t = 370MPa$$

In order to determine the safety factor, the allowable bending stress needs to be determined (Eq 2-8). The factors that play a role are the:

- allowable bending stress of the material,
- stress cycle factor for bending,
- reliability factor, and
- temperature factor.

The material to be used for gears is BS970: 655M13 steel, that have been typically developed for gear manufacturing/production. The material is carburized and case hardened to a surface hardness of $58 - 64HRC$. In this condition AGMA allows a bending stress of $\sigma_{FP} = 380MPa$ in the material and a contact stress of $\sigma_{xx} = 1550MPa$. Material data is presented in Annexure C.

The calculations for the various factors are presented in Annexure C, and their calculated values are as follows:

- $Y_N = 1.185$
- $Y_\theta = 1$
- $Y_Z = 1$

The allowable bending stress is calculated as follows:

$$\begin{aligned}\sigma_{all} &= \frac{\sigma_{FP} Y_N}{Y_\theta Y_Z} \\ \sigma_{all} &= \frac{450 \times 1.185}{1} \\ &= 450.3MPa\end{aligned}$$

The safety factor for bending is thus:

$$\begin{aligned}S_F &= \frac{\sigma_{all}}{\sigma_{st}} \\ &= \frac{450.3}{370} = 1.4\end{aligned}$$

The calculated safety factor for bending is 1.4, which satisfies the design requirement of $S_F = 1.4$ in Table 3-2.

The contact stress on the gear teeth were calculated using Equation 2-9 as follows:

$$\sigma_c = Z_E \sqrt{W^t K_o K_v K_s \frac{K_H}{d_{w1} b} \frac{Z_R}{Z_I}}$$

Where W_t, K_o, K_s, K_v and b are the same terms that were used in the calculation of the bending stress. The additional factors were calculated in Annexure, and were determined to be as follows:

- $Z_E = 191 GPa$
- $Z_R = 1$
- $Z_I = 0.06$
- $Z_N = 1.14$
- $Z_W = 1$

The contact stress thus is:

$$\begin{aligned} \sigma_c &= 191 \sqrt{3600 \times 1 \times 1.1 \frac{1.123}{50 \times 24} \frac{1}{0.06}} \\ &= 1501 MPa \end{aligned}$$

The contact stress allowed is:

$$\begin{aligned} \sigma_{all,c} &\leq \frac{s_{ac}}{S_H} \frac{Z_N}{K_T} \frac{C_H}{K_R} \\ \sigma_{all,c} &\leq \frac{1550 \times 1.14}{1} \\ &= 1767 MPa \end{aligned}$$

Accordingly, the safety factor for contact stress or resistance against pitting, was calculated as:

$$S_H = \frac{1767}{1501}$$

$$= 1.2$$

The calculation of the safety factor for surface durability of 1.2 satisfies the design requirement in Table 3-2 of $S_H = 1.1$.

Gearbox shaft design

The function of shafts in gearboxes is to transfer torque and to position the gears very accurately in order to maintain the desired working center distance of intermeshing gears.

The forces developed by the gearing are directly transferred to the shafts. The radial force F_r induces a bending moment on the shaft in a plane through the length of the shaft. A typical example is a beam carrying a load. However, the rotation of the shaft causes the bending of the beam to change angle, exposing the shaft to fatigue. The tangential force F_t , transfers the torque between two gears and induces a bending moment on the shaft on a plane through the length of the shaft, 90° to the plane of the radial force (Figure 3-3). Thus there is a resultant bending moment on the shaft caused by these two forces.

If the gearing has a helix angle, force F_a will not be 0N which in turn induces a third moment on the shaft, due to the distance from the point of contact of the gear to the center of the shaft.

Another consideration is the angle of the shaft due to bending at the positions of the bearings (reaction support of beam). Bearings have a limit in which the shaft is allowed to bend before the bearing life reduces dramatically.

Figure 3-2 is a graphical representation of the gearbox. The input shaft contains the pinion gears, which transfers the torque to the two adjacent gears on the output shafts.

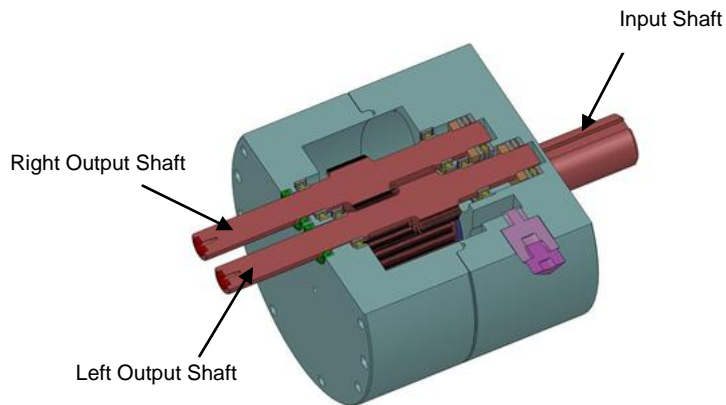


Figure 3-2: CAD model of the designed splitter gearbox (CFAM Technologies (Pty) Ltd, 2011).

Figure 3-3 is a free body diagram of the left output shaft. The forces developed by the gears, as well as the planes in which these forces lie is shown. A and B represents the bearing support on the shaft.

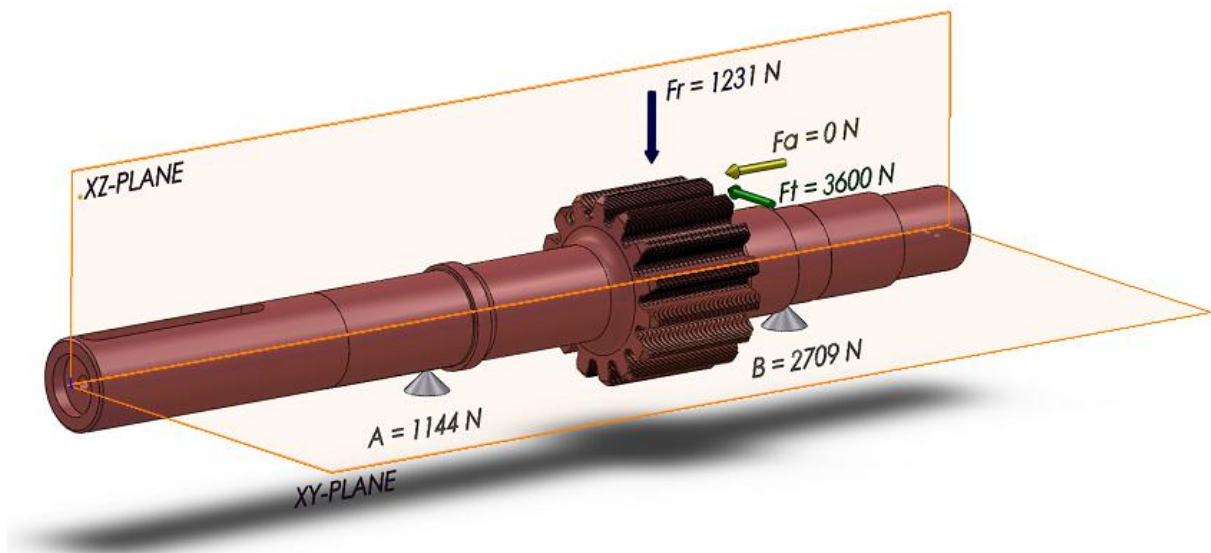


Figure 3-3: CAD model of the gearbox shaft illustrating the calculated sizes and directions of acting forces.

In the design of the shafts, the primary focus was the displacement of the shaft at the position of the gear, the angle at the supports and the minimum coefficient for dynamic and static safety in the shaft.

This section presents the calculation results of the shear and bending moment diagrams, the deflection, angular deflection as well as the bending and torsional stress in the shaft. A summary of the results of all the shafts is presented at the end of the section.

Figures 3-4 and 3-5 respectively show the shear force and bending moment diagrams of the shaft. The shear force and bending moment represented by the blue line, is a result of the radial force $F_r = 1318N$, and lies in the $XZ - Plane$. The green line represents the tangential force $F_t = 3622N$ which lies in the $XY - Plane$, (see Figure 3-3 for force and plane orientation). The resultant force of F_r and F_t is indicated as the red line. This gives an indication of the maximum shear force well as the maximum bending moment. The maximum shear force and maximum bending moment are respectively $2709N$ and $56Nm$. At the bearing locations, $78.5mm$ and $147.5mm$, from the front of the shaft, the reaction force is respectively, $1144N$ and $2709N$.

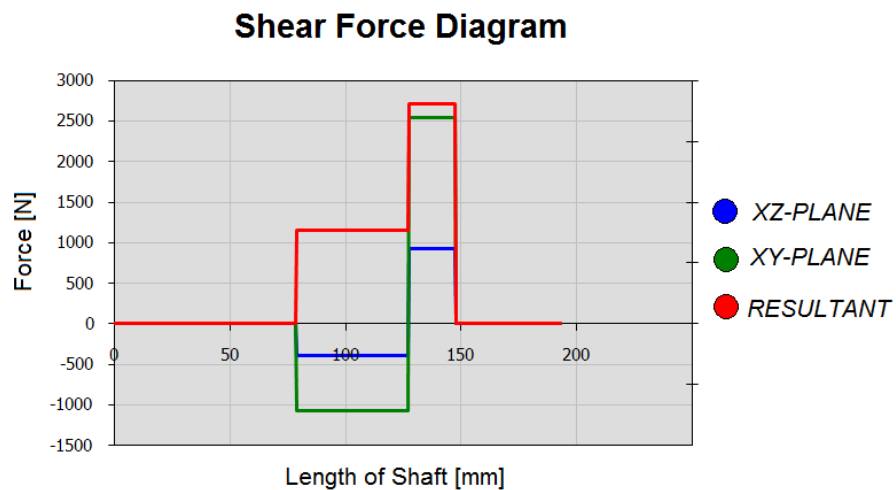


Figure 3-4: Shear Force Diagram

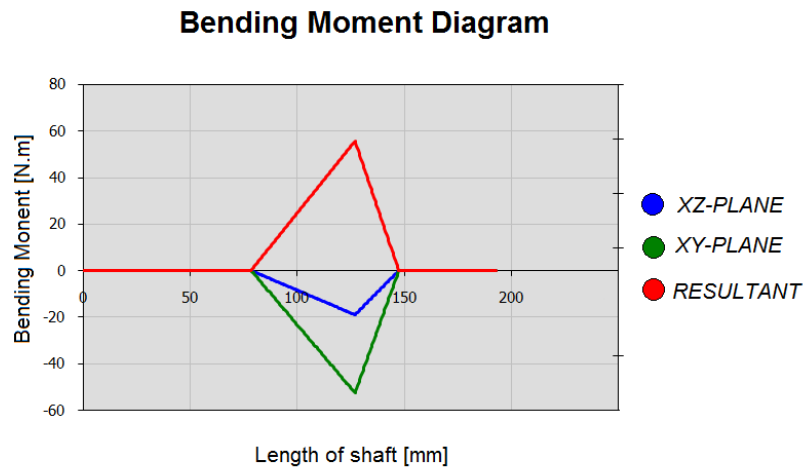


Figure 3-5: Bending Moment Diagram

The deflection of the shaft due to the tangential force of the gear pair F_t lies in the $XY - plane$, and is represented as the green line in Figure 3-6. The deflection due to the radial force of the gears F_r , lies in the $XZ - plane$ and is represented as the blue line. These two forces create a resultant force F_n , (Figure 2-7). The deflection caused by the resultant force is shown as the red line. The point of interest is at the middle of the gear, a distance of $127mm$ from the front of the shaft. The maximum deflection (red line) at this point is $0.01mm$ which is much smaller than the gear's acceptable backlash range of $0.038mm$ to $0.152mm$.

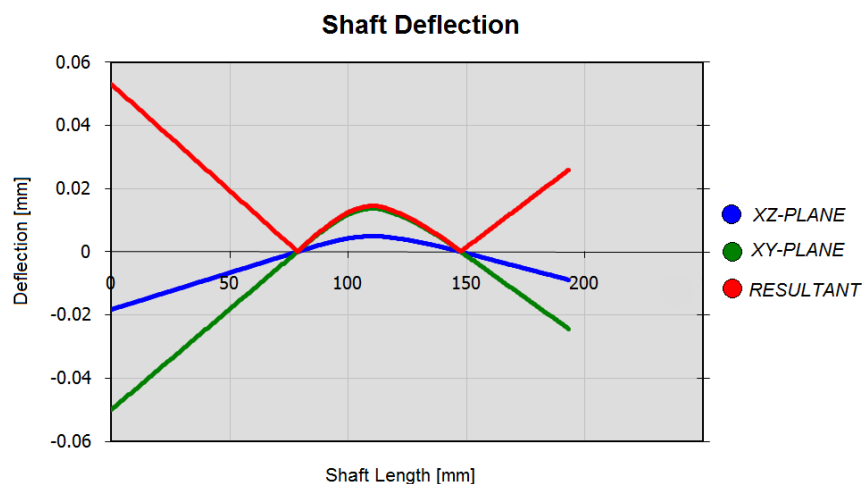


Figure 3-6: Deflection of the shaft

Forces, F_t and F_r , developed by the gear causes the shaft to deflect (Figure 3-6). This deflection causes the shaft to contact the shaft supports (bearings) at an angle (Figure 3-7). Bearings which are not self-aligned have limits in which the angle of the shaft can be. For ball bearings the angle limit is 0.27° , and for roller bearings the angle limit is 0.058° (<http://www.skf.com>). The bending angle at the bearing locations, $78.5mm$ and $147.5mm$ from the front of the shaft is 0.038° and 0.032° respectively. The shaft angles at both locations are less than the minimum angle for both deep groove and roller bearings, providing the freedom to use any of the two types of bearings.

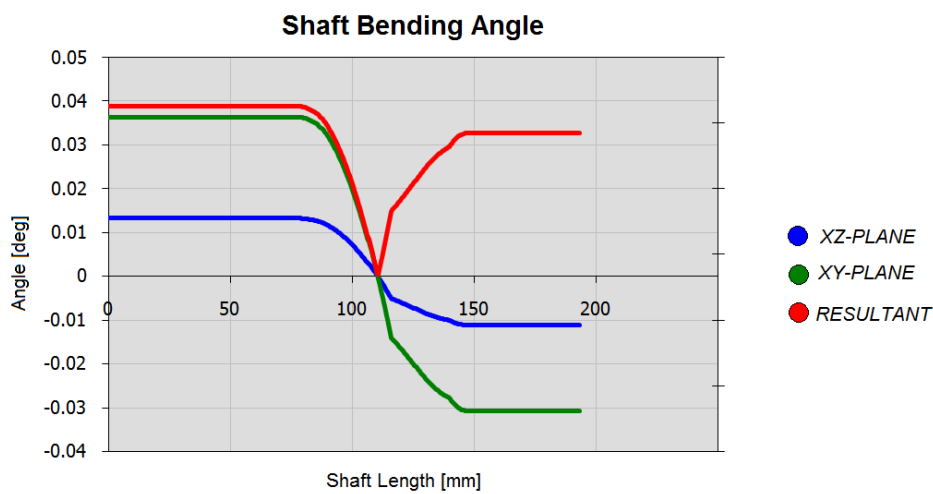


Figure 3-7: Bending angle of the shaft

The bending stress in the shaft is shown in Figure 3-9 and is calculated by Equation 2-3.

$$\sigma_{max} = \frac{M \times c}{I}$$

The bending moment together with the moment of inertia is used to calculate the bending stress at each change in shaft diameter. This provides a graph showing the maximum normal stresses in the shaft (Figure 3-8). From Figure 3-5 the maximum bending moment is $127mm$ from the front of the shaft at the middle of the gear teeth. The maximum bending stress in the shaft of $88.5MPa$ is $115mm$ from the front where the shaft diameter increases from $17mm$ to $25mm$, which is the root of the gear teeth (Figure 3-8).

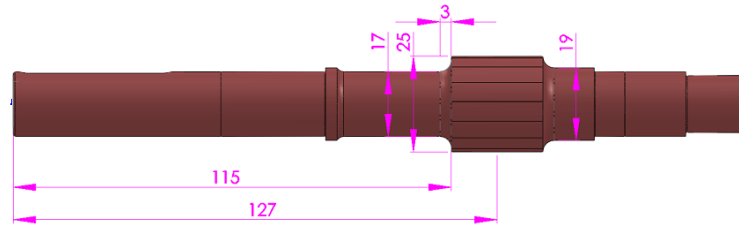


Figure 3-8: Location of maximum bending stress in shaft

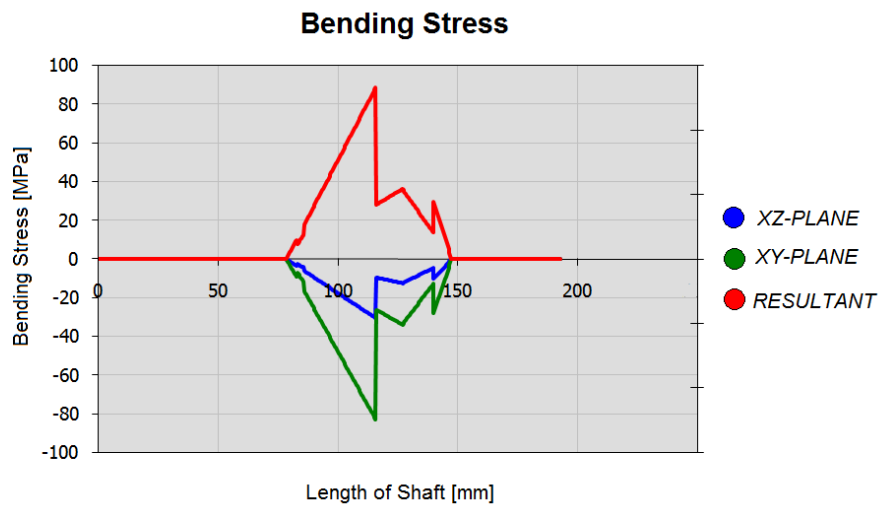


Figure 3-9: Bending Stress of the shaft

The torsional moment as well as the torsional stress in the shaft is presented in Figure 3-11. The torsion in the shaft is constant from the point on the shaft where the gear transfers the torque to the shaft to where the shaft transfers it to the extruder shaft. The torsional stress follows the same route, but changes as the diameter of the shaft changes. The torsional stress is expressed by Equation 2-2.

$$\tau = \frac{T \times \rho}{J}$$

The maximum torsional stress in the shaft is 62 MPa where the keyway starts. The effective diameter at this location is reduced from 17 mm to 12 mm as shown in Figure 3-10.

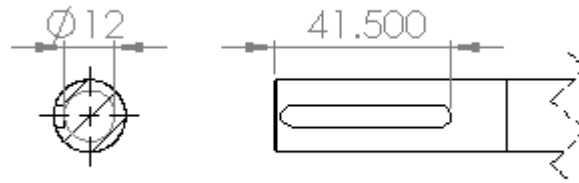


Figure 3-10: Effective diameter of the shaft at the keyway

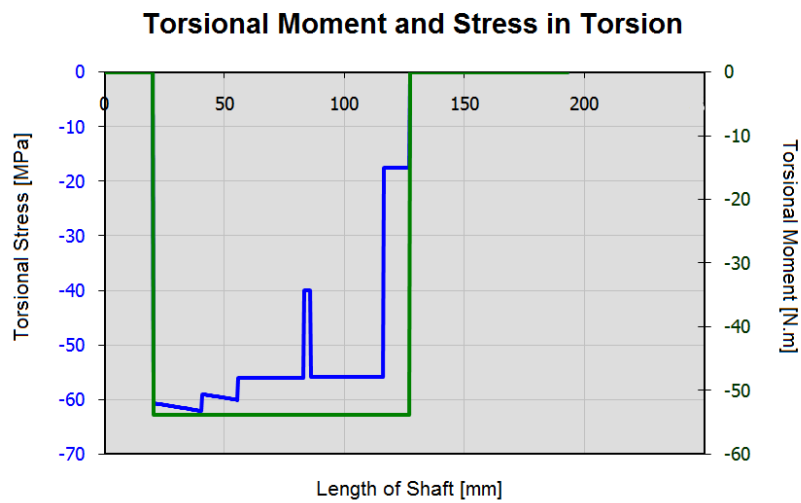


Figure 3-11: Torsional moment and stress in torsion of the shaft

The point of interest for the calculation of the factor of safety for the shaft is 115mm from the front of the shaft (Figure 3-8). This point is of interest because the maximum bending stress (88.5MPa) occurs there, the shaft is in torsion (54Nm) and a stress concentration is present due to the large diameter change. The calculation for the static factor of safety was done for Von Mises stresses and is expressed by Equation 3-6 and the dynamic factor of safety was calculated for an alternating bending moment and a mean torsional moment, Equation 3-7.

$$\frac{1}{n} = \frac{16}{\pi d^3 S_y} \sqrt{4M_a^2 + 3T_m^2} \quad [3-6]$$

$$\frac{1}{n} = \frac{16}{\pi d^3} \sqrt{4 \left(\frac{K_f M_a}{S_e} \right)^2 + 3 \left(\frac{K_{fs} T_m}{S_y} \right)^2} \quad [3-7]$$

Where:

- n is the factor of safety
- d is the smallest diameter of the shaft at the point of interest [mm]
- M_a is the alternating bending moment [Nmm]
- T_m is the mean torsional moment [Nmm]
- K_f and K_{fs} is the stress-concentration factor for both bending and torsion
- S_y is the yield stress of the shaft material
- S_e is the endurance limit of the shaft material

The calculations of the concentration factors and endurance limit are presented in Annexure C. The material to be used for the shaft is BS970: 655M13 steel, as this is the gear material and the gears are integrated on the shafts.

- $K_f = 1.3$
- $K_{fs} = 1.25$
- $S_y = 765MPa$
- $S_e = 247MPa$

At the point of interest the bending moment in the shaft is $41.5Nm$, the minimum diameter is $17mm$. The factor of safety for static and dynamic loading is calculated as:

Static

$$\frac{1}{n} = \frac{16}{\pi \cdot 17^3 \cdot 765} \cdot [4 \cdot (41.5 \times 10^3)^2 + 3 \cdot (54 \times 10^3)^2]^{0.5}$$

$$n = 5.8$$

Dynamic

$$\frac{1}{n} = \frac{16}{\pi \cdot 17^3} \sqrt{4 \cdot \left(\frac{1.3 \cdot 41.5 \times 10^3}{247} \right)^2 + 3 \cdot \left(\frac{1.25 \cdot 54 \times 10^3}{765} \right)^2}$$

$$n = 2.1$$

From the calculation both the static safety factor as well as the dynamic safety factor satisfies the design specification of a minimum of 2. A summary of the calculated safety factors, deflection and angular deflection for both the output shafts as well as the input shaft, are presented in Table 3-5. The detail design drawings of the gearbox shafts and housing are presented in Annexure A.

Table 3-5: Summary of the deflections, angular bending and safety factors of the input and two output shafts of the gearbox.

Description	Output shaft 1	Output shaft 2	Input shaft
Deflection at gear	0.01mm	0.012mm	0.001mm
Bending angle at support A	0.038°	0.041°	0.0038°
Bending angle at support B	0.032°	0.044°	0.0039°
SF Dynamic	2.1	2.77	7.28
SF Static	5.8	3.31	5.22

3.3.2 Process section

3.3.2.1 Barrel design

From the technical specification for a standard 28mm twin screw extruder, in Section 3.2 Table 3-1, the extruder requires a length to diameter ratio (L/D) of 19:1, should be equipped with a clamshell barrel, hosting replaceable liner segments and have 3 temperature controlling zones.

Barrel geometry

It sometimes happens that the melted product cures inside the barrel during production due to mechanical failures or production flaws. It was therefore necessary to use a clamshell barrel so that the barrel could easily be opened and cleaned.

The screw package that the extruder must facilitate has a 19:1 length to diameter ratio. This means that the length of the barrel will be.

$$L = 19 \times 28 = 532mm$$

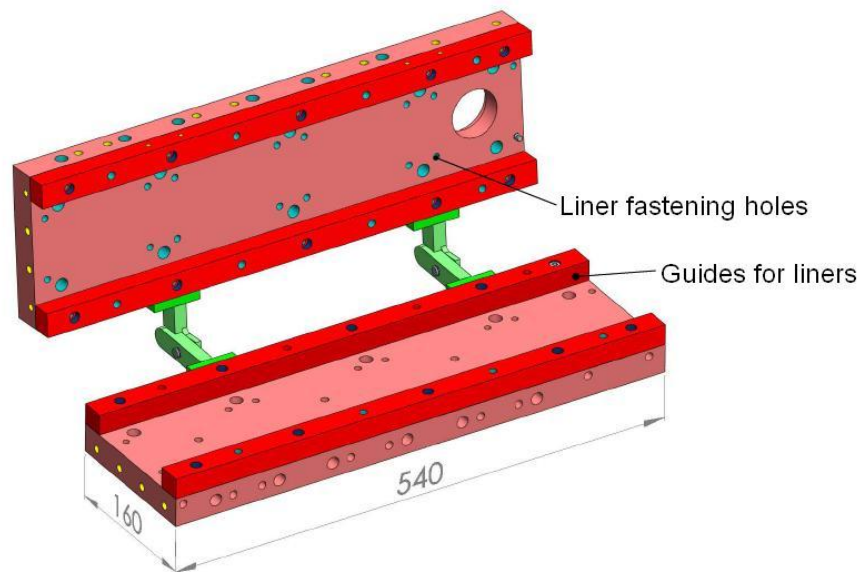


Figure 3-12: Basic geometry of the clam shell barrel (CFAM Technologies (Pty) Ltd, 2011).

Figure 3-12 shows the basic geometry of the barrel. It shows that the barrel length is 540mm, the extra 8mm is to compensate for a shoulder on the shaft at the back of the screw set. The shoulder serves as an axial stop to provide a reaction force to the screw set, as the screws is pushed towards the gearbox when conveying product.

The liners were divided into segments in order to be able to replace a single liner at a time as they wear down. The set of liners is therefore guided so that the bore of each liner aligns with the one next to it. The liner guides are presented in Figure 3-12, as the red bars running through the length of the barrel. These liner guides are located very accurately on the cooling block to ensure correct liner alignment. After all the liners have been placed into position, they are fastened with cap screws that are counter sunk into the barrel.

Processing capabilities

The process capability of the barrel is to fine tune the temperatures inside the liners. This capability is achieved by making use of cartridge elements in conjunction with cooling ports, pared into 3 sections distributed evenly across the processing section of the screws. The processing section of the screws is presented in Figure 3-13.

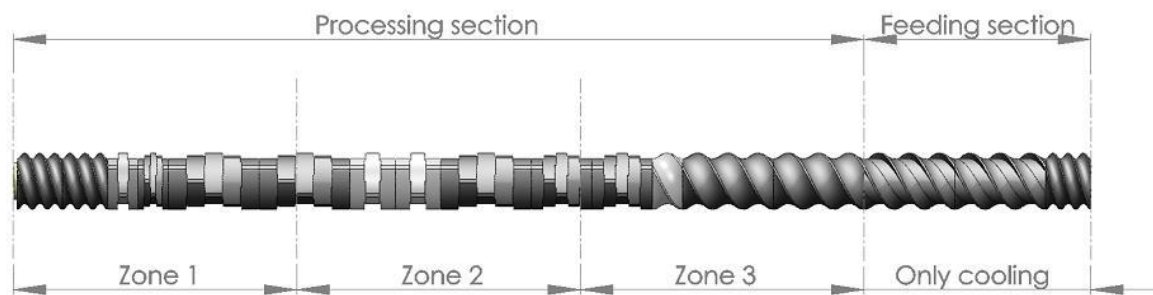


Figure 3-13: Processing zones on the screw configuration.

The screw configuration in Figure 3-13 is a typical configuration used for the production of powder coating powders.

Each processing zone has a separate set of cooling ports and heaters in order to achieve accurate process temperature control. Figure 3-14 shows the cartridge heater holes (red) and the cooling ports (blue) for both the bottom and top cooling block respectively.

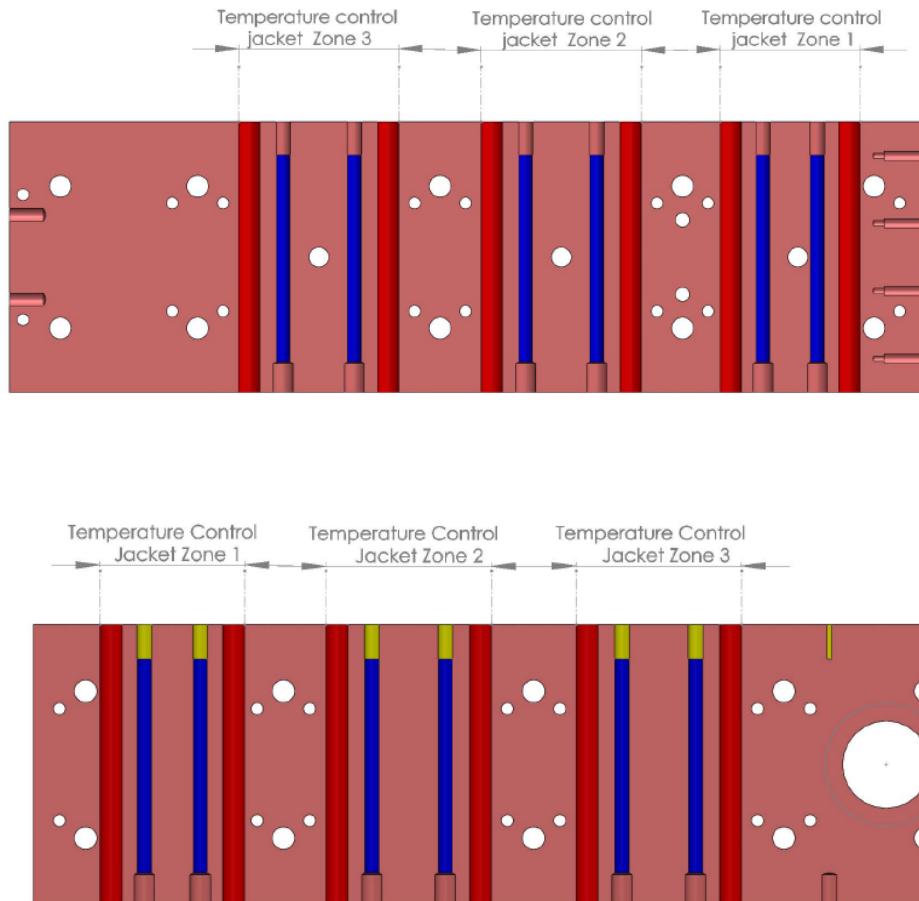


Figure 3-14: Bottom and top barrel temperature control zones (CFAM Technologies (Pty) Ltd, 2011).

The feed port section has permanent cooling so that the product does not melt in the feeding section, and to prevent the barrel temperature from being conducted to the splitter gearbox and extruder frame. Conduction of heat to the splitter gearbox can result in damaging of the shaft seals causing oil leaks and it raises the temperature of the oil inside the gearbox, reducing the lubrication capability of the oil. Figure 3-15 shows a graphical illustration of the permanent cooling ports inside the barrel.

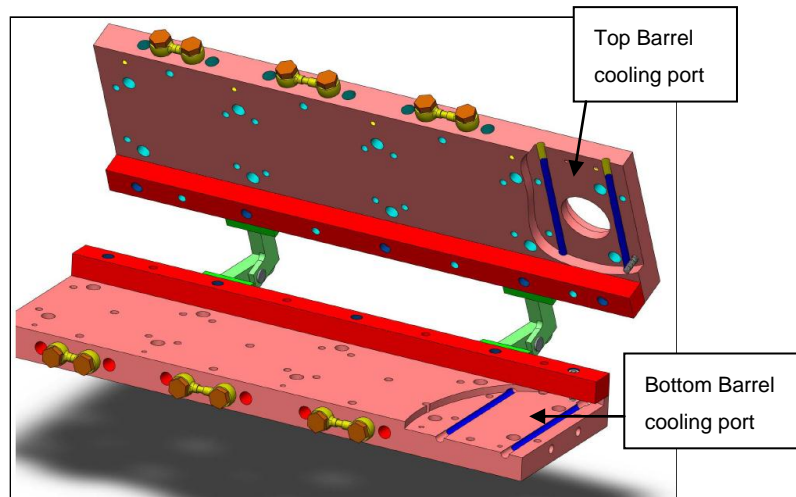


Figure 3-15: Barrel permanent cooling ports (CFAM Technologies (Pty) Ltd, 2011).

The complete barrel assembly open and closed is presented in Figure 3-16. The barrel sections are fixed by two hinges, making it easy to open the barrel for cleaning and inspection.

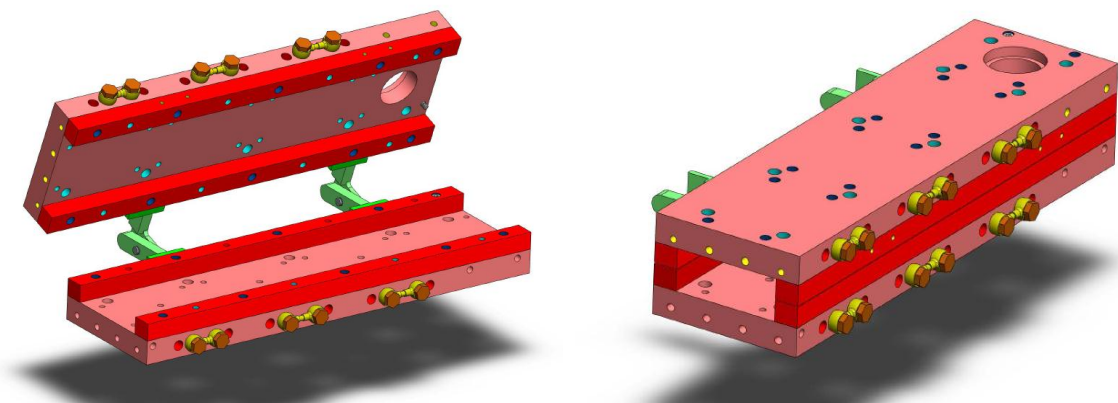


Figure 3-16: Clam shell barrel assembly (CFAM Technologies (Pty) Ltd, 2011).

Interfacing of barrel with extruder frame

During operation the temperature of the barrel increases to 250°C . This results in elongation of the barrel material with respect to its width, height and length. The barrel must thus be able to expand freely, and not be held in a fixed position. There is a fixed distance from the extruder gearbox to the back of the barrel; thus, if the barrel is free to elongate it still must be fixed at this point. The barrel is therefore fixed to a structure, namely the backing plate.

The backing plate has more than one feature as follows:

- The backing plate sets the height so that the bores align with the output shafts of the gearbox.
- It serves as a stuffing box that keeps the product from leaking backwards.
- It hosts two bushes that fix the extruder screws to the bore centerline distance, in order to prevent the screws from rubbing against the liner wall, and also prevents cyclic bending moments on the output shafts of the gearbox.

The elongation of the barrel due to the increase in temperature can be accommodated by designing a foot at the front of the barrel that enables the barrel to move freely in the axial direction of the shafts. The backing plate as well as the front foot is shown with the barrel assembly in Figure 3-17.

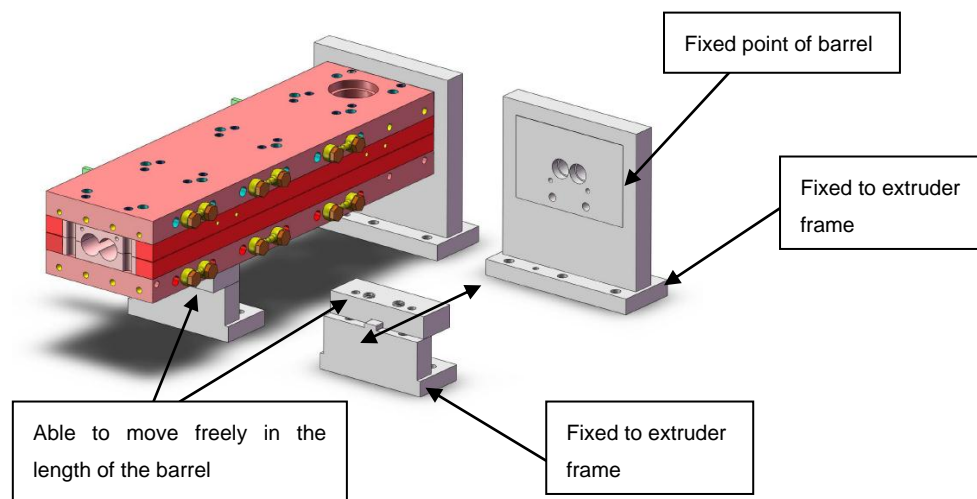


Figure 3-17: Interfacing components of the barrel with the rest of the extruder (CFAM Technologies (Pty) Ltd, 2011).

3.3.2.2 Liner design

The cavities, in which the extruder screws operate, are called the bores of the extruder. These bores, as mentioned in Section 2.6.2.2, are subject to extensive wear due to the amount of product and its abrasive characteristics as it is pumped through the bores. In order to compensate for the wear, the extruder barrel is equipped with a series of liner segments specially treated and manufactured to resist wear.

The different types of liners are described in section 2.6.2.2. In this clam shell barrel design, the liners are separate parts that fit into the barrel. Thus it is advantageous to use through-hardened liners. The liners are manufactured from K110 (<http://www.bohler-edelstahl.at>), a high-carbon, high-chromium tool steel alloyed with molybdenum and vanadium. The material is characterized by the following:

- High wear resistance
- High compressive strength
- Good through-hardening properties
- High stability in hardening
- Good resistance to tempering-back

Liner geometry

For a twin screw extruder with a diameter of 28mm , the industry standard extruder with a triple flight profile, the center distance for the two intermeshing screw profiles is 26.2mm . The geometry of the liner bore is shown in Figure 3-18.

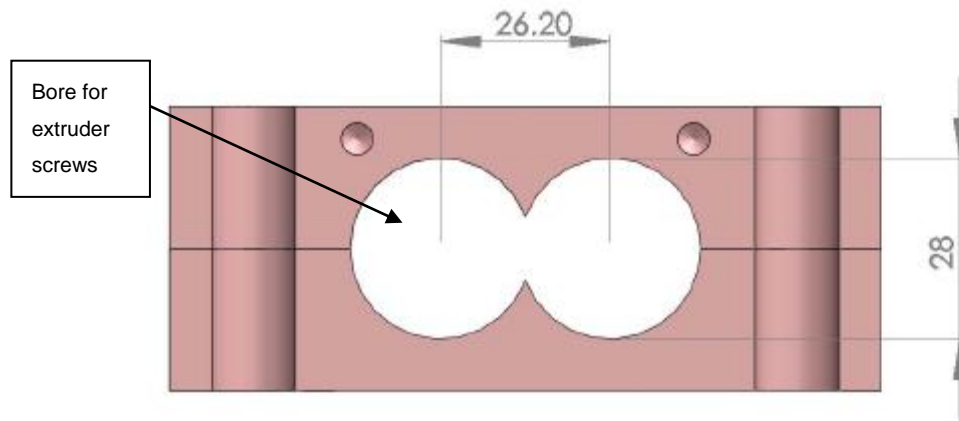


Figure 3-18: Liner bore dimensions (CFAM Technologies (Pty) Ltd, 2011).

In order for the bores of the different liner segments to line up perfectly after installation into the barrel between the liner guides, the liners segments have to be carefully manufactured to a high accuracy and tolerance. A fit is thus calculated for accurate location. The width of the liner is manufactured with a K7/h6 tolerance providing a maximum clearance of $32\mu\text{m}$ and minimum clearance of $-25\mu\text{m}$. Figure 3-19 presents a graphical illustration of the liner segment geometry.

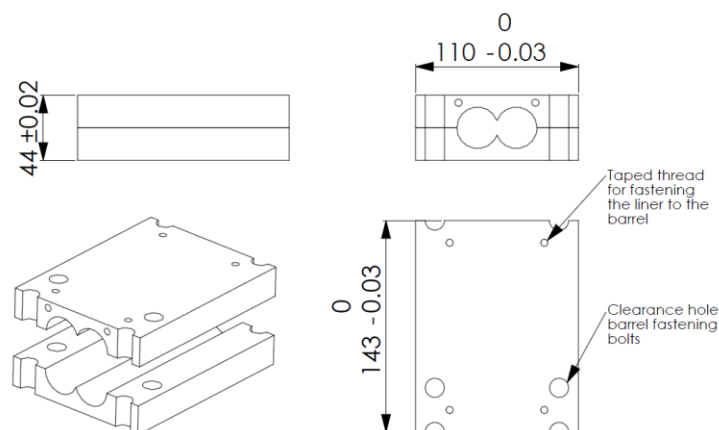


Figure 3-19: Liner inserts geometry (CFAM Technologies (Pty) Ltd, 2011).

3.3.2.3 Knife plate design

The function of the knife plate, as described in Section 2.6.3, is to provide a slight increase in the pressure inside the barrel in order to ensure proper fill of the processing section. Secondly, it assists in the manner in which the product exits the barrel, by projecting flow away from the barrel.

The knife plate is a very simple component. It has 4 basic characteristics:

1. A flat surface facing the screws that causes pressure to increase.
2. An angled front that determines the flow direction.
3. Internal cooling to prevent the knife plate from overheating.
4. Corrosion resistant material that prevents product contamination.

The knife plate is positioned next to the final heating zone of the barrel. Therefore, the temperature of the knife plate is regulated by a final temperature zone. A graphical illustration of the internal cooling of the knife plate is shown in Figure 3-20.

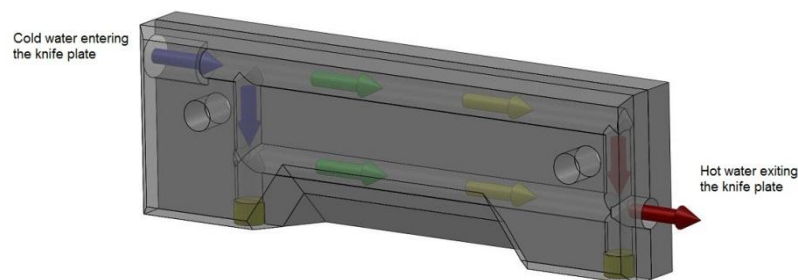


Figure 3-20: Knife plate cooling (CFAM Technologies (Pty) Ltd, 2011).

The angle that provides assistance to the flow direction is 45°. The design is presented in Figure 3-21.

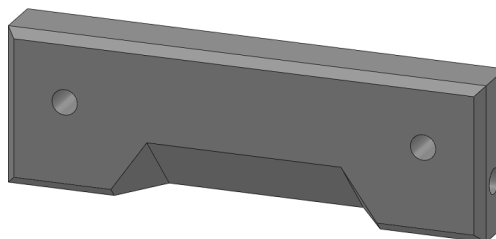


Figure 3-21: Final design of knife plate (CFAM Technologies (Pty) Ltd, 2011).

3.3.3 Final design of twin screw extruder

Having completed the design of the drive and processing sections, the components are assembled to complete the design. Both units are to be fitted on a frame fabricated from grade 350W structural steel and grade 300W steel plate. The assembly is shown in Figure 3-22 and Figure 3-23.

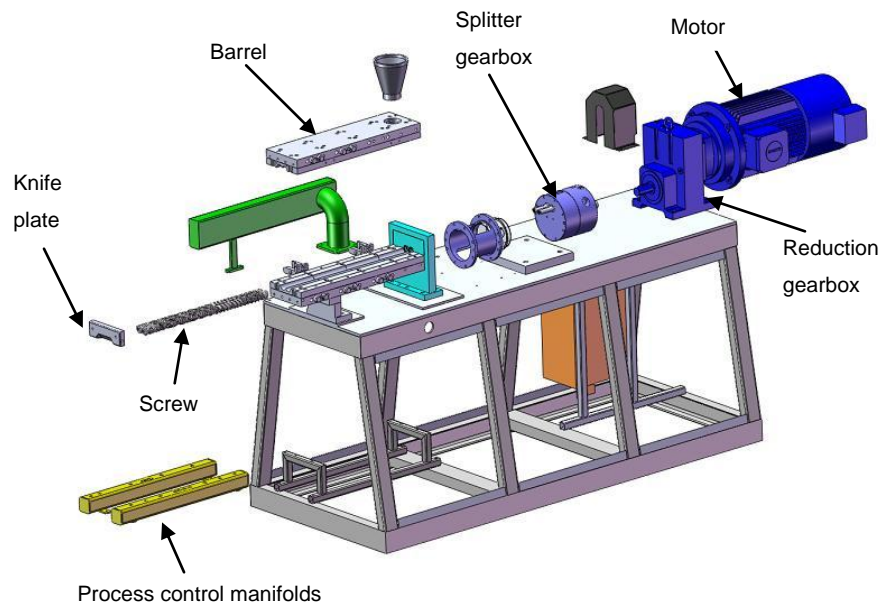


Figure 3-22: Exploded view of 28mm twin screw extruder (CFAM Technologies (Pty) Ltd, 2011).

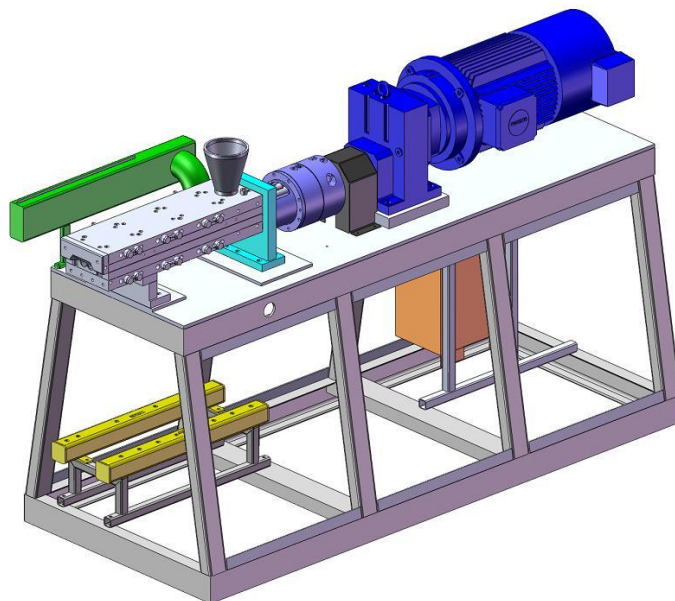


Figure 3-23: Twin screw extruder 28mm (CFAM Technologies (Pty) Ltd, 2011).

3.3.4 Cooling unit design

Introduction

Traditionally the product is rolled into a thin sheet by a pair of chill rollers and laid onto a conveyor belt which is cooled from underneath by means of a sprinkler system. The product is then fed into a kibler⁸ which breaks it into flakes. A schematic illustration of the process is presented in Figure 3-24.

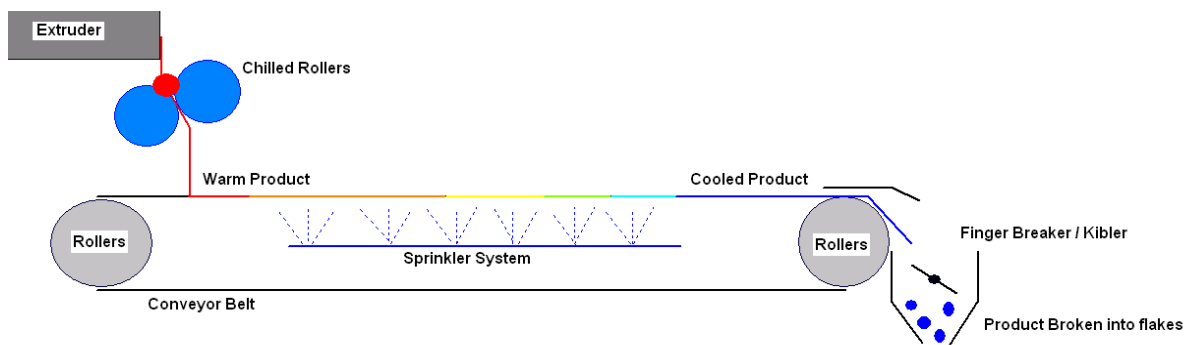


Figure 3-24: Traditional product cooling method.

Section 2.9 stipulates that the two different types of cooling mechanisms have both advantageous and negative properties. The aim here is to provide a single solution as an improvement on both of these cooling units.

⁸Kibler: Apparatus that breaks the powder coating powder film into smaller pieces of about 10mm x 10mm.

Concept

The design is done, based on the concept shown in Figure 3-25.

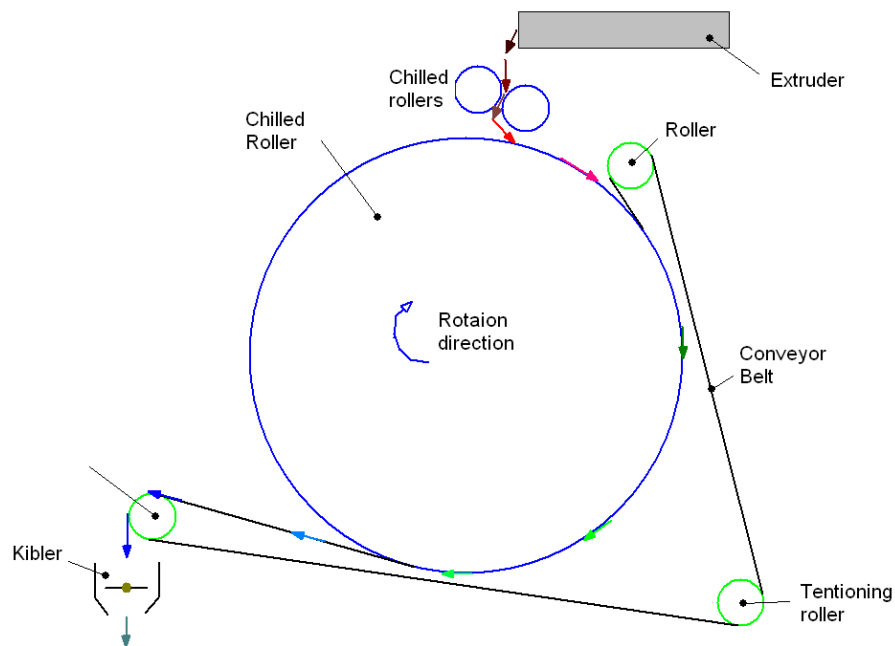


Figure 3-25: Wrapping belt concept.

The large roller is the main heat transfer mechanism. In this concept the conveyor belt is wrapped around this roller by jockey rollers. During production the product is fed between the conveyor and the cooling roller. This should ensure good contact between the product and the cooling roller. The wrapping of the belt around the roller also provides an extended contact distance – in other words, improved contact time which ensures proper cooling of the product.

Finally, the conveyor is used to transport the product to the kibler or finger breaker where it is reduced to flakes for the pulverization process.

Cooling roller unit design

The cooling roller unit design is based on the concept shown in Fig 3-25. The calculations include the cool-down time of the extrudate (powder coating extruded product), the calculation of the roller diameter and the rotation speed of the roller. The design specifications the unit is designed to are presented in Table 3-6.

Table 3-6: Cooling roller design specifications

Desired flake/film thickness	2mm
Extrudate exit temperature at extruder discharge	130°C
Desired temperature of extrudate after chilled roller	40°C
Chilled water input temperature	3 – 5°C

The thermo physical properties of the powder coating extrudate are presented in Table 3-7.

Table 3-7: Thermo Physical properties of extrudate

Thermal conductivity of the extrudate	4 W/m . K
Specific heat of the extrudate at constant pressure	2500 J/kg . K
Density of the extrudate	437 kg/m ³

In order to be able to calculate the roller diameter and speed, it was necessary to calculate the cooling characteristics of a thin layer of the powder coating material (extrudate) in contact with a cooling surface. This was done by the Semi-Infinite Solid Method with constant surface temperature, which is a transient conduction calculation model (Incropera, F., Frank, P. & De Wit, D., 2002). The calculation was done for a number of time increments, where the point of interest was the point furthest away from the cooling surface. The mathematical model followed for the calculation is presented in Equation 3-8.

$$\frac{T_{(x,t)} - T_s}{T_i - T_s} = \operatorname{erf}\left(\frac{x}{2\sqrt{(\alpha \times t)}}\right) \quad [3-8]$$

Where

- $T_{(x,t)}$ is the temperature of the material at a distance x from the surface with constant temperature and t the time in seconds, from the moment the material comes in contact with the surface with constant temperature.
- T_s is the constant temperature of the contact surface.
- T_i is the initial temperature of the material before it comes in contact with the surface which is at constant temperature.
- $\alpha = \frac{K}{\rho \cdot C_p}$, with K the thermal conductivity [$W/m \cdot K$], ρ the density [kg/m^3] and C_p the specific heat at constant pressure [$J/kg \cdot K$].
- $erf()$ is the Gaussian error function.

With a roller surface temperature of 5°C, extrudate temperature of 130°C and material properties from Table 3-7, and using Eq 3-8 it follows that:

$$\frac{T_{(0.002,t)} - 5}{130 - 5} = erf\left(\frac{0.002}{2\sqrt{\left(\frac{4}{(2500 \cdot 437)} \times t\right)}}\right)$$

$$T_{(0.002,t)} = 125 \times erf\left(\frac{0.002}{2\sqrt{3.66 \times 10^{-6} \times t}}\right) + 5$$

The temperature calculation was done on the surface of the product, on the side not in contact with the drum, for time intervals of 0.1sec. Figure 3-26 presents a graphical illustration of the film on the chilled roller.

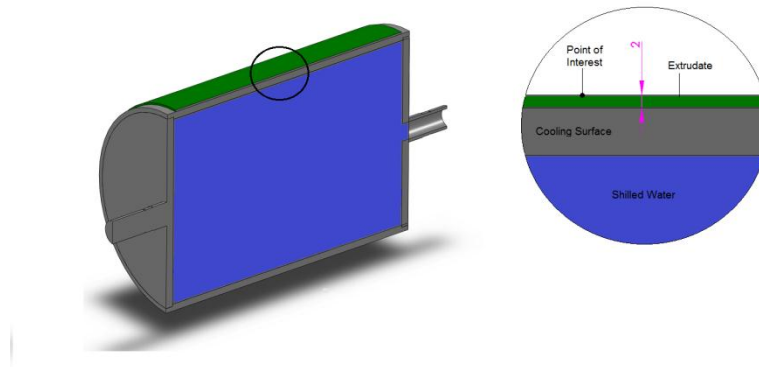


Figure 3-26: Extrudate film on chilled roller.

A plot of the extrudate temperature ($^{\circ}\text{C}$) against time (s) is shown in Figure 3-27.

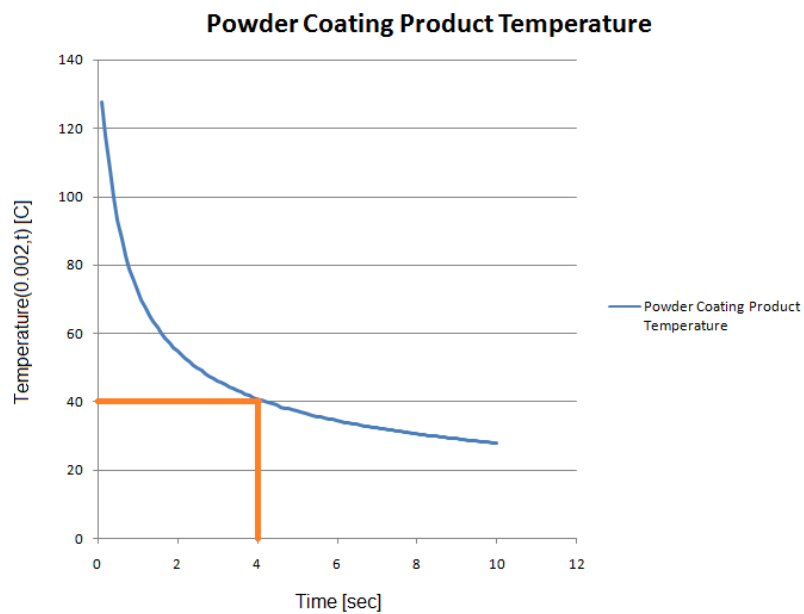


Figure 3-27: Temperature against time plot for the cooling of the extrudate.

From Figure 3-27, the time for the extrudate to cool to 40°C is 4 *seconds*. With the cooling time of the product known, the roller diameter and its rotational speed were calculated.

From the extruder design specifications Table 3-1, the maximum mass flow of the extruder is 70kg/h . With a density of the product of 437kg/m^3 the flow volume, using Equation 3-9, is calculated as:

$$\dot{V}(\text{volume flow}) = \frac{\text{Mass flow}}{\text{Density}} \quad [3-9]$$

$$\dot{V}(\text{volume flow}) = \frac{70}{437} = 0.16 \text{ m}^3/\text{h}$$

$$= \frac{0.16}{3600} = 4.4 \times 10^{-5} \text{ m}^3/\text{s}$$

For the iterative calculation proses, the initial product film width on the roller was chosen as 280mm . The tangential speed the roller needs to turn with a film thickness of 2mm (t_F) and width of 280mm (w_F) is:

$$w_F = 0.280\text{m and } t_F = 0.002\text{m}$$

The sectional area is

$$\begin{aligned} A_F &= w_F \times t_F = 0.28 \times 0.002 \\ &= 0.00056\text{m}^2 \end{aligned}$$

The tangential speed is:

$$v_t = \frac{\dot{V}}{A_F} = \frac{4.4 \times 10^{-5}}{0.00056} = 0.08 \text{ m/s}$$

The distance the product is in contact with the roller is:

$$\begin{aligned} \text{contact distance} &= 0.08 \text{ m/s} \times 4 \text{ s} \\ &= 0.32\text{m} \end{aligned}$$

Figure 3-28 presents the contact angle of the product with the roller according to the current concept. The angle is measured as 170° .

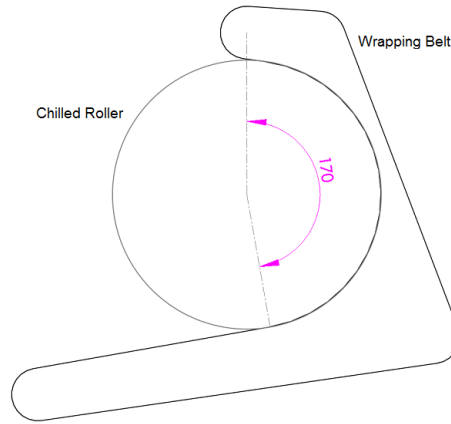


Figure 3-28: Contact angle of product with the chilled roller

The diameter of the roller is calculated by the fraction the circumference of the roller is in contact with the product.

$$\text{contact circumference} = \pi \times D_{\text{ROLLER}} \times \frac{170^\circ}{360^\circ}$$

$$D_{\text{ROLLER}} = \frac{0.32}{(0.47 \times \pi)}$$

$$D_{\text{ROLLER}} = 0.217\text{m}$$

$$= 217\text{mm}$$

The calculated roller diameter is 217mm . For the manufacturing of the roller a standard seamless pipe with diameter of 219.1mm can be used and machined to the required diameter of 217mm . Therefore the chosen film width of 280mm is correct and no further iterations of the calculation is necessary.

The rotational speed of the roller is calculated using the tangential speed v_t and the roller diameter D_{ROLLER} .

$$v_t = \omega \cdot r$$

Where:

- ω is the rotational speed [rad/s]
- r is the roller radius [m]

Thus is the rotational speed of the roller:

$$\begin{aligned}\omega &= v_t/r \\ &= \frac{0.08}{0.1085} = 0.737 \text{ rad/s} \\ &= \frac{0.737 \times 60}{2\pi} \\ &= 7 \text{ rpm}\end{aligned}$$

The layout for the design is presented in Figure 3-29. The tension in the belt is set by an adjustable roller (yellow arrow). From the concept design Figure 3-25, the belt is wrapped around the large chilled roller by means of smaller rollers. In Figure 3-29, the belt extends over the forming roller (red arrow). This is to ensure that the product does not stick to the forming roller.

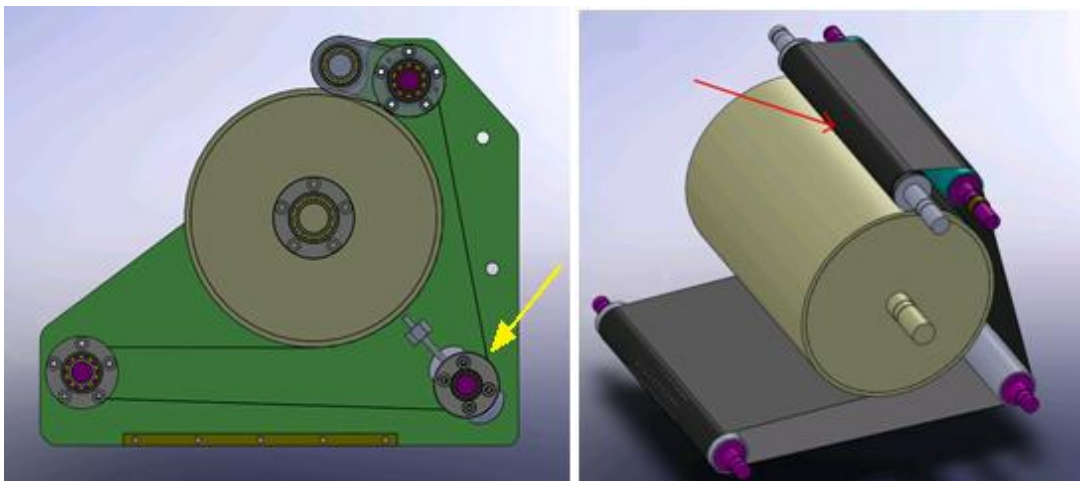


Figure 3-29: Belt wrapped around cooling roller (CFAM Technologies (Pty) Ltd, 2011).

The final design is presented in Figure 3-30.

- The conveyor belt used is a PTFE belt. The advantage of a PTFE belt is that it has an outstanding temperature resistance of up to 260°C, a non-stick surface, strong resistance to chemicals, good dimensional stability and is easy to clean.
- The heat from the product is extracted through the roller surface with chilled water that is circulated through the cooling roller. The water exchange is done by making use of a double passage rotary union as discussed in section 2.10.1.
- The main cooling roller is the only roller that comes in contact with the product. It is important that this roller does not corrode in order to prevent contamination of the manufactured product. Therefore, the roller is manufactured from corrosion resistant steel or as a more cost-effective option, from a mild steel pipe, side plates and shafts. The shafts and roller surface are machined concentric to one another. The roller surface that comes into contact with the product is hard chromed and ground to a very fine finish. This prevents the product from sticking to the roller surface.
- The roller unit is powered by a 3-phase geared motor, which is controlled by a frequency converter to enable the roller system's speed to be adjusted to the throughput of the extruder.

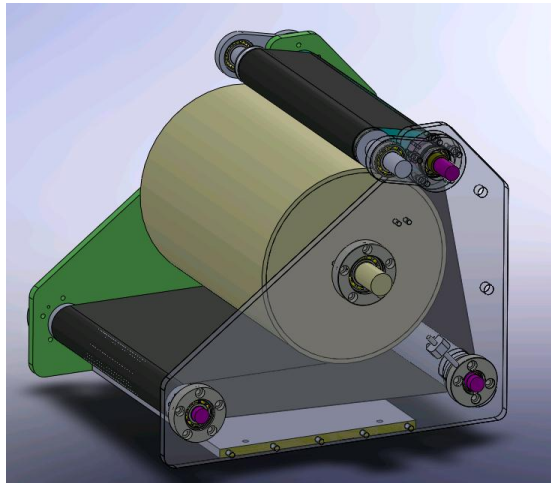


Figure 3-30: Cooling roller system (CFAM Technologies (Pty) Ltd, 2011).

3.4 Conclusion

Geared motor selection

The selection of the geared motor was essentially the selection of the reduction gearbox for the motor, where the motor size was stipulated in the design specifications. The ratio of the gearbox had to be calculated with the splitter gearbox ratio in mind. Therefore, a ratio was chosen for the splitter gearbox. The reduction gear ratio was calculated as 5:1.

Gear geometry

The geometry for the splitter gearbox was calculated with driving factors like output shaft center distance and gear ratio. From these factors the tooth module was calculated as 2 and the number of teeth for the pinion and gear is respectively 25 and 15.

Gear strength

The gear strength was calculated according to the AGMA tooth strength methodology. The gear strength was calculated for tooth failure due to bending and pitting. Pitting fatigue is slowly progressive and failures are not usually catastrophic. Bending fatigue frequently occurs without warning and the resulting damage may be catastrophic. The safety factors for both bending as well as surface durability was calculated as 1.4 and 1.18 respectively, which satisfied the required safety factors from the design specification.

Shaft design

In the shaft design the focus was to determine the deflection of the shaft at the gear location, the bending angle of the shaft at the bearing locations, and finally the static as well as the dynamic safety factors of the shaft.

The deflection of the shaft at the gear location was calculated as $0.01mm$ which is a fraction of the allowable tolerance on the backlash of the gear.

Non self-aligning bearings have limits in which the shaft angle can change. The maximum angle the shaft will reach at the bearing locations is $0.038mm$, which is less than the maximum shaft angle for roller bearings (0.05°).

The safety factors of the shaft were calculated at a location where the shaft is subjected to maximum bending moment, torsional moment and a large stress concentration. The bending moment however, is generated by the tangential and radial forces of the gears, making the bending moment alternating, causing the shaft to fail as a result of fatigue. Both the static and dynamic safety factors were calculated as 5.8 and 2.1 respectively, which satisfy the minimum safety factor of 2 from the design specifications.

Barrel design

The barrel is a clam shell barrel design, providing the capability of opening the barrel for easy cleaning in case the product cures inside the barrel due to mechanical failure or production flaws. The barrel contains 3 temperature control zones in order to create different temperature profiles over the length of the barrel for different products.

Liner inserts are used for the screw cavity of the barrel. These inserts fits accurately in the barrels and can be replaced when worn.

The pressure increase in the barrel is achieved with a knife plate. The knife plate is designed with cooling ports allowing its temperature to be controlled by the final temperature control zone.

Cooling unit design

The cooling unit is designed to form the product to a 2mm thick by 280mm wide sheet and cools it to the specified temperature of 40°C . It is calculated that at a cooling surface temperature of 5°C , the 2mm thick film will reach 40°C in 4sec . A mass flow of 70kg/h will therefore be cooled by a chilled roller with a diameter of 217mm rotating at a speed of 7rpm .

CHAPTER 4

MANUFACTURING AND ASSEMBLY

*The detail design described in **Chapter 3** leads to the manufacturing phase of the extruder.*

Appropriate machining processes have been chosen for every component to optimize between machining quality and manufacturing time.

Finally, the chapter concludes with the fitting of all of the components, providing the developed twin screw extruder with integrated cooling.

4.1 Introduction

The detail design provides 3D rendered models. These models are used to produce manufacturing drawings which are used for the manufacturing of each component of the extruder.

Each component is manufactured by the most suitable process. Each process is carefully chosen depending on the geometric accuracy required, material used and the value of the component. Highly accurate manufacturing processes are expensive, and therefore the manufactured components have to justify the cost.

4.2 Manufacture and assembly

The extruder frame was fabricated from grade 350W structural steel and grade 300W steel plate. Figure 4-1 shows the frame after fabrication. The design drawings for the frame are presented in Annexure A.



Figure 4-1: Extruder frame (CFAM Technologies (Pty) Ltd, 2011).

The purpose of the frame is for accurate mounting of the primary systems that consists of the motor, gearbox, and barrel, as well as the auxiliary systems consisting of the junction box, cooling manifolds, etc.

Components such as liners, barrels, screws and gearbox are geometric accurate components. They were therefore machined with high accuracy on CNC lathes and 3-axis machining centers and wire cutters. Figure 4-2 shows the machining of the splitter gearbox housing on a 3-axis CNC machining center. Annexure A presents detail drawings of the gearbox.



Figure 4-2: Machining of splitter gearbox housing (CFAM Technologies (Pty) Ltd, 2011).

The assembled splitter gearbox is fitted to the backing plate of the barrel and finally fitted to the extruder frame as shown in Figure 4-3.

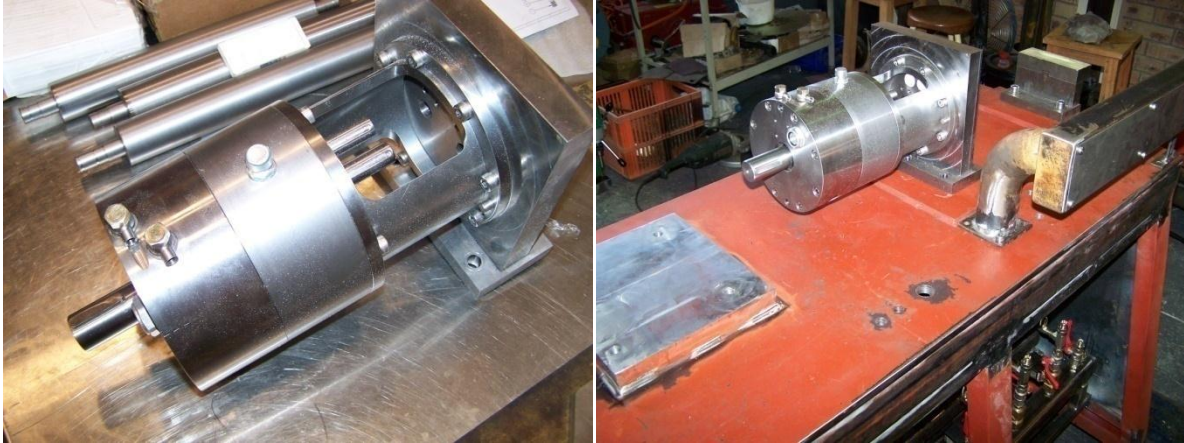


Figure 4-3: Splitter gearbox and Barrel backing plate (CFAM Technologies (Pty) Ltd, 2011).

After assembly of the barrel, it was fitted to the frame as shown in Figure 4-4. Notice the sliding mechanism that compensates for elongation of the barrel on the connection piece to the frame.

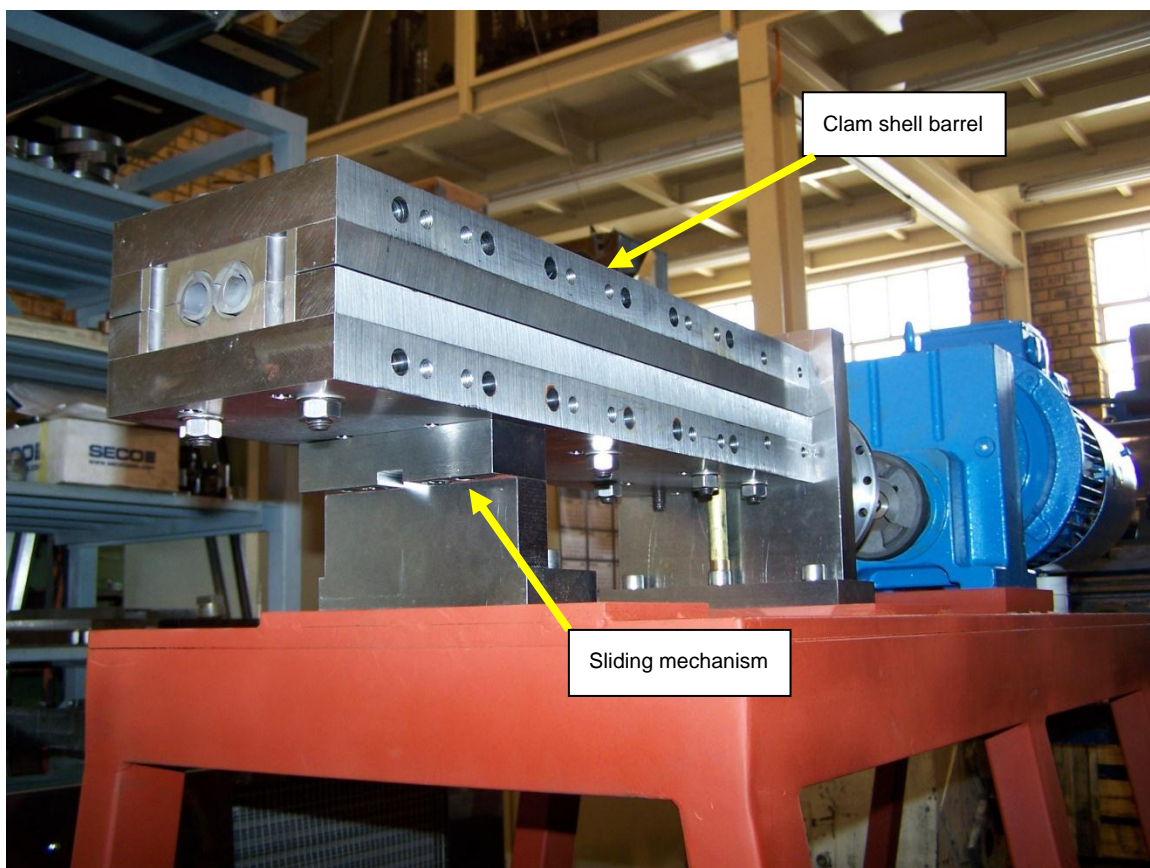


Figure 4-4: Extruder barrel or processing section fitted to the frame (CFAM Technologies (Pty) Ltd, 2011).

The motor, reduction gearbox and splitter gearbox are presented in Figure 4-5. These parts form the drive unit of the machine. The barrel process cooling, process heaters and knife plate form the processing section of the extruder.

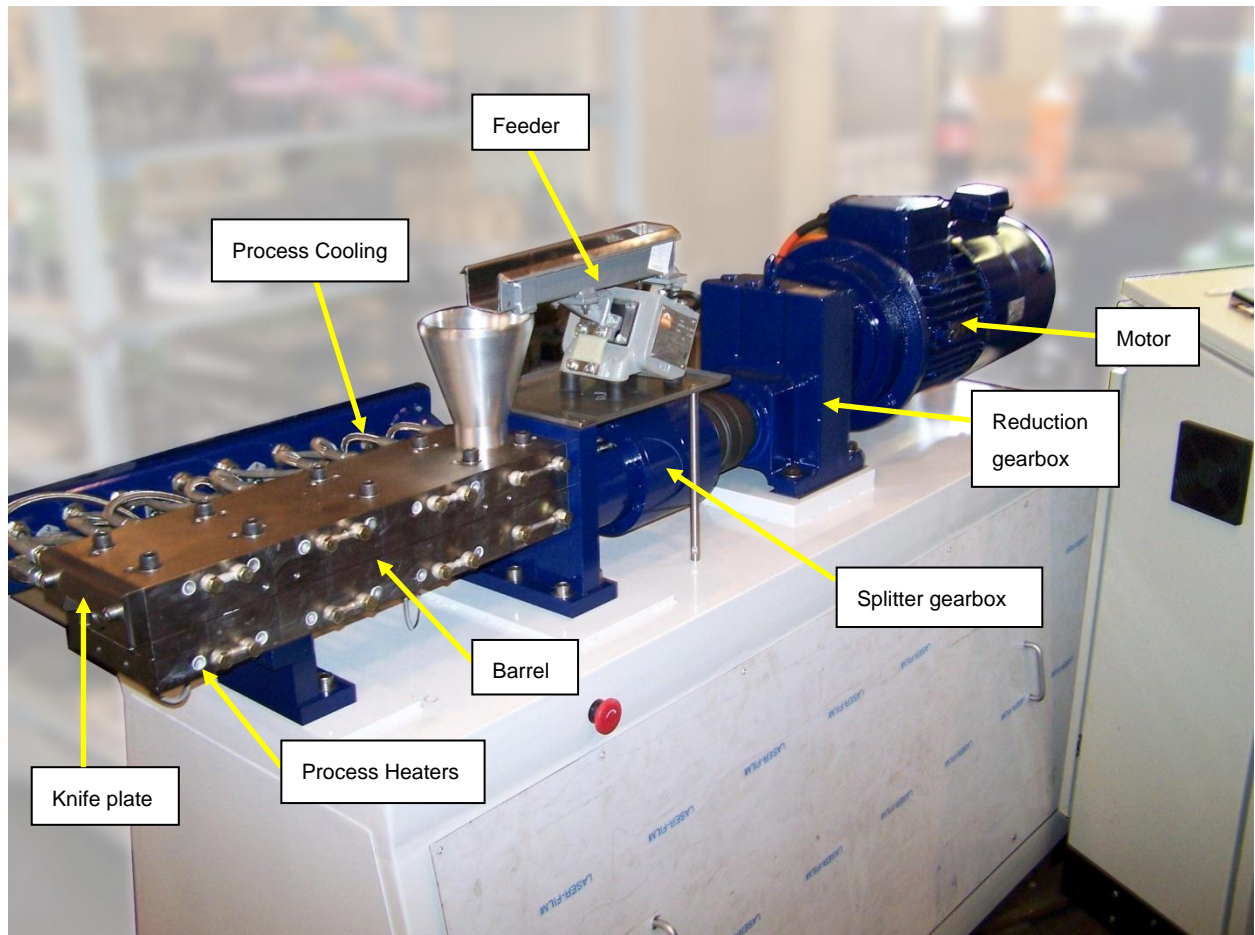


Figure 4-5: Processing section and drive unit of the extruder (CFAM Technologies (Pty) Ltd, 2011).

The basic components of the cooling roller unit are shown in Figure 4-6. The large cylinder is the main cooling mechanism. Notice the hole in the shaft of the roller that is the opening through which the rotary union circulates the water. The conveyor belt is wrapped around the main cooling roller by the guide rollers and tensioning roller. The detail drawings for the main cooling roller are presented in Annexure A.



Figure 4-6: Cooling roller unit components (CFAM Technologies (Pty) Ltd, 2011).

In Figure 4-7 the forming roller is shown holding the wrapping belt at a pre-set distance away from the main roller ensuring that the product is rolled into a uniform sheet. The scraper shown in Figure 4-7 prevents cooled product from re-entering the wrapped belt.

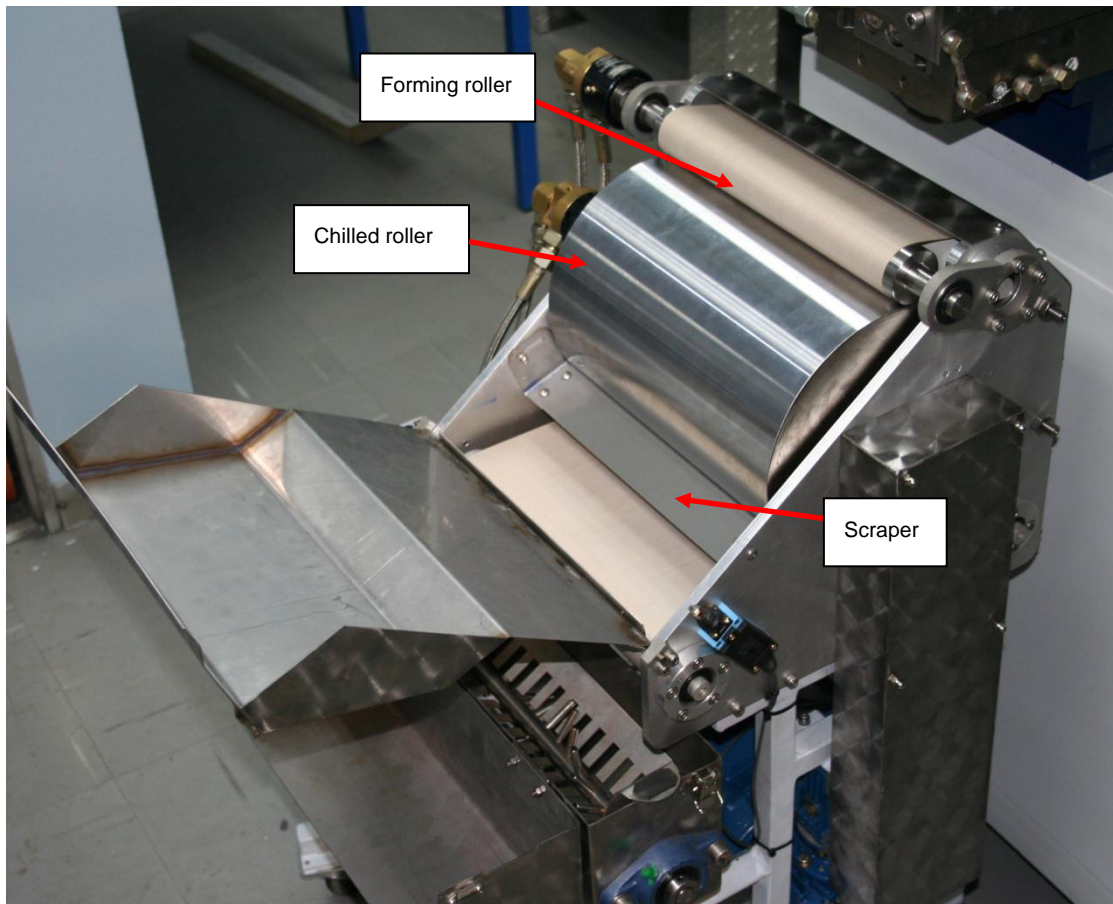


Figure 4-7: Chilled roller unit with installed conveyor belt (CFAM Technologies (Pty) Ltd, 2011).

The completed extruder is shown in Figure 4-8 with the cooling roller unit in front. The panel on the right hand of Figure 4-8 is the control panel of the extruder. The control panel enables the operator to set the desired temperature profile over the barrel, the screw speed, feed rate and cooling roller speed.



Figure 4-8: Twin screw extruder with integrated cooling unit (CFAM Technologies (Pty) Ltd, 2011).

4.3 Conclusions

The twin screw extruder designed during this project was successfully designed and built. The manufacturing process of the extruder is depicted in Figures 4-1 through to 4-8. The machine was commissioned successfully and a good quality product was successfully produced.

CHAPTER 5

TESTING OF THE PERFORMANCE OF A TWIN SCREW EXTRUDER

Part 2

Part 1 of the study concerns the development of a twin screw extruder with an integrated cooling roller system applied in the powder coating manufacturing industry is successfully completed.

Part 2 comprises the evaluation of the performance of a twin screw extruder. The aspects addressed include the understanding of the energy transfer through the extruder processing section and the measuring and evaluation of energy consumption. This section is divided into two chapters namely: 1.) testing of the performance of a twin screw extruder and 2.) testing and evaluation thereof.

Chapter 5 investigates the energy transfer through the extruder. It defines the different types of energy input to the processing section. Finally, it investigates how the energy consumption of an extruder can be measured.

Chapter 6 Contains the test procedure for measuring the energy consumption of an extruder, as well as the results obtained from measuring the energy consumption of an extruder.

5.1 Introduction

Extrusion lines consume a huge amount of energy. The wrong equipment, unsuitable screw configurations, and poor operating parameters and conditions cause even higher energy consumption, poor production and product quality. Therefore, measuring the energy consumption of the different systems in the processing section of an extruder enables the manufacturer to identify possible improvements to the process.

5.2 The energy balance of an extruder

Before an energy balance⁹ can be generated, the system boundaries have to be defined. A system can be defined as any enclosed volume, process, processing equipment, etc., that is of interest – thus the system boundary includes only the processing section. This provides a basis for the derivation of an equation for the transfer of energy into and out of the processing section of the extruder (Mian, R.N., Aldrich, G., 2007). Figure 5-1 shows the chosen boundary.

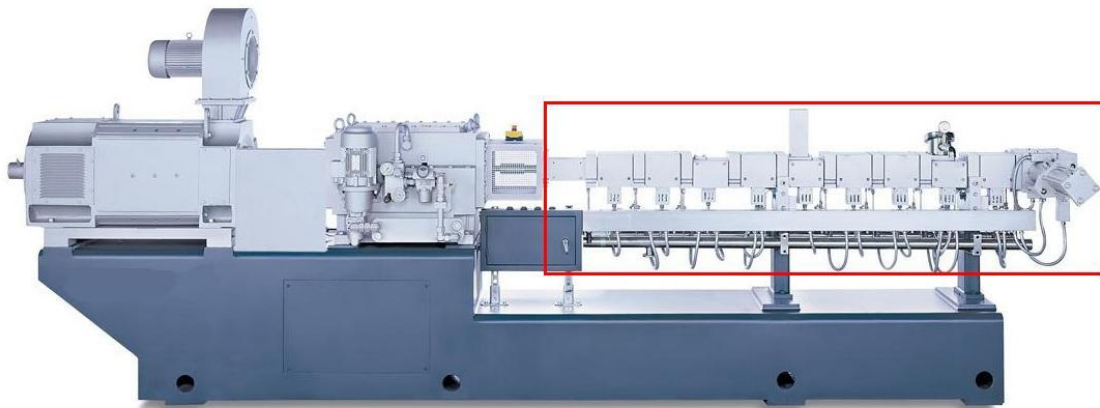


Figure 5-1: System boundary for energy balance Courtesy of (COPERION, 2010).

The extruder is considered as a thermodynamic unit. Thus, for steady-state operation, it means all energy that is introduced into the system must also exit the system. The energy balance consists of the following terms:

- Mechanical energy added by screw rotation.
- Heat transferred through the barrel wall.

⁹Energy balance: A systematic presentation of energy flows and transformations in a system.

- Mechanical energy partly used to increase the pressure of the material.
- Mechanical energy partly converted into heat by viscous dissipation.

In an adiabatic process the thermal energy generated by viscous dissipation (mechanical energy converted into internal energy of the material) results in an increase in the temperature and possible phase change of the product (Janssen, 2002; Kohlgruber, 2007). The energy balance for an extruder is therefore as follows:

$$P_{shaft} = \dot{m}C_p\Delta T + \dot{Q}\Delta p + \dot{m}U_p \quad [5-1]$$

Where:

P_{shaft} is the power delivered to the processing section by the extruder drive section [W]

\dot{m} is the mass flow of the product through the extruder in [kg/h]

C_p is the specific heat capacity of the product [kJ/kg K]

ΔT is the change in temperature during the extrusion process [K]

\dot{Q} is the volume flow of the product through the extruder [m³/s]

Δp is the difference in pressure between the tip of the screws to the intake at the feed port P_a

U_p is the phase change enthalpy per unit weight, which includes the energy needed for chain splitting, cross-linking in protein rich materials and for the generation of new surfaces when the material expands [kJ/kg]

If the temperature is measured after the product has left the die, before any convective and radiation losses occur, the pressure energy is also transferred to heat, then the energy balance can be reduced to:

$$P_{shaft} = \dot{m}C_p\Delta T + \dot{m}U_p \quad [5-2]$$

Assuming that the energy needed for melting solid fractions of the material is much smaller for the heating of the material and evaporation of moisture, the last term in Equation 5-2 can be neglected and the equation reduces to simply:

$$P_{shaft} = \dot{m}C_p\Delta T \quad [5-3]$$

If no evaporation of moisture at the die end occurs, the final product temperature T_f is given as:

$$T_f = T_o + \frac{P_{shaft}}{\dot{m}C_p} \quad [5-4]$$

When the moisture content of fraction f evaporates at the die the equation [5-4] can be modified as:

$$T_f = T_o + \frac{P_{shaft} - f e_w \dot{m}}{\dot{m}C_p} \quad [5-5]$$

Where e_w is the phase change enthalpy for the vaporizing component. For water $e_w = 2257.8 \text{ kJ/kg}$ at 100°C (Janssen, L. 2002; Kohlgruber, K. 2007).

The energy balance in Equation [5-1] is for an ideal situation. There are, however, energy losses due to factors such as evaporation, heat conduction to the extruder frame, convection of heat to air flowing over the barrel as well, as radiation from the barrel.

Another factor that has an effect on the energy balance is temperature profile. Some products have more complex process constraints that require a more complicated temperature profile throughout the barrel. For example, a higher or lower temperature at the kneading section which the kneaders can deliver through mechanical shear, or a low temperature in the die preventing the product from expanding at exit.

The energy balance can thus be written as:

$$P_{shaft} + \dot{H}_{Barrel} = \Delta\dot{U} + \dot{Q}\Delta p + \dot{m}U_p + \dot{H}_{evaporation} + \dot{H}_{Conduction} + \dot{H}_{Convection} + \dot{H}_{Radiation} \quad [5-6]$$

In order to compensate for heat losses and regulation of the temperature profile, external heat sources can be applied to the barrel. (Section 2.6.2.1, Extruder barrel and process control). External heat source in the energy balance (Equation 5-6) is the term \dot{H}_{Barrel} . Thus, the losses can be neglected and the energy balance written as:

$$P_{shaft} + \dot{H}_{Barrel} = \Delta\dot{U} + \dot{Q}\Delta p + \dot{m}U_p \quad [5-7]$$

following

$$T_f = T_o + \frac{P_{shaft} + \dot{H}_{Barrel}}{\dot{m}C_p} \quad [5-8]$$

5.3 Specific mechanical energy

Specific mechanical energy (*SME*) is a characteristic value for every extrusion process (Kohlgruber, K., 2007). It provides an indication of the unit measure of energy required to process a given product. This value is one of the most important values used in extruder scale-up because it gives an indication of the mechanical and geometrical configuration of the processing section and the size required of the drive section of an extruder.

The value of *SME* is determined by measuring the energy consumption of the drive system (*watt*) and throughput (*kg/h*) simultaneously. It can also be calculated by measuring the percentage of torque and rotational speed of the motor. Equations 5-9 and 5-10 are used for the calculation of *SME* for both DC and AC motors, respectively.

$$SME = (PN\tau)t/N_m m \quad [5-9]$$

and

$$SME = \eta P_r t / m \quad [5-10]$$

Where *SME* [*kWh/kg*] is Specific Mechanical Energy, *P* the rated motor power in *kW*. *N* is the motor speed and *N_m* maximum motor speed, both measured in *rotations*⁻¹. Time *t* in *h*, *τ* the percentage of torque and *m* is the mass of the extrudate in *kg*. (Lei, H., 2005; Wójtowicz, A. & Mocicki, L., 2008).

By incorporating *SME* into the energy balance, the energy balance changes to unit measure, simplifying the energy equation and calculations for any throughput, in other words any screw diameter.

Equation 5-1 can be written as:

$$T_{out} - T_{in} = \frac{P_{shaft} - \dot{Q}\Delta p - \dot{m}U_p}{\dot{m}C_p} \quad [5-11]$$

Examine the first term right of the Equation 5-11

$$\frac{P_{shaft}}{\dot{m}C_p} = \frac{P_{shaft}}{\dot{m}} \times \frac{1}{C_p}$$

The units for $\frac{P_{shaft}}{\dot{m}}$ is:

$$\frac{P_{shaft}}{\dot{m}} = \frac{W}{kg/h} = \frac{Wh}{kg}$$

But $\frac{Wh}{kg}$ is the measure for specific mechanical energy (*SME*). By inserting this term and

$\dot{m} = \rho \times \dot{Q}$, the equation can be written as:

$$T_{out} - T_{in} = \frac{SME}{C_p} - \frac{\Delta p}{\rho C_p} - \frac{U_p}{C_p} \quad [5-12]$$

(Kohlgruber, K., 2007).

5.4 Specific thermal energy

Specific thermal energy (*STE*) can be defined as the sum of all the energy losses in the processing section of the extruder (Equation 5-6), as well as the energy contributions of all the raw materials, for example (Janssen, L., 2002):

- Energy contribution from water
- Energy contribution from steam
- Energy contribution from dry mix

STE thus provides an indication of the external thermal input or extraction of energy per unit measure.

The measurement of *STE* is not simple, due to convective and radiation losses to the environment and the heat input and losses from electrical coils or jackets, as well as the heat transferred by direct steam injection or venting.

By introducing *STE* to the energy balance for a non-adiabatic process, Equation 5-8 and the manipulation of 5-12, the energy balance can be written as follows:

$$T_{out} - T_{in} = \frac{SME}{c_p} - \frac{STE}{c_p} - \frac{\Delta p}{\rho c_p} - \frac{U_p}{c_p} \quad [5-13]$$

5.5 Measurement of energy consumption of an extrusion system

Measuring the energy consumption of an extruder provides valuable information regarding the product being manufactured. This information includes production costs and pre-conditioning requirements for optimization of the manufacturing process. It gives a good indication of the correctness of the design and setup (screw configuration, L/D ratio, die configuration, etc.) of the processing section of the extruder, providing the capability for optimizing the processing section.

The energy consumption is measured by measuring the energy consumed by the drive system (mechanical energy) and the process temperature control zones. The process temperature control zones (Section 2.6.2.1) usually consist of two systems, one adding heat to the process and the other extracting heat from the process.

5.5.1 Measurement of energy consumed by the drive system

The drive system consists of the variable speed drive which powers either an AC or DC motor which powers the intermeshing screws that provides mechanical shear in the processing section (Section 2.6.1).

The energy consumption is determined by measuring phase to phase voltage of the supply power (3-phase) to the variable speed drive, as well as the current passing through each of the three supply lines. The value of each current reading should be the same, depending on the electrical balance of the motor. Therefore, for the calculations a mean value can be calculated. The active power consumed by the drive system can then be calculated by:

$$P_a = \sqrt{3} \times V_L \times I_L \times \cos \theta \quad [5-14]$$

Where P_a is the active power consumed [watt], V_L the phase to phase voltage [V], I_L the line current [A] and $\cos \theta$ the power factor of the motor.

5.5.2 Measurement of the energy consumed by the process temperature control zones

The process temperature control zones usually consist of two systems where one adds heat to the process and the other extracts heat from the process.

The addition of heat is typically achieved by electrical heaters distributed between the temperature control zones. These heaters can either be single or 3-phase.

Although the heaters are divided into a number of zones, it is only necessary to measure the total energy consumption of all the heaters.

To determine the energy consumption for a processing section with single phase heaters the following equation is used:

$$P_a = \sum_{i=1}^n [(V \times I)_1 + (V \times I)_2 + \dots (V \times I)_n] \quad [5-15]$$

Where P_a is the active power [watt] consumed by the heater, V is the voltage [V] over the heater and I the current through the heater [A]. n is the number of heaters present.

For the energy consumption for a processing section with 3 phase heaters:

$$P_a = \sum_{i=1}^n [(\sqrt{3} \times V_L \times I_L)_1 + (\sqrt{3} \times V_L \times I_L)_2 + \dots (\sqrt{3} \times V_L \times I_L)_n] \quad [5-16]$$

Where P_a is the active power [watt] consumed by the heater, V_L is the line voltage [V] over the heater and I_L the line current through the heater [A]. n is the number of heaters present.

The measurement of energy consumed by the extraction of energy from the processing section is a bit more dependent on the process that is used for the extraction of energy.

In some cases the heat is extracted by blowing air over the barrel. Determining the consumed energy is very difficult due to the unknown efficiency of the heat transfer from the barrel to the air.

Another method of extracting heat from the barrel is by running chilled water through cavities inside the barrel. The energy consumption for such a system can be determined easily by measuring the temperature difference of the water before it enters and after it leaves the barrel, as well as the flow rate of the water through the barrel. Once these values are captured, the energy extracted from the processing section is determined by:

$$Q = \dot{m}C_p(T_{out} - T_{in}) \quad [5-17]$$

Where Q is the heat energy, extracted from the barrel [watt]. \dot{m} is the mass flow rate of the water passing through [kg/s] and T_{out} and T_{in} is the temperature of the water exiting and entering the barrel, respectively.

5.6 Conclusion

This chapter focused on the energy consumption of the different systems of the processing sections of an extruder. The aim was to get a better understanding of the energy consumed by the extruder, as well as the technique to measure the energy consumption.

Specific mechanical energy (SME) is the amount of mechanical energy used to process a given product. Mechanical energy is converted to heat energy by the rotation of one or more screw sets. The mechanical shear from the screws increases the internal heat of the product through viscous dissipation.

Specific thermal energy (STE) is the amount of energy required to maintain the required temperature of the processing section for extruding a given product. STE is the amount of thermal energy introduced or extracted from the processing section, depending on the amount of heat losses and the amount of mechanical energy input to the system.

Finally the chapter showed how to calculate the energy usage of the drive system as well the thermal energy applied to the system.

CHAPTER 6

TESTING AND EVALUATION

Chapter 5 focused on the theories regarding the evaluation of the performance of a twin screw extruder.

In **Chapter 6** these theories are applied in practice by setting up and measuring the performance characteristics of an extruder.

6.1 Introduction

This chapter starts by explaining how test equipment is used to determine the energy consumption during test runs. It also describes the procedure followed during tests. The chapter explains the interpretation of test data. Finally the energy consumption and efficiency of different mechanical setups of an extruder are determined.

6.2 Setup of test equipment

In order to measure the energy consumption of an extruder, specific measuring equipment needs to be installed onto the machine.

Due to logistical difficulties, the extruder developed in this study could not be used for the testing of the energy consumption therefore an available Baker Perkins APV 2050 twin screw extruder was used as suggested by the study leader.

The APV 2050 extruder is equipped with a 30kW DC motor. The processing section consists of a clam shell barrel with a Length/Diameter (L/D) ratio of 20 and 7 different temperature controlling zones. Process heating is done with cartridge heaters and the cooling with chilled water circulated through the barrel.

Energy consumption is determined by measuring the current supply to the electric drive (power converter) of the drive motor, the current supplied to the cartridge heaters and finally the temperature difference of the cooling water flowing through the barrel, as well as the flow rate. Figure 6-1 presents a graphical illustration of the location of the installed equipment.

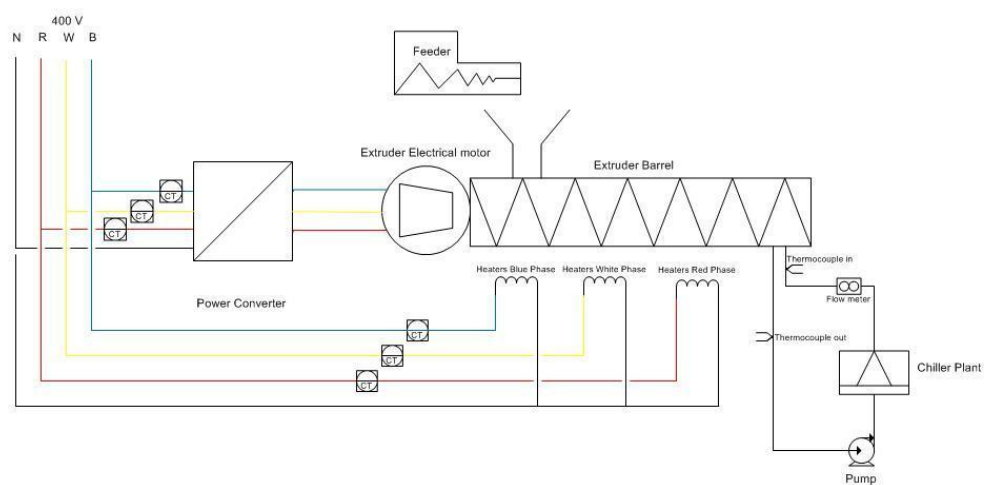


Figure 6-1: Instrumentation for measuring of energy consumption of extruder

The measuring equipment consists of data loggers with current transformers, thermocouples for measuring the water temperature and a flow meter. The instrumentation used were Tinytag Plus (Pt100) temperature measuring units and a SWHlog flow meter, which have built in data logging capability. For the measurement of current to the power converter and barrel heaters, 100A and 50A current transformers were respectively used in conjunction with data loggers.

Take note that the cartridge heaters are single phase, but that they are divided as evenly as possible between the red, white and blue phases of the supply power. This means that in order to attain the total amount of heating power applied to the process, the current has to be measured in each phase and added together.

Photos of the built-in water flow-meter and thermocouples are presented in Figure 6-2. By measuring the difference in temperature of the cooling water flowing through the barrel as well as the mass flow of the water, the cooling power used can be calculated using Equation 5-17 ($Q = \dot{m} \cdot C_p(T_{out} - T_{in})$).



Figure 6-2: Test facility and test equipment.

The current transformers and data loggers are shown in Figure 6-3. The current transformers indicated by Block 1 in Figure 6-3, is used to measure the current through the electric drive. Using Equation 5-14 ($P_a = \sqrt{3} \cdot V_L \cdot A_L$) in Section 5.5.1, the power consumed by the electric motor driving the extruder screws can be calculated and used to determine the Specific Mechanical Energy. The current transformers in Block 2 of Figure 6-3, measures the current through each phase, providing power to the heaters in the processing section of the extruder. With Equation 5-15 ($P = V \cdot I$), and the current known, the power consumed by the heaters can be calculated. With the power consumed by the heaters and the coolers known, it is possible to calculate the Specific Thermal Energy.

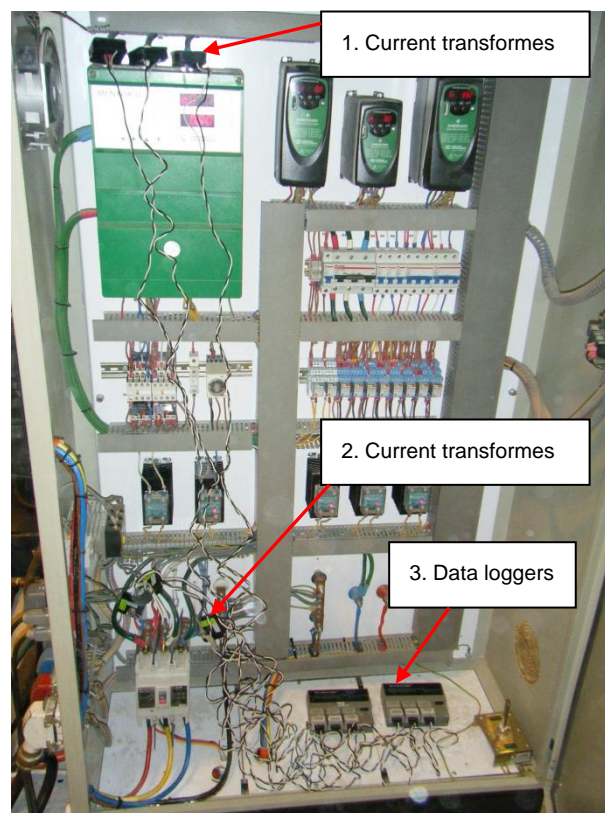


Figure 6-3: Current transformers and data loggers

6.3 Test procedure

As prescribed by the study leader, the test was run by the extrusion of a soy product. The quality of the product is kept constant throughout the test. The tests were conducted with three different screw configurations. Changing of the mechanical setup (screw configuration), changes the amount of mechanical energy the extruder is able to introduce to the extruded product.

The three screw configurations used for the tests are presented in Figure 6-4

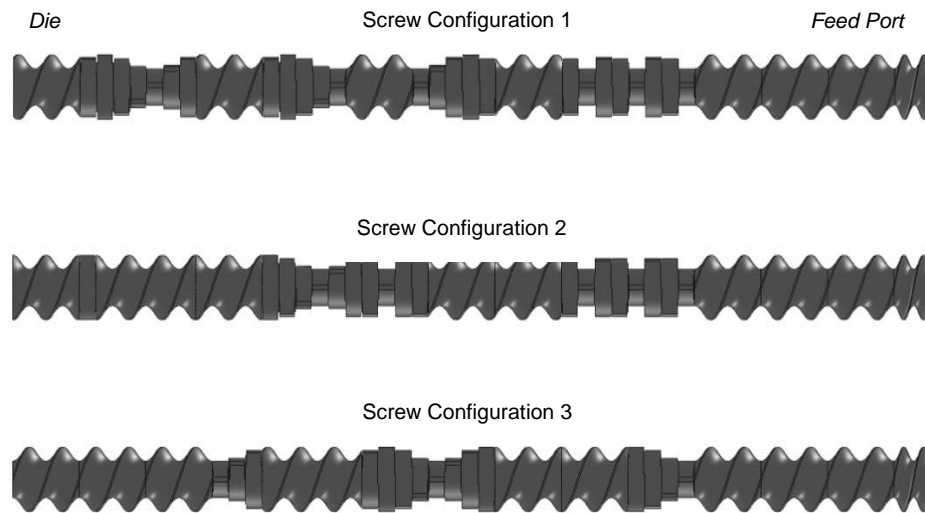


Figure 6-4: Screw configuration 1, 2 and 3.

The temperature profile over the barrel is predicted and set as constant before the initiation of the test. The prediction is based on known values from a similar previously extruded product. Table 6-1 presents the predicted temperature values and the temperature profile over the barrel is shown in Figure 6-5.

Table 6-1: Barrel temperature set values

Zone	Set Temperature
Zone 1 (Feed port)	19°C
Zone 2	60°C
Zone 3	130°C
Zone 4	126°C
Zone 5	132°C
Zone 6	140°C
Zone 7 (Die)	152°C

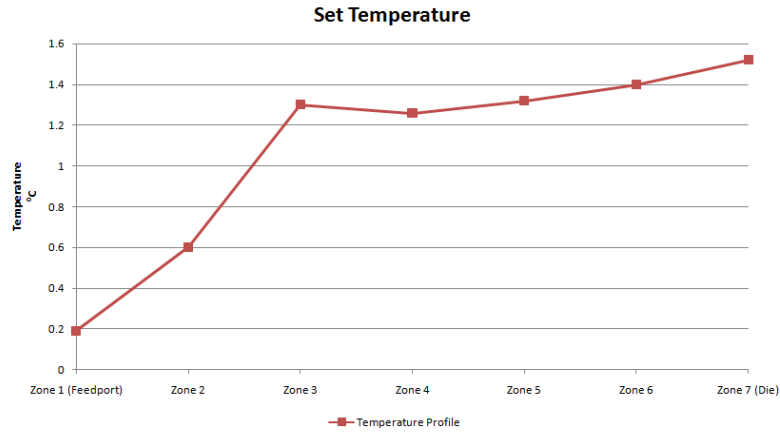


Figure 6-5: Temperature profile over barrel

The temperature profile is kept constant for all the tests in order for the product to be extruded under the same conditions, as well as to demand the same external heat transfer to enable the different results to be compared.

Figure 6-6 presents the test procedure followed. After completion the tests for all three screw configurations, the data was downloaded from the data loggers.

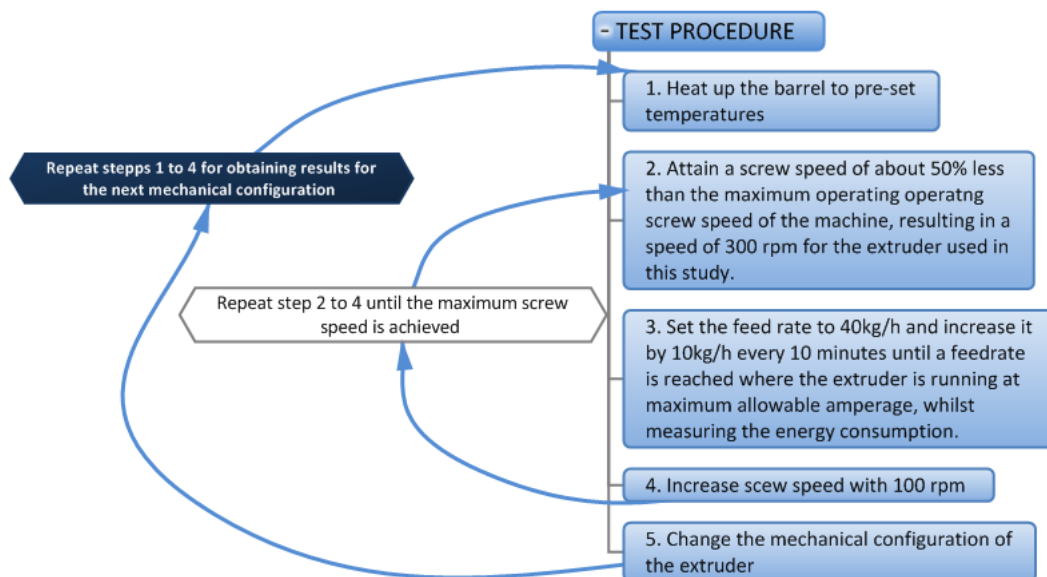


Figure 6-6: Test procedure

The conduction of these tests enabled the ascertainment of the extruder's energy consumption profile at different screw speeds, throughputs and mechanical configurations. These energy consumption profiles were analyzed and compared in order to find the most cost-effective and production enhanced configuration.

6.4 Test results

The test results attained in the extrusion of the product is presented in this section.

6.4.1 Introduction

The tests were conducted as described in Section 6.3. The product used was a soy product. The quality of the product was kept constant, through visual inspection of the appearance of the product.

There were some issues that were identified during the testing. The product had a very low viscosity that resulted in low viscous dissipation of mechanical shear into thermal energy. This prevented the screws from attaining high torque values, resulting in lower energy consumption. It was also quite difficult to cook, which left little room for changes of settings. In general the product could easily be either overcooked or undercooked. It also required a large amount of moisture before texturing could occur. Figure 6-7 shows an example of the product in an overcooked and undercooked state.



Figure 6-7: Extruded product. Overcooked left, undercooked right.

As stated in the test procedure, tests were done with 3 different screw configurations. Configuration 3 however, did not texturize the product at all and the captured data was so inconclusive that no conclusion could be made. Thus the results represent only two of the initial three tests.

The tests from configuration 1 and 2 both produced properly texturized products. The extruded products are shown in Figure 6-8 and Figure 6-9 respectively for configuration 1 and 2.



Figure 6-8: Extruded product from screw configuration 1.



Figure 6-9: Extruded product from screw configuration 2.

6.4.2 Detail results

The first 6 graphs show a comparison of the two configurations for 3 different screw speeds, 400rpm, 500rpm and 600rpm. The graphs show the specific mechanical energy (*SME*), specific thermal energy (*STE*) and the total energy usage (*TEU*) per throughput. All these values are measured in $W/kg.h$. The horizontal scale is the throughput of the extruder in kg/h . The graphs give an indication of the specific energy required to process a given material at different feed rates.

Figures 6-10 to 6-12 indicate that the *STE* decreases with an increase in feed rate. This is primarily due to the percentage fill of the barrel, leading to an increase in specific density of the product. An increase in specific density increases the mechanical dissipation of the product, in

other words an increase in heat. The temperature control zones thus use less energy to obtain the set temperature value.

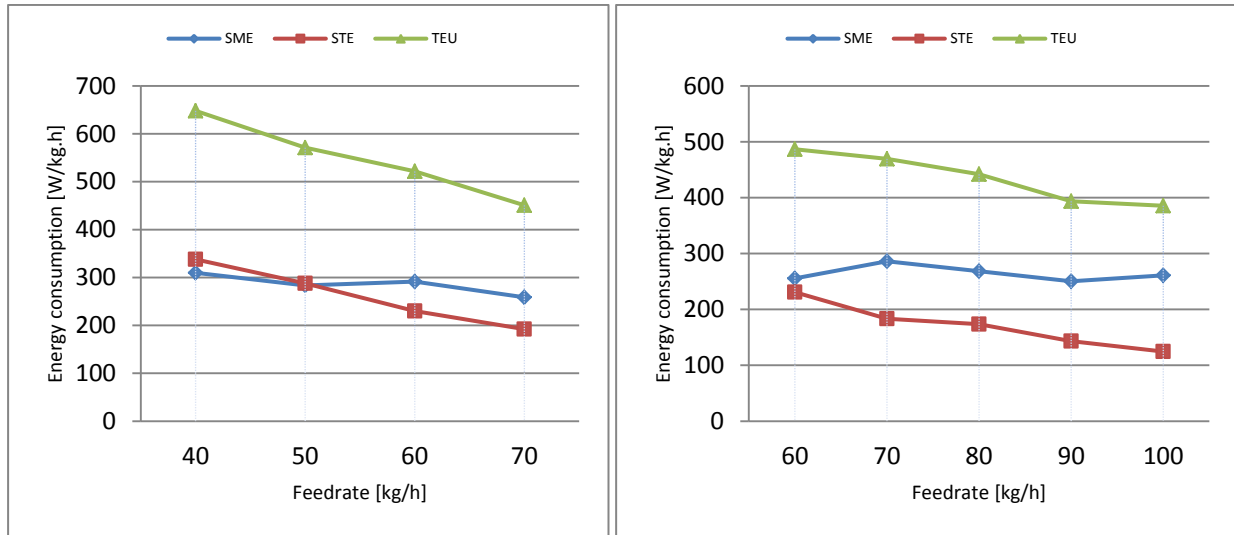


Figure 6-10: Comparison of configurations 1 and 2 at 400rpm.

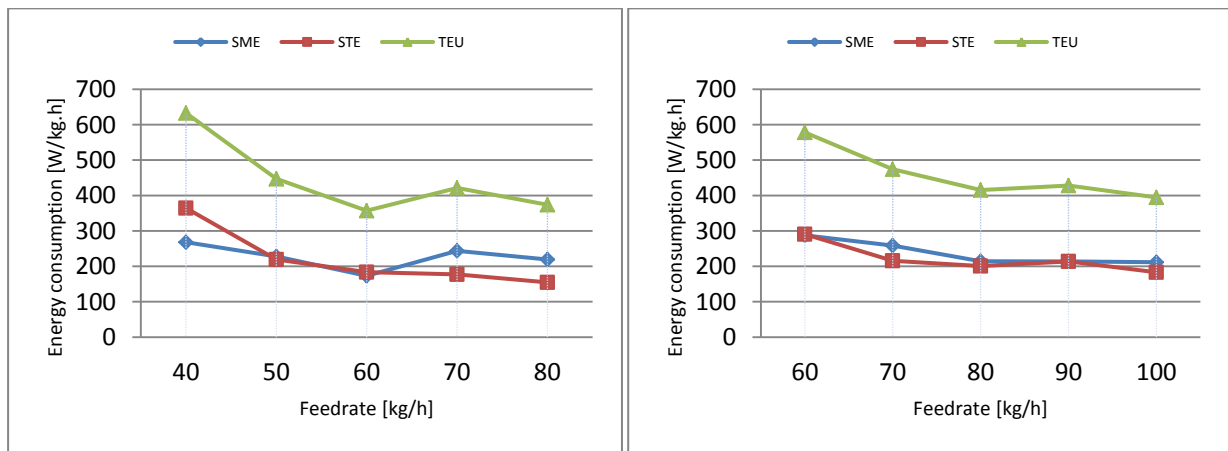


Figure 6-11: Comparison of configurations 1 and 2 at 500rpm.

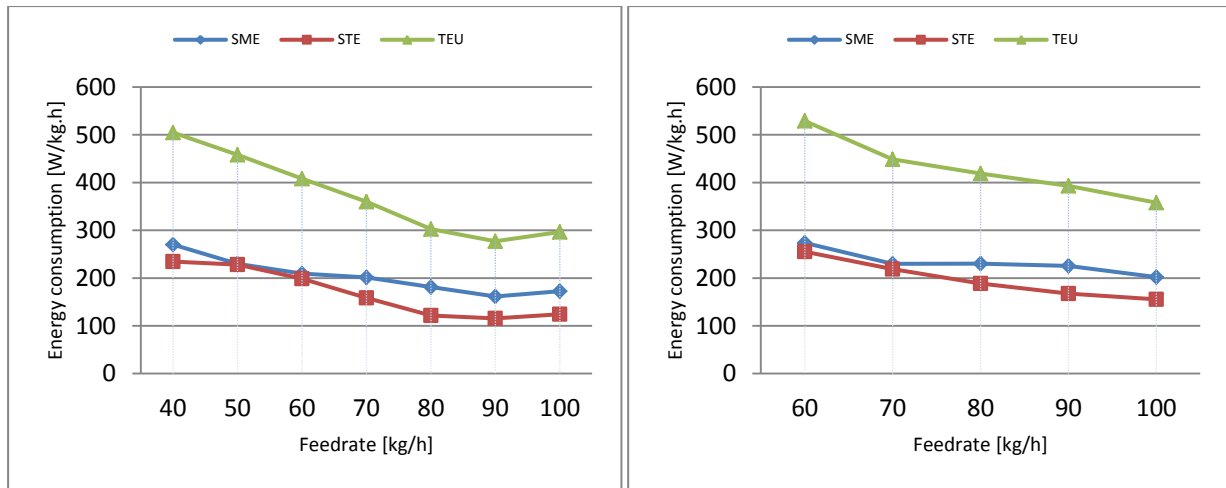


Figure 6-12: Comparison of configurations 1 and 2 at 600rpm.

Overall the total energy usage has decreased with an increase in flow rate, meaning that it is more cost-effective to run the extruder at high feed rates.

Figure 6-13, 6-14 and 6-15 show the *TEU*, *STE* and *SME* for the different screw speeds against the throughput.

The comparison of *STE* for the two configurations shown in Figure 6-13 indicates that the lowest *STE* of 115W/kg.h is achieved in configuration 1 with a screw speed of 600rpm and a feedrate of 90kg/h.

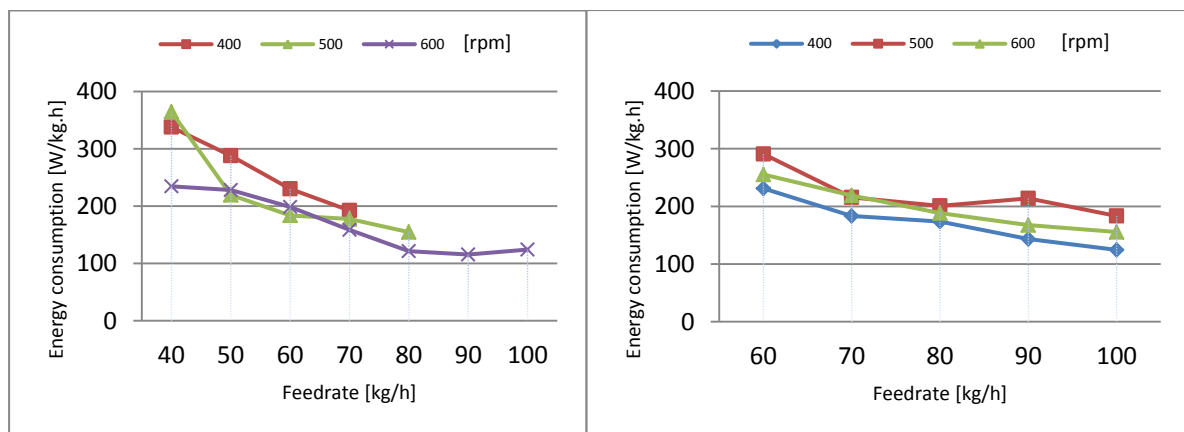


Figure 6-13: Comparison of STE of configurations 1 and 2

Evaluation of the *SME* for the two configurations shows that the mechanical energy needed to process the product is much lower in the first configuration than the second. Configuration 1 also indicates a low *SME* of 162W/kg.h at 90kg/h and 600rpm , where the corresponding *SME* value for Configuration 2 is 225W/kg.h .

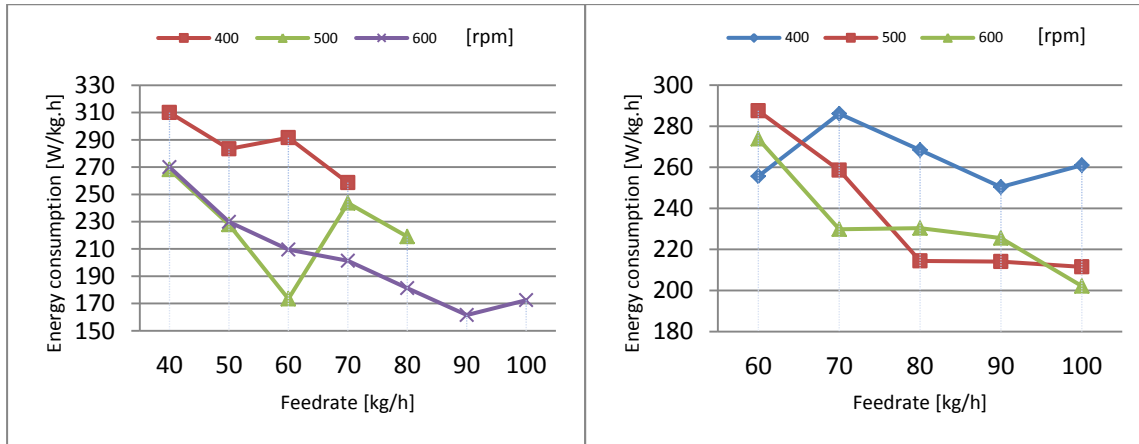


Figure 6-14: Comparison of SME of configurations 1 and 2

Looking at the total energy consumption of the two configurations, configuration 2 does not show a clear difference between the different screw speeds. However, the total energy consumption reduces with an increase in feed rate. The overall energy usage for configuration 1 is less than for configuration 2. As shown in Figure 6-15, the total energy usage reduces as the throughput increases. It also indicates that the most cost-effective operating condition is reached at a speed of 600rpm and a feed rate of 90kg/h .

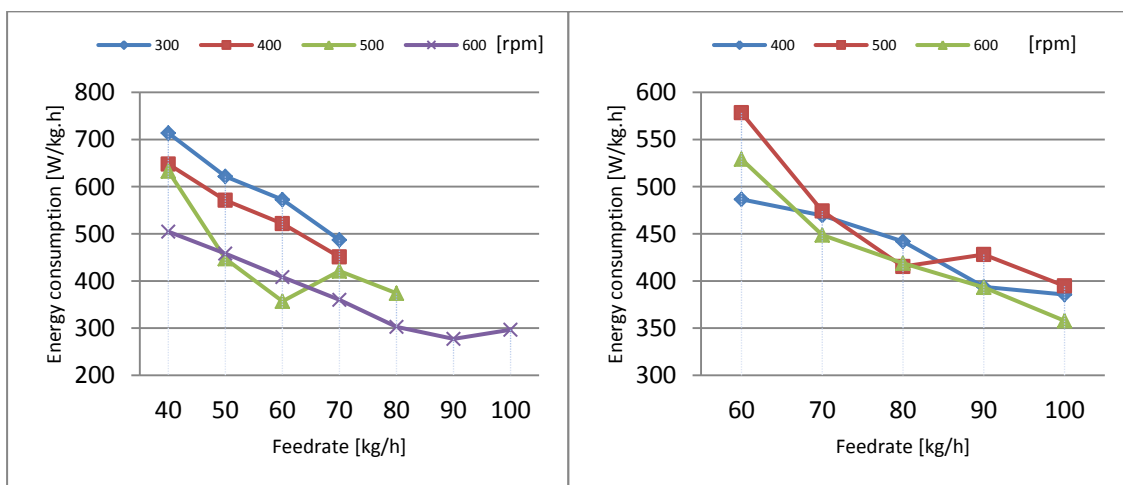


Figure 6-15: Comparison of the total energy usage (TEU) of configurations 1 and 2.

6.5 Interpretation of results

The measurement of the energy consumption of the processing section gives an indication of the power consumption of the extruder for a given product. This is valuable information in order to determine the efficiency in which the product is being manufactured.

What follows are possible assumptions that can be made while evaluating the data.

Specific Thermal Energy (*STE*) values can possibly be explained by the following (can also be in combinations):

- Large temperature losses due to radiation and convection to air flowing over the barrel.
- Low *SME* value, causing high energy input from the elements to provide the correct barrel temperature.
- High *SME* value, resulting in requiring high energy extraction from the barrel by cooling.
- Energy extensive temperature profile demanding steep temperature changes over sections of the barrel.

In Figure 6-13 it is shown that for both configurations, the *STE* decreases with an increase in feed rate. This is an indication that as the percentage fill of the barrel is increased with an increase in feed rate the specific density of the product is increased leading to an increase in mechanical dissipation. The increase in mechanical dissipation increases the heat inside the barrel, causing less energy needed to maintain the barrel at the set temperature values.

As indicated by Figure 6-13 Configuration 1, the *STE* for a rotational speed of 600rpm at a feed rate of 90kg/h is 115W/kg.h, from here it increase to 124W/kg.h at a feed rate of 100kg/h This increase in energy usage, is due to the increase in mechanical dissipation up to a point where the barrel needs to be cooled in order to maintain the set values of the temperature of the barrel. The desirable operating conditions for a low *STE* value for the given product, is thus at a rotational speed of 600rpm and a feed rate of 90kg/h.

Low *STE* is an indication that there is low external energy exchange necessary to acquire the correct barrel temperature. This means that the mechanical energy input is doing the correct amount of work, due to very good process variables which are the combination of the following:

- screw configuration
- screw speed
- feed rate
- L/D ratio
- die design

Specific Mechanical Energy (*SME*) is an indication of the amount of mechanical shear going into the product. The *SME* values can be due to the following and combinations of the following:

- High feed rate causing a highly filled barrel
- High shear screw configuration. A screw configuration with aggressive shear can have a negative effect on production tempo and can easily burn the product
- High viscosity product. A higher viscosity increases the viscous dissipation of mechanical energy to thermal energy.
- Low moisture content
- Increase in screw speed reduces the degree of barrel fill, resulting in a lower torque required.
- Screw speed. An increase in screw speed increases the shear rate on the product inside the barrel. Depending on the product, the shear rate can either have a direct or indirect relationship with the apparent viscosity of the product, which in return has a significant effect on the power required to the extruder screw (Janssen, L. 2002; Chakradorty, P. & Banerjee, S., 2009).
- Increases the shear inside the barrel which results in an increase in *SME*
- Die design. The number of holes and their sizes have an effect on the back pressure inside the barrel which increases the fill of the barrel

Low *SME* is an indication that there is very low energy transferred from the screws to the product. This can be explained by the following:

- Low feed rate. A low feed rate causes an insufficient amount of product inside the barrel
- Low shear, screw configuration
- A product that has a low viscosity
- High moisture content
- Low screw speed

In Figure 6-14 it is shown that the *SME* value for both Configuration 1 and 2 decreases with an increase in screw speed. The decrease in *SME* can be a result of the reduction in the percentage fill of product inside the barrel reducing the required torque to the screws.

The *SME* values for Configuration 1 and 2 in Figure 6-14 decreases with an increase in feed rate. In some cases depending on the activation energy and temperature of the product an increase in mechanical shear can reduce the viscosity of the product, reducing the required torque (Janssen, L., 2002). The increase in feed rate for the tests of both configurations increases the product fill in the barrel increasing the amount of shear, which could be the reason for the reduction in the mechanical energy consumption.

The optimum operating point would be where the feed rate is a maximum and the energy usage is a minimum. A minimum energy usage will be where the *STE* as well as the *SME* values are a minimum.

From the results presented in Figures 6-13 and 6-14 the lower energy usage occurs at high rotation speeds and high feed rates. This can be confirmed by looking at the total energy usage graphs shown in Figure 6-15. For Configuration 1 the minimum energy usage of $277W/kg.h$ is at a screw speed of $600rpm$ and feed rate of $90kg/h$ and for Configuration 2 is $358W/kg.h$ with a screw speed of $600rpm$ and feed rate of $100kg/h$.

The difference between the energy consumption of the two Configurations at a feed rate of $90kg/h$ and rotation speed of $600rpm$ is $81W/kg.h$ in favor of Configuration 1. This indicates that Configuration 1 is a more cost effective configuration to use than Configuration 2.

6.6 Conclusion

Setup of equipment

In order to measure the energy consumption of the extruder it was necessary to equip the extruder with the necessary instrumentation to measure the amount of energy consumed by the processing section. The equipment consists of thermocouples, a flow meter, current transformers and data loggers in order to capture the measured data.

Test procedure

The measurement of the energy usage of the extruder was done by 3 different screw configurations. The configurations were mainly changed by changing the screw configuration. Changing of the mechanical configuration of the extruder changes the amount of mechanical energy the screw set is able to introduce into the product, it also changes the rate of conveying of the material which changes the percentage fill of the barrel.

A procedure in which the tests were conducted is presented as well as the pre-determined temperature values of the barrel, providing a temperature profile over the barrel, setting the basis of the cooking process.

Test results and interpretation of the results

The test results were presented in the chapter in the form of graphs, showing the energy consumption of the processing section against the feed rate, for different screw speeds.

From the test results, both screw configurations presented that the *STE* value decreased with an increase in feed rate. The increase of *STE* values are due to the increase of mechanical dissipation of the product increasing the heat of the product, which reduces the amount of energy needed to maintain the pre-set temperature values of the barrel.

The *SME* values from the results were decreasing with an increase in screw speed. The increase in screw speed increases the shear rate of the product, reducing the viscosity. A reduction in viscosity reduces the required power to drive the screw set.

The total energy usage for extruding the product for both screw configurations, were at its lowest, where the *STE* and *SME* values were low. For Configuration 1 the lowest energy consumption was $277W/kg.h$ at a feed rate of $90kg/h$ and a rotation speed of $600rpm$ and $358W/kg.h$ for Configuration 2 at a $100kg/h$ feed rate. Overall Configuration 1 was the more energy efficient configuration of the two.

In general

This chapter proves that it is possible to measure certain parameters during the extrusion process of a product in order to determine the energy consumed of an extruder for a given product. This valuable information can be used to improve the mechanical setup as well as process parameters for a given product. By reducing both the specific thermal as well as the specific mechanical energy of the extrusion process will reduce the cost per unit weight of the product increasing the profit margin of the product.

CHAPTER 7

CONCLUSIONS AND RECOMMENDATIONS

*This chapter concludes **Part 1** and **Part 2** of the study.*

7.1 Conclusions

This section concludes the findings for the problem statement in chapter 1, as well as the issues to be addressed as described in section 1.3 of chapter 1.

Extruder drive section

The extruder drive system for a small scale extruder was found to be cost-effective and simple if a 3-phase AC geared motor was used, which provided the desired output speed to the splitter gearbox. Secondly, the study proved that a reliable splitter gearbox could be designed and built cost-effectively.

Extruder processing section

The different design considerations for extruder barrels were studied. It was found that the difference in barrel design is determined by the product being processed. For the manufacturing of powder coating powder, the clam shell barrel was the most advantageous to use due to its features allowing easy cleaning.

Cooling roller unit

The design of the cooling roller unit was improved, resulting in a compact machine suitable for laboratory use. It also provided very good heat extraction from the product because of the extended contact time of the product with the chilled roller, due to the wrapping-belt concept.

Final outcome

The final outcome was achieved by the design and manufacturing of a complete 28 mm extruder, capable of processing powder coatings powders.

Twin screw extruder performance testing

In this section the energy consumption of an extruder was investigated. The aspect that was addressed was the understanding of the energy transfer through the extruder processing section. Furthermore, the measuring and evaluation of energy consumption were investigated. A product was manufactured with a twin screw extruder with different mechanical

configurations. The energy consumption was measured and evaluated, indicating the performance difference for different mechanical setups.

7.2 Recommendations

The recommendations for part 1 and 2 of the study are as follows.

Part 1

During operation of the cooling roller unit, it was found that the conveyor belt used, started to tear when solidified product got between the cooling roller and the belt. The belt also lost tracking during operation resulting in a shift to one side. It was found that the traction problem was due to the inability of the belt to stretch. Furthermore, it was found to be a time-consuming task to replace the belt. Thus, the recommendation is made to replace the conveyor belt with a tougher belt with the ability to stretch.

Further studies regarding the twin screw extruder and cooling unit include the following:

- An investigation of the splitter gearbox in order to change the design so that the gearbox will be able to handle large axial thrust from the extruder shafts. This will provide the capability of developing an extruder with a large length to diameter ratio for the compounding of polymers.
- A study regarding the design of the cooling roller unit in order to improve the maintainability of the machine. This will include the ease in which the conveyor belt can be exchanged, as well as tracking of the belt during operation.
- The development of a similar cooling roller unit for large production lines, which then provide an effective product cooling machine that takes up less space as traditional cooling units and requires less maintenance.

Part 2

The tests conducted in Chapter 6 were done with a product that was very difficult to process therefore, the test results could not be established for all possible conditions in the manufacturing process. The recommendation is to re-do the tests with a product that has a higher viscosity and a higher ability to gelatinize. It might be advantageous to do the test on a polymer extruder, because there is no moisture to be added to the product.

Future studies may include the following:

- A study regarding test equipment, to determine the best methods for measuring the required parameters in order to determine an extruder's performance.
- A study regarding the chemical reactions of the product during extrusion in order to better define and interpret the test results.
- The development of an electronic system that can be integrated into any extruder, capable of providing live feedback of the extruder's performance characteristics during operation. This will not only save the manufacture time during the optimization of the mechanical setup of the machine, but will also assist in attaining the best possible operation parameters.

References

AKzo Nobel Powder coatings. Available from: <http://www.akzonobel.com> (Accessed 20 September 2010).

AGMA (American Gear Manufacturing Association. (1988). *Fundamental Rating Factors and Calculation Methods for Involute Spur and Helical Gear Teeth*. Alexandria: AGMA.

AZOM. (2008). *The AZO Journal of Materials Online*. Available from: <http://www.azom.com> (Accessed 12 December 2008).

Bezenka, E. (2000). *Tandem Bearings in twin screw extruder gearboxes*. Available from: <http://www.ina.com> (Accessed 18 September 2010).

Bohler Udeholm. (2011). *Bohler-edelstahl*. Available from: www.bohler-edelstahl.at (Accessed 15 October 2011).

Budinski, K.G. & Budinski, M.K. (2002). *Engineering Materials*. New Jersey: Prentice Hall.

CFAM Technologies (Pty) Ltd. (2011). Available from: www.cfam.co.za (Accessed 22 Oct 2011).

Chakraborty, P. & Banerjee, S. (2009). Optimization of extrusion process for production of expanded product from green gram and rice by response surface methodology. *Journal of Scientific & Industrial Research*, 68(1):140-148.

Classifier milling systems. (2000). *Powder Processing Equipment*. Available from: www.classifiermillingssystems.com (Accessed 22 October 2011).

Deublin. (2006). *Precision rotating connections for water*. Available from: www.deublin.com (Accessed 14 January 2008).

Coperion. (2010). *Coperion-compounding-extrusion*. Available from: <http://www.coperion.com/en/compounding-extrusion> (Accessed 04 Nov 2010).

- Corre, J.B. and Le, A. (2008). Food Extrusion-cooking Technology. *Technical Bulletin*, 1(1):10.
- Dumain, E. *Novel acrylic cure polyester powder coating resin technology*. Available from: www.p2pays.org/ref/10/09793.pdf (Accessed 9 November 2011).
- Extruder gearboxes*. Available from: www.CenturyExtrusion.com (Accessed 20 September 2010).
- Fabrycky, W.J. & Blanchard, B.S. (2006). Advanced System Planning. In *Systems Engineering and Analysis*. New Jersey: Pearson Prentice Hall.
- Fabrycky, W.J. & Blanchard, B.S. (2006). Detailed Design Requirements. In *Systems Engineering and Analysis*. New Jersey: Pearson Prentice Hall.
- Fabrycky, W.J. & Blanchard B.S. (2006). Development, Product, Process, and Material Specifications. In *Systems Engineering and Analysis*. New Jersey: Pearson Prentice Hall.
- Fabrycky, W.J. & Blanchard, B.S. (2006). System Specification. In *Systems Engineering and Analysis*. New Jersey: Pearson Prentice Hall.
- Frame, N.D. (1993). *The Technology of Extrusion Cooking*. New York: Springer.
- SKF. (2010). *SKF rating life*. Available from: www.skf.com (Accessed 28 October 2010).
- Harper, M.J. (1981). *Extrusion of Foods*. Florida: CRC Press.
- Hensen, F. (1997). *Plastics Extrusion Technology*. New York: Hanser.
- Incropera, F.P. & De Wit, D.P. (2002). *Fundamentals of Heat and Mass Transfer*. Hobogen: John Wiley & Sons.
- Janssen, L., Moscicki, L. & Mitrus, D. (2002). Energy aspects in food extrusion-cooking. *International agrophysics*, 16(3):191-196.

Janssen, L.P.B.M. & Van Zuilichem, D.J. (1980). *Rheology of reacting biopolymers during extrusion*. New York: Plenum Press.

Karwe, R. & Godavari, J. (1997). Accurate measurement of extrudate temperature and heat loss on a twin-screw extruder. *Journal of Food Science*, 62(2):367-372.

Tiger Coatings. Available from: <http://tiger-coatings.com/index.php?id=368&L=1> (Accessed 28 September 2011).

Kohlgruber, K. (2007). *Co-Rotating Twin Screw Extruders*. Munich: Hanser.

Lei, H., Fulcher, G., Ruan, R. & Van Lengerich, B. (2005). SME-Arrhenius Model for WSI of Rice Flour in a Twin-Screw Extruder. *Cereal Chemistry*, 82(5):574-581.

Levin, L. (1997). Estimating moisture flash upon discharge from an extruder die. *Cereal foods world*, 42(3):144.

Mccauley, C. (2000). *Machinery's Handbook*. New York: Industrial press.

Mian, R.N. (2009). *The role of extrusion technology on feed safety and hygiene*. Paper presented at the 17th Annual ASAIM SEA Feed Technology and Nutrition Workshop: Hue, Vietnam.

Mian, R.N. & Aldrich, G. (2007). *Extruders and expanders in pet food, aquatic and livestock feeds*. Madison: Agrimedia.

Micro Powder Tech. Available from: <http://www.micropowdertech.com> (Accessed 05 Aug 2010).

Mitrus, M. (2005). Changes of specific mechanical energy during extrusion cooking of thermoplastic starch. *Commission of Motorization and Power Industry in Agriculture*, 5(1):152-157.

- Baker Perkins. (2006). *Production Extruders for Powder Coatings*. Available from: www.bakerperkinsgroup.com (Accessed 05 April 2010).
- Potente, J.L., Helmut & White. (2003). *Screw Extrusion*. Munich: Hanser.
- Rapp, P. (2004). *Engineers Black Book*. Perth: Pat Rapp Enterprises.
- Rauwendaal, C. (2001). *Polymer Extrusion*. Munich: Hanser.
- Shigley, J.E., Mischke, R.C. & Budynas, R.G. (2004). *Mechanical Engineering Design*. New York: McGraw-Hill.
- Smith, E.H. (2000). *Mechanical Engineer's Reference Book*. Lancashire: Reed Educational and Professional Publishing Limited.
- Solomon, S. (1999). *Understanding variable speed drives*. Available from: http://ecmweb.com/mag/electric_understanding_variable_speed_3/ (Accessed 06 June 2010).
- Superior bearings for extruder gearboxes*. Available from: www.gearsolutionsonline.com (Accessed 08 September 2010).
- Special steels*. Available from: <http://www.specialsteels.co.za> (Accessed 06 October 2011).
- Spectra Consultech*. Available from: <http://www.indiamart.com/spectra-consultech/#profile> (Accessed 2 August 2010).
- Talco Inc*. Available from: <http://www.rotaryunions.net/index.htm> (Accessed 22 October 2011).
- Van Niekerk, W. (2008). *Development of an multi-purpose twin-screw extruder*. Unpublished masters thesis. Potchefstroom: North-West University.
- White, J.L. (1991). *Twin Screw Extrusion Technology and Principles*. Munich: Hanser.

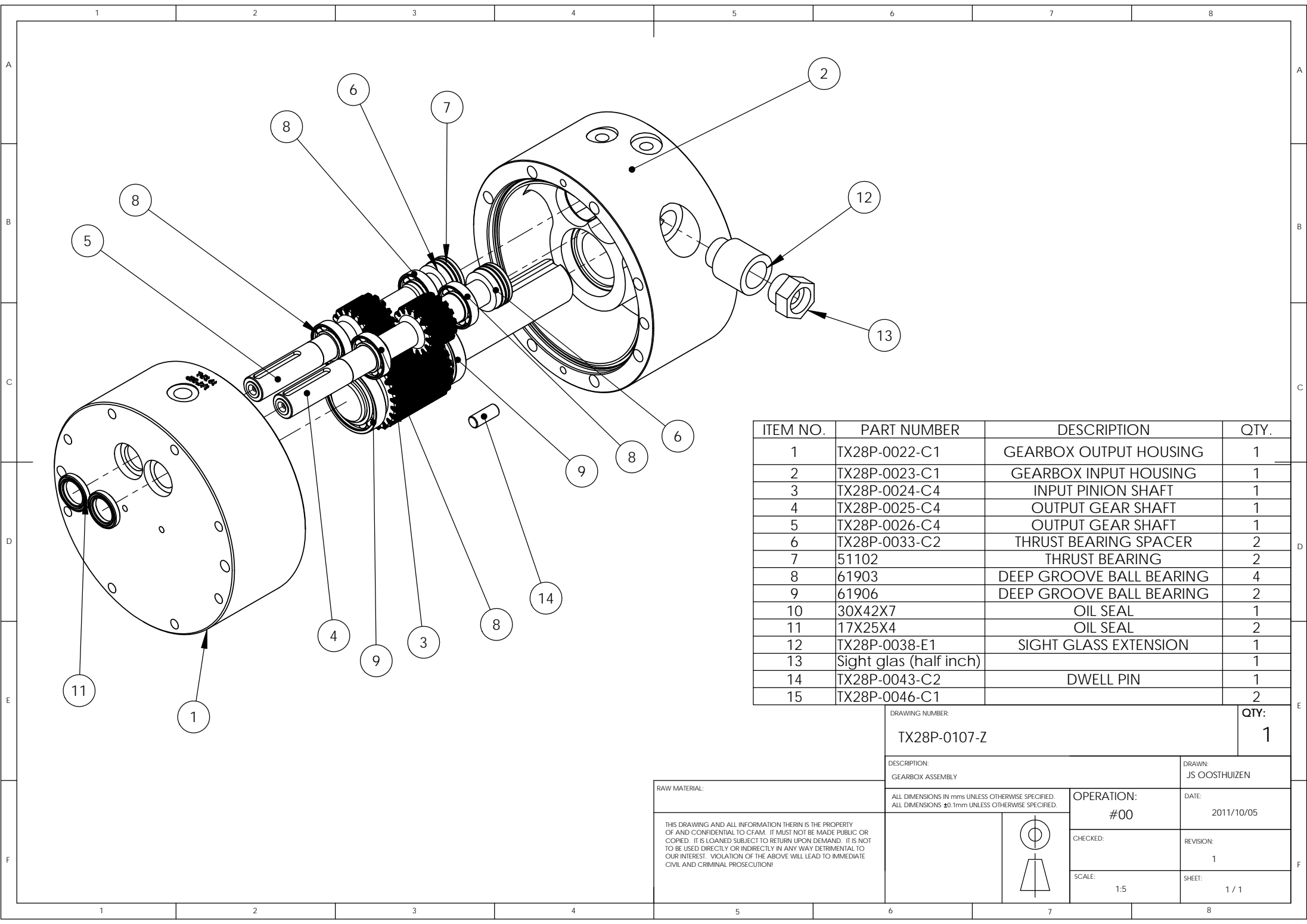
Wiedmann, W. & Strobel, E. (1991). Compounding of thermoplastic starch with twin-screw extruders. *Starch*, 43(4):138-145.

Wójtowicz, A. & Mocicki, L. (2008). Energy consumption during extrusion-cooking of pre-cooked pasta. *Commission of Motorization and Power Industry in Agriculture*, 8(1):311-318.

Zobon conveyor belt company. Available from: <http://www.china-ptfebelt.com> (Accessed 7 October 2011).

ANNEXURE A

Design drawings

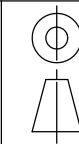


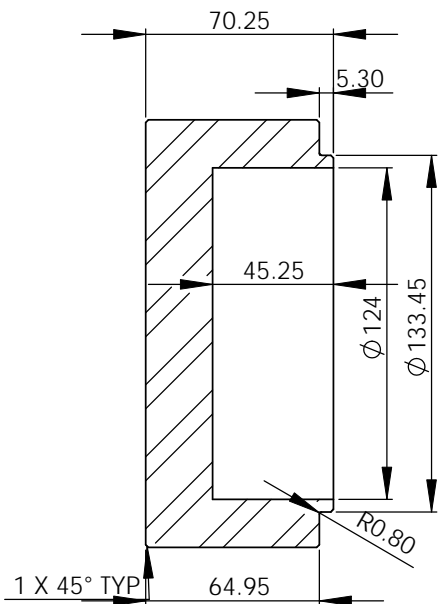
ITEM NO.	PART NUMBER	DESCRIPTION	QTY.
1	TX28P-0022-C1	GEARBOX OUTPUT HOUSING	1
2	TX28P-0023-C1	GEARBOX INPUT HOUSING	1
3	TX28P-0024-C4	INPUT PINION SHAFT	1
4	TX28P-0025-C4	OUTPUT GEAR SHAFT	1
5	TX28P-0026-C4	OUTPUT GEAR SHAFT	1
6	TX28P-0033-C2	THRUST BEARING SPACER	2
7	51102	THRUST BEARING	2
8	61903	DEEP GROOVE BALL BEARING	4
9	61906	DEEP GROOVE BALL BEARING	2
10	30X42X7	OIL SEAL	1
11	17X25X4	OIL SEAL	2
12	TX28P-0038-E1	SIGHT GLASS EXTENSION	1
13	Sight glas (half inch)		1
14	TX28P-0043-C2	DWELL PIN	1
15	TX28P-0046-C1		2

DRAWING NUMBER: TX28P-0107-Z		QTY: 1	
DESCRIPTION: GEARBOX ASSEMBLY		DRAWN: JS OOSTHUIZEN	
ALL DIMENSIONS IN mms UNLESS OTHERWISE SPECIFIED. ALL DIMENSIONS ± 0.1 mm UNLESS OTHERWISE SPECIFIED.		OPERATION: #00	DATE: 2011/10/05
		CHECKED:	REVISION: 1
		SCALE: 1:5	SHEET: 1 / 1

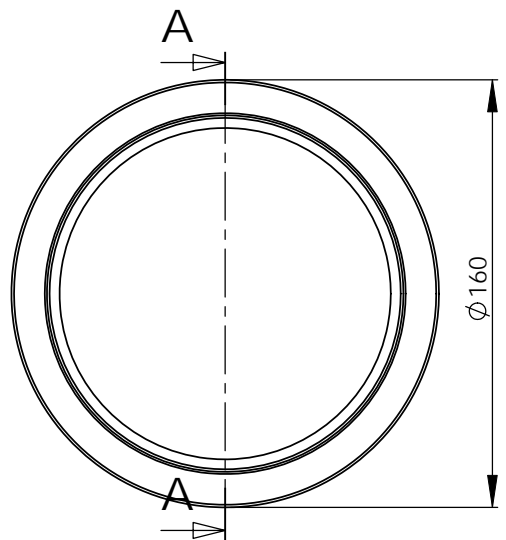
RAW MATERIAL:

THIS DRAWING AND ALL INFORMATION THERIN IS THE PROPERTY OF AND CONFIDENTIAL TO CFAM. IT MUST NOT BE MADE PUBLIC OR COPIED. IT IS LOANED SUBJECT TO RETURN UPON DEMAND. IT IS NOT TO BE USED DIRECTLY OR INDIRECTLY IN ANY WAY DETRIMENTAL TO OUR INTEREST. VIOLATION OF THE ABOVE WILL LEAD TO IMMEDIATE CIVIL AND CRIMINAL PROSECUTION!

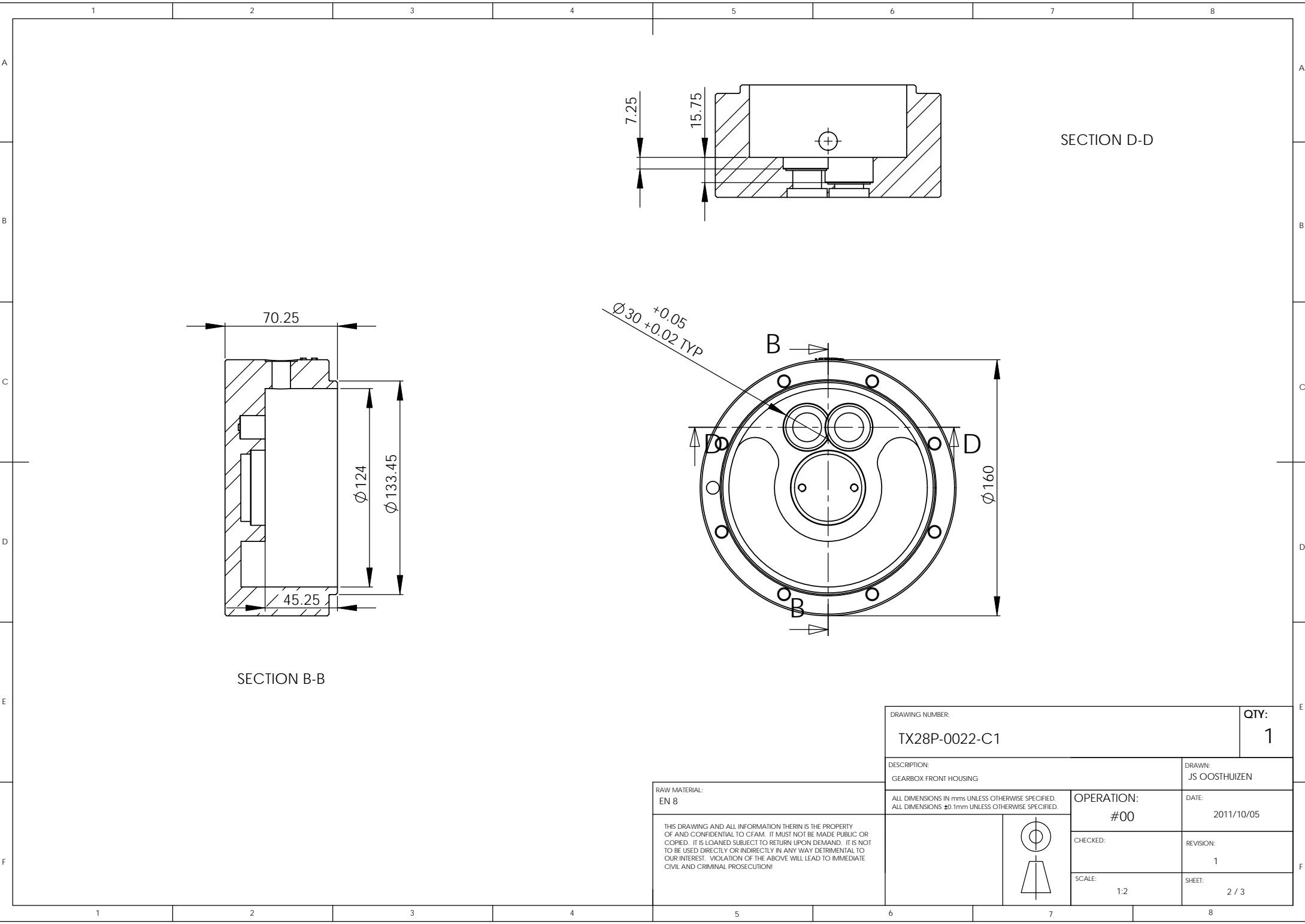




SECTION A-A



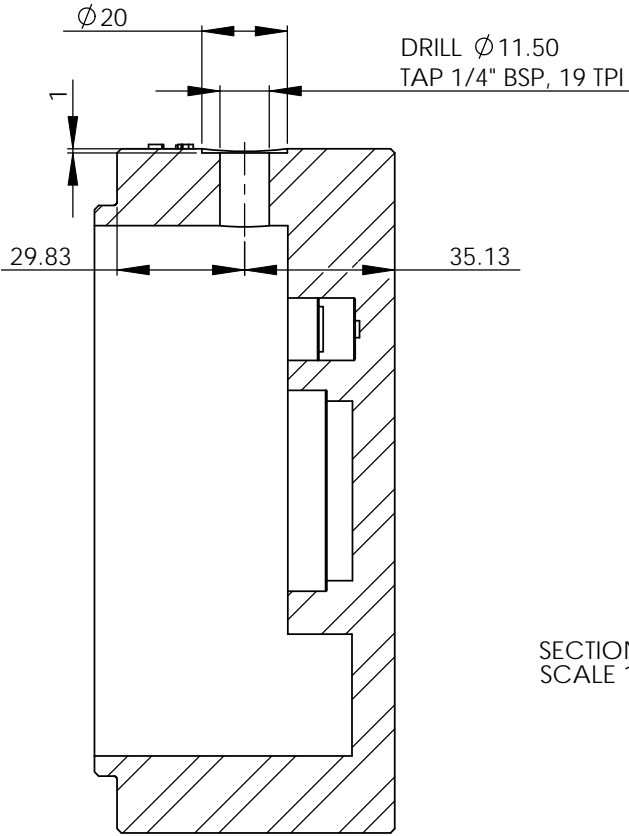
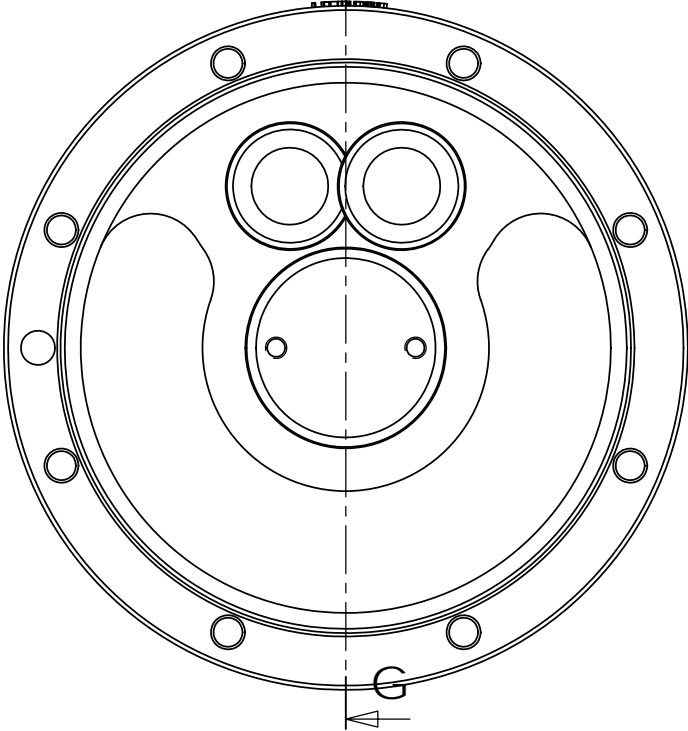
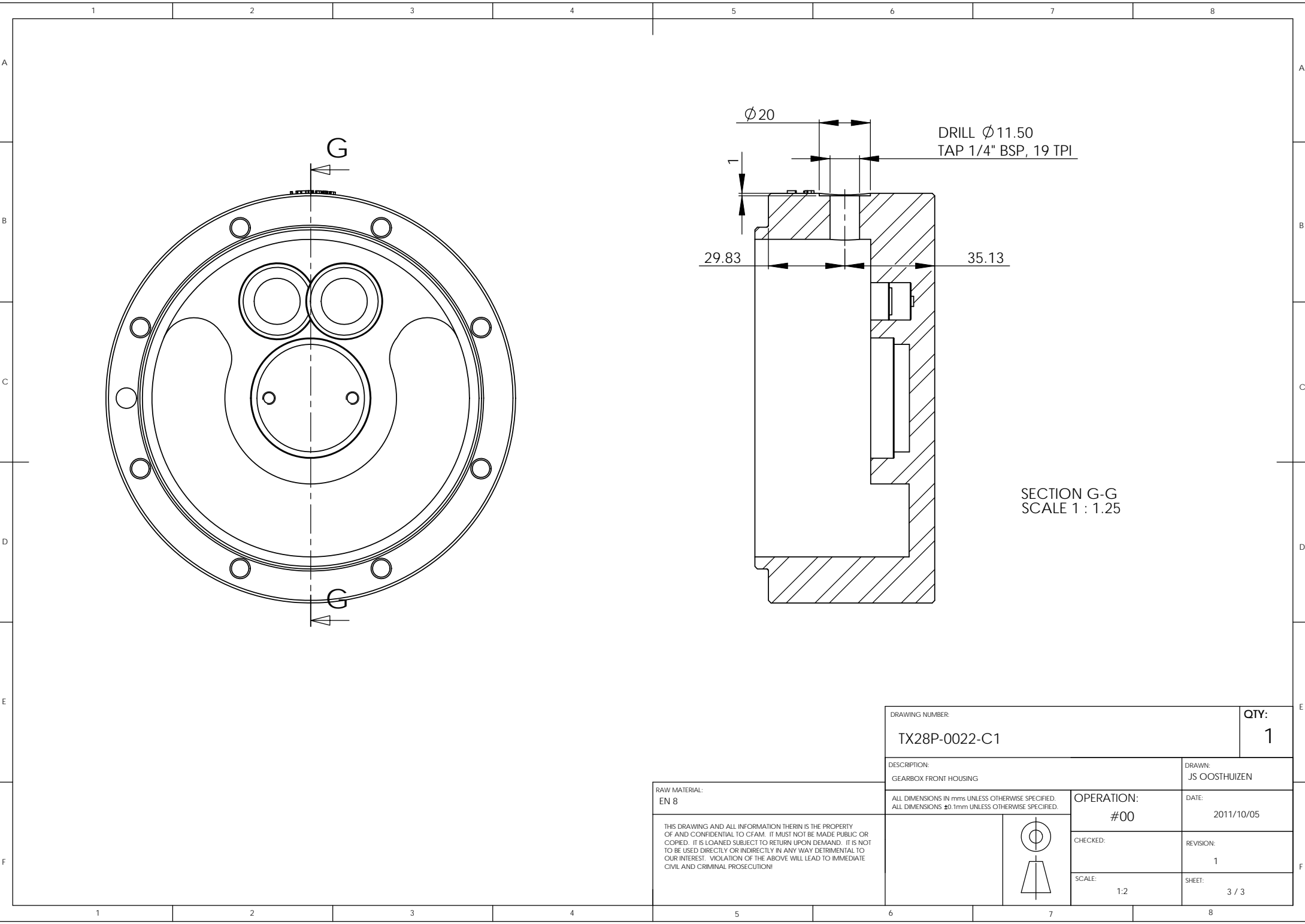
RAW MATERIAL: EN 8		DRAWING NUMBER: TX28P-0022-C1		QTY: 1	
THIS DRAWING AND ALL INFORMATION THERIN IS THE PROPERTY OF AND CONFIDENTIAL TO CFAM. IT MUST NOT BE MADE PUBLIC OR COPIED. IT IS LOANED SUBJECT TO RETURN UPON DEMAND. IT IS NOT TO BE USED DIRECTLY OR INDIRECTLY IN ANY WAY DETRIMENTAL TO OUR INTEREST. VIOLATION OF THE ABOVE WILL LEAD TO IMMEDIATE CIVIL AND CRIMINAL PROSECUTION!		DESCRIPTION: GEARBOX FRONT HOUSING		DRAWN: JS OOSTHUIZEN	
		ALL DIMENSIONS IN mms UNLESS OTHERWISE SPECIFIED. ALL DIMENSIONS $\pm 0.1\text{mm}$ UNLESS OTHERWISE SPECIFIED.		OPERATION: #00	
				DATE: 2011/10/05	
				REVISION: 1	
		SCALE: 1:2		SHEET: 1 / 3	



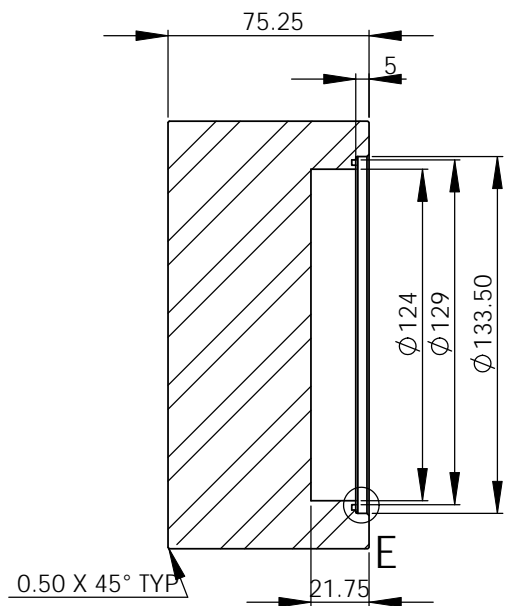
SECTION B-B

SECTION D-D

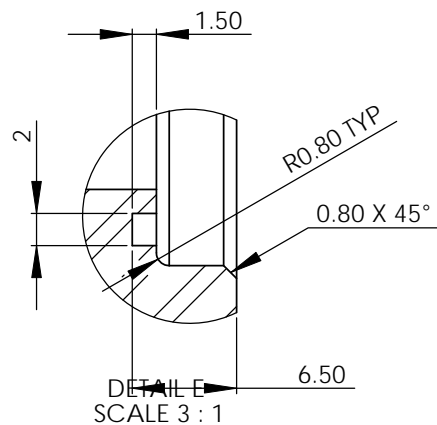
DRAWING NUMBER: TX28P-0022-C1			QTY: 1
DESCRIPTION: GEARBOX FRONT HOUSING		DRAWN: JS OOSTHUIZEN	
RAW MATERIAL: EN 8		OPERATION: #00	DATE: 2011/10/05
ALL DIMENSIONS IN mms UNLESS OTHERWISE SPECIFIED. ALL DIMENSIONS ±0.1mm UNLESS OTHERWISE SPECIFIED.		CHECKED:	REVISION: 1
THIS DRAWING AND ALL INFORMATION THERIN IS THE PROPERTY OF AND CONFIDENTIAL TO CFAM. IT MUST NOT BE MADE PUBLIC OR COPIED. IT IS LOANED SUBJECT TO RETURN UPON DEMAND. IT IS NOT TO BE USED DIRECTLY OR INDIRECTLY IN ANY WAY DETRIMENTAL TO OUR INTEREST. VIOLATION OF THE ABOVE WILL LEAD TO IMMEDIATE CIVIL AND CRIMINAL PROSECUTION!		SCALE: 1:2	SHEET: 2 / 3



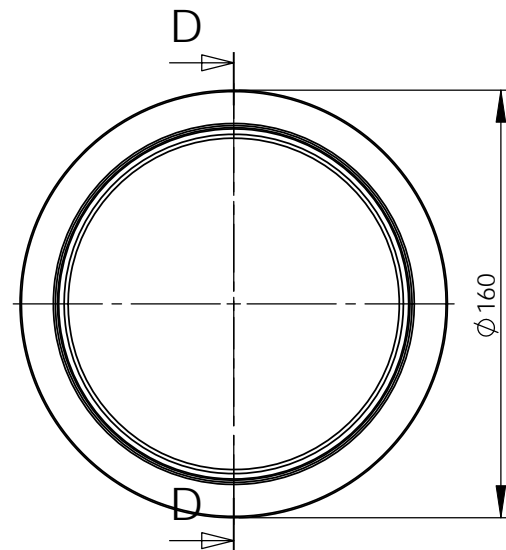
DRAWING NUMBER: TX28P-0022-C1			QTY: 1
DESCRIPTION: GEARBOX FRONT HOUSING		DRAWN: JS OOSTHUIZEN	
RAW MATERIAL: EN 8		OPERATION: #00	DATE: 2011/10/05
ALL DIMENSIONS IN mms UNLESS OTHERWISE SPECIFIED. ALL DIMENSIONS ±0.1mm UNLESS OTHERWISE SPECIFIED.		CHECKED:	REVISION: 1
THIS DRAWING AND ALL INFORMATION THERIN IS THE PROPERTY OF AND CONFIDENTIAL TO CFAM. IT MUST NOT BE MADE PUBLIC OR COPIED. IT IS LOANED SUBJECT TO RETURN UPON DEMAND. IT IS NOT TO BE USED DIRECTLY OR INDIRECTLY IN ANY WAY DETRIMENTAL TO OUR INTEREST. VIOLATION OF THE ABOVE WILL LEAD TO IMMEDIATE CIVIL AND CRIMINAL PROSECUTION!		SCALE: 1:2	SHEET: 3 / 3

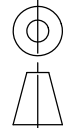


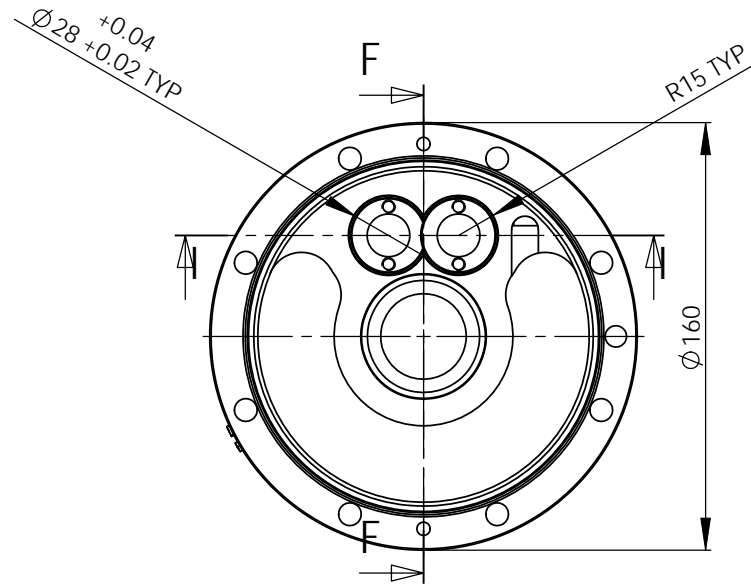
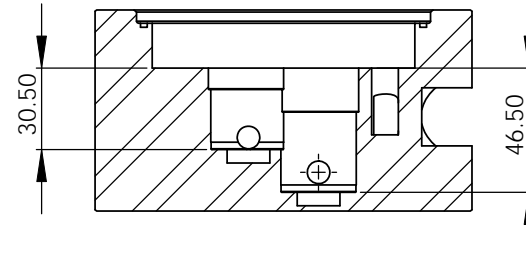
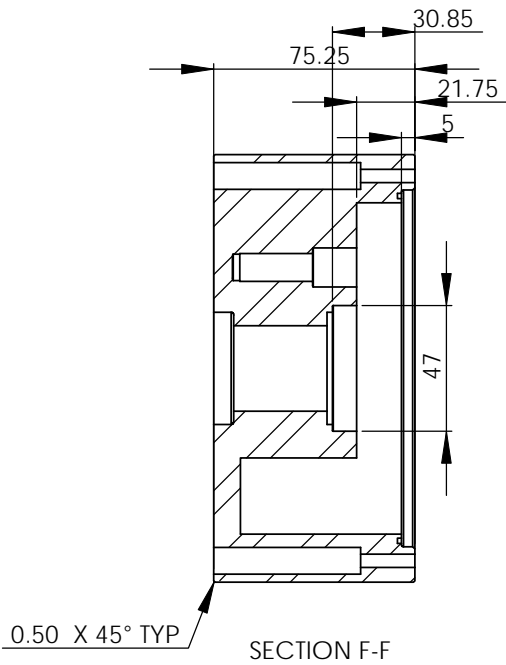
SECTION D-D



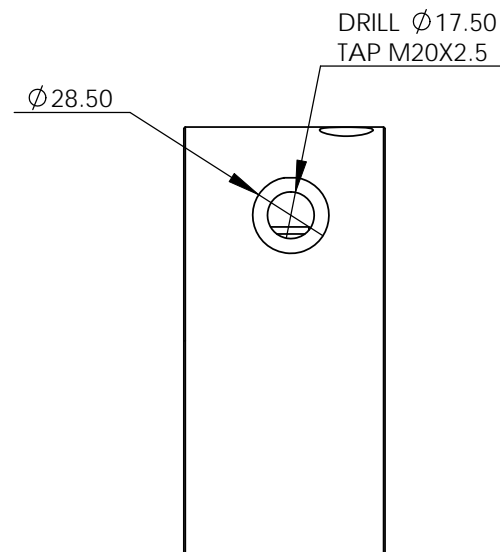
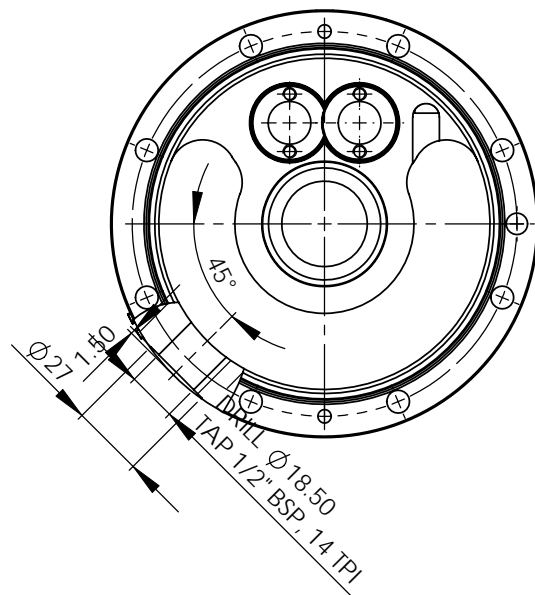
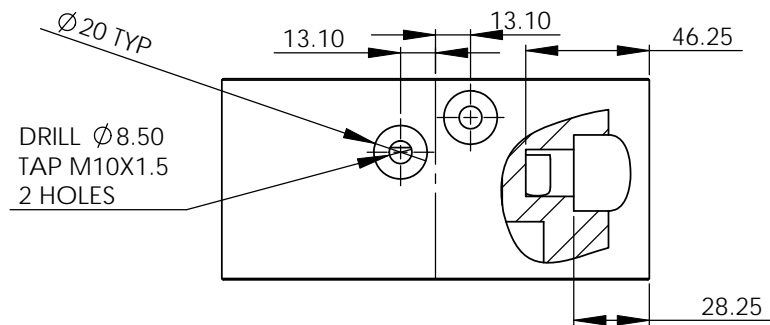
DETAIL E
SCALE 3 : 1



DRAWING NUMBER: TX28P-0023-C1				QTY: 1
DESCRIPTION: GAERBOX BACK HOUSING			DRAWN: JS OOSTHUIZEN	
RAW MATERIAL: EN 8		ALL DIMENSIONS IN mms UNLESS OTHERWISE SPECIFIED. ALL DIMENSIONS $\pm 0.1\text{mm}$ UNLESS OTHERWISE SPECIFIED.	OPERATION: #00	DATE: 2011/10/05
THIS DRAWING AND ALL INFORMATION THERIN IS THE PROPERTY OF AND CONFIDENTIAL TO CFAM. IT MUST NOT BE MADE PUBLIC OR COPIED. IT IS LOANED SUBJECT TO RETURN UPON DEMAND. IT IS NOT TO BE USED DIRECTLY OR INDIRECTLY IN ANY WAY DETRIMENTAL TO OUR INTEREST. VIOLATION OF THE ABOVE WILL LEAD TO IMMEDIATE CIVIL AND CRIMINAL PROSECUTION!			CHECKED:	REVISION: 1
			SCALE: 1:2	SHEET: 1 / 3

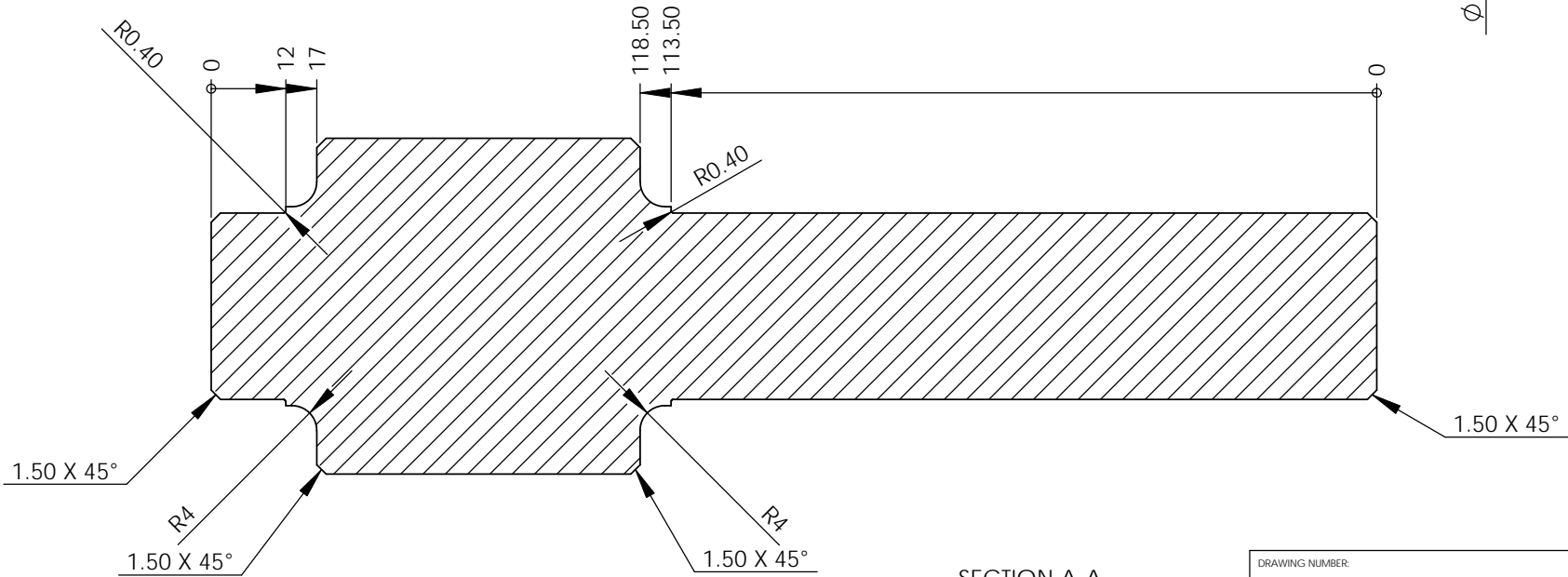
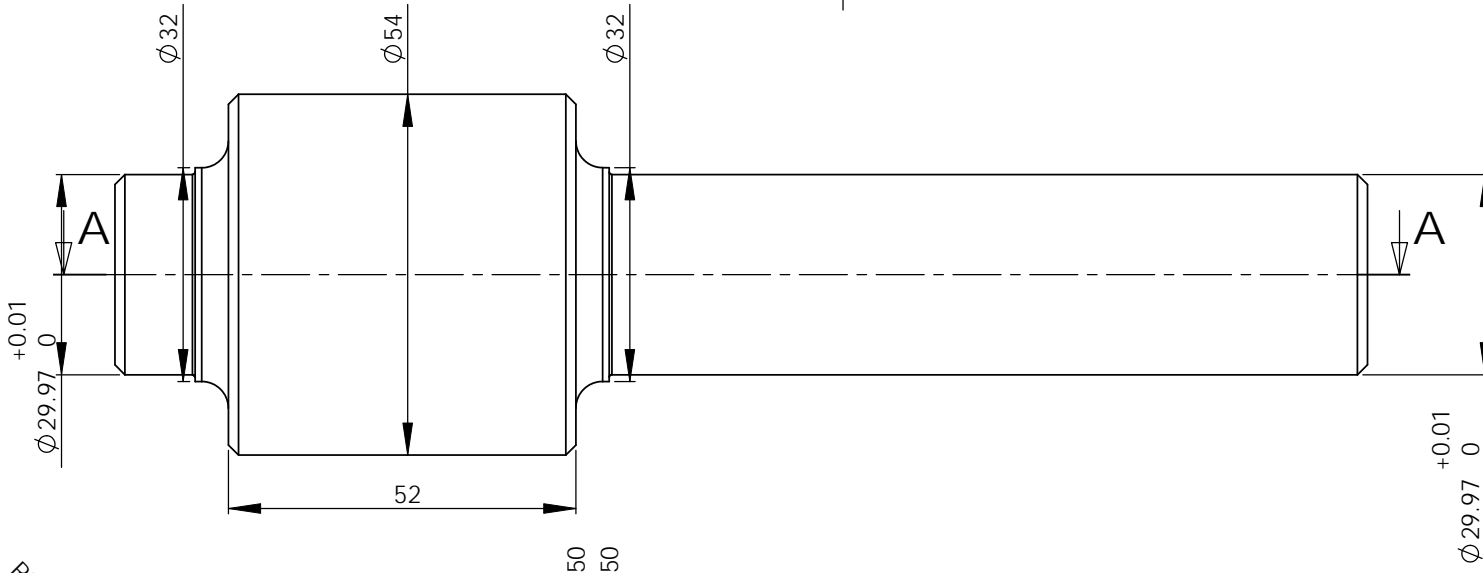


DRAWING NUMBER: TX28P-0023-C1			QTY: 1
DESCRIPTION: GEARBOX BACK HOUSING		DRAWN: JS OOSTHUIZEN	
RAW MATERIAL: EN 8		OPERATION: #00	DATE: 2011/10/05
THIS DRAWING AND ALL INFORMATION THERIN IS THE PROPERTY OF AND CONFIDENTIAL TO CFAM. IT MUST NOT BE MADE PUBLIC OR COPIED. IT IS LOANED SUBJECT TO RETURN UPON DEMAND. IT IS NOT TO BE USED DIRECTLY OR INDIRECTLY IN ANY WAY DETRIMENTAL TO OUR INTEREST. VIOLATION OF THE ABOVE WILL LEAD TO IMMEDIATE CIVIL AND CRIMINAL PROSECUTION!			REVISION: 1
			SHEET: 2 / 3



DRAWING NUMBER: TX28P-0023-C1			QTY: 1
DESCRIPTION: GEARBOX BACK HOUSING		DRAWN: JS OOTHUIZEN	
RAW MATERIAL: EN 8		OPERATION: #00	DATE: 2011/10/05
ALL DIMENSIONS IN mms UNLESS OTHERWISE SPECIFIED. ALL DIMENSIONS ± 0.1 mm UNLESS OTHERWISE SPECIFIED.		CHECKED:	REVISION: 1
THIS DRAWING AND ALL INFORMATION THERIN IS THE PROPERTY OF AND CONFIDENTIAL TO CFAM. IT MUST NOT BE MADE PUBLIC OR COPIED. IT IS LOANED SUBJECT TO RETURN UPON DEMAND. IT IS NOT TO BE USED DIRECTLY OR INDIRECTLY IN ANY WAY DETRIMENTAL TO OUR INTEREST. VIOLATION OF THE ABOVE WILL LEAD TO IMMEDIATE CIVIL AND CRIMINAL PROSECUTION!		SCALE: 1:2	SHEET: 3 / 3



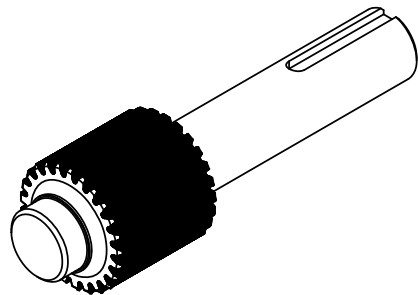
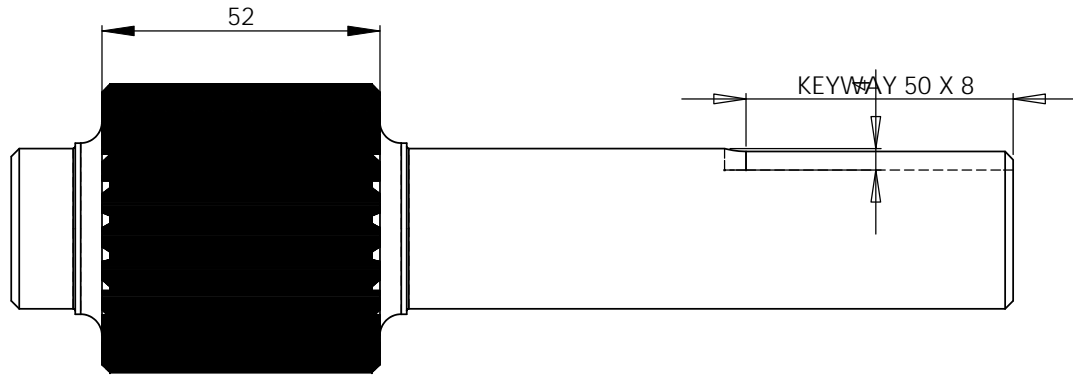
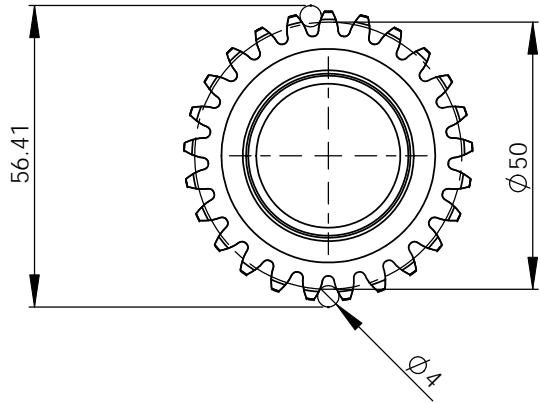


SECTION A-A
SCALE 1.25 : 1

NOTE: CORNER RADIUS VERY IMPORTANT

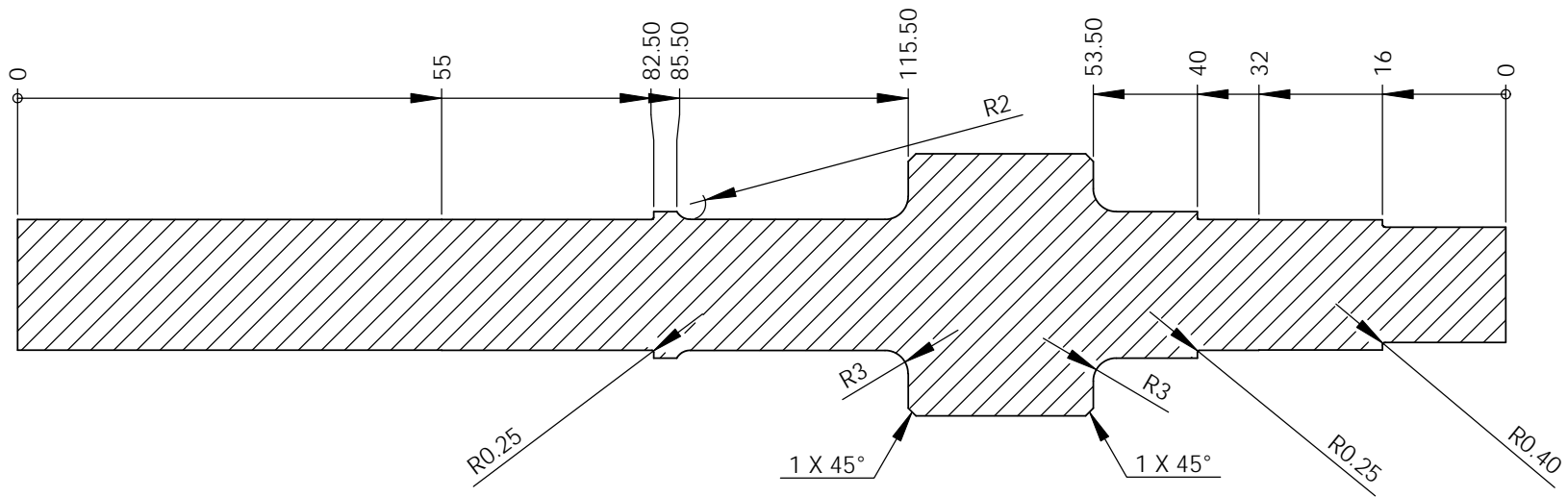
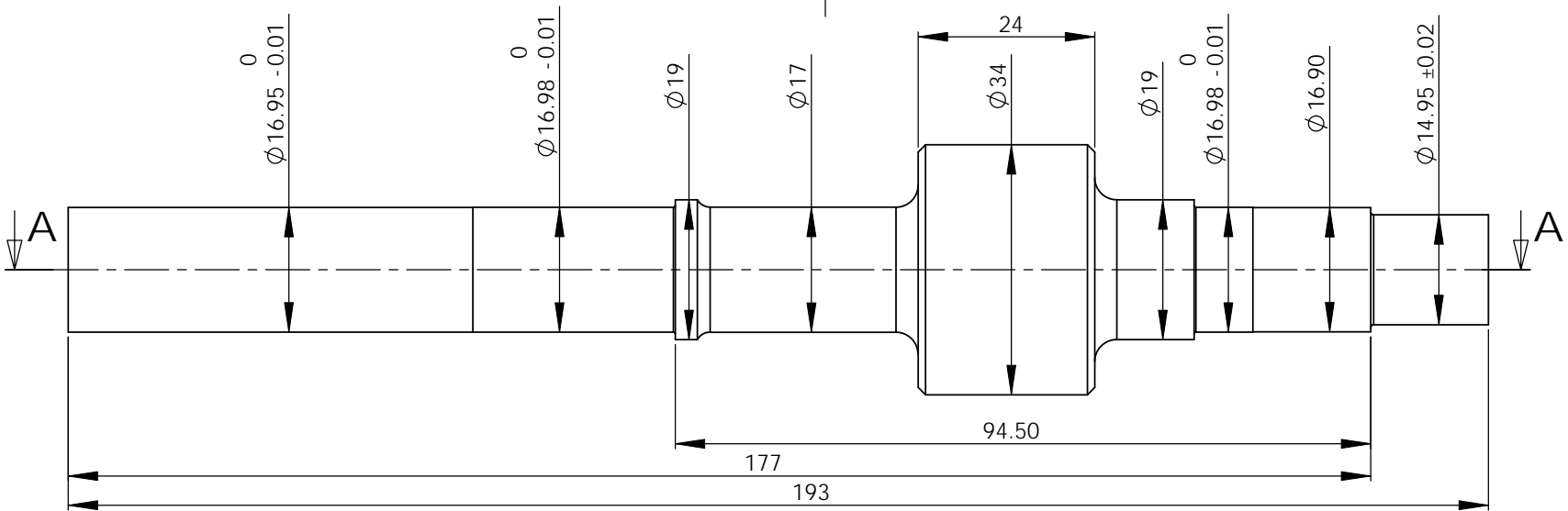
RAW MATERIAL: EN 36		DRAWING NUMBER: TX28P-0024-C4		QTY: 1	
THIS DRAWING AND ALL INFORMATION THERIN IS THE PROPERTY OF AND CONFIDENTIAL TO CFAM. IT MUST NOT BE MADE PUBLIC OR COPIED. IT IS LOANED SUBJECT TO RETURN UPON DEMAND. IT IS NOT TO BE USED DIRECTLY OR INDIRECTLY IN ANY WAY DETRIMENTAL TO OUR INTEREST. VIOLATION OF THE ABOVE WILL LEAD TO IMMEDIATE CIVIL AND CRIMINAL PROSECUTION!		DESCRIPTION: INPUT SHAFT		DRAWN: JS OOTHUIZEN	
		ALL DIMENSIONS IN mms UNLESS OTHERWISE SPECIFIED. ALL DIMENSIONS ± 0.1 mm UNLESS OTHERWISE SPECIFIED.		OPERATION: #00	
				DATE: 2011/10/05	
				REVISION: 1	
				SHEET: 1 / 3	
				SCALE: 1:2	





GEAR DATA	
NO OF TEETH	25
MODULE	2
PRESSURE ANGLE	20
HELIX ANGLE	0
FACE WIDTH	52

DRAWING NUMBER: TX28P-0024-C4		QTY: 1
DESCRIPTION: INPUT SHAFT		DRAWN: JS OOSTHUIZEN
RAW MATERIAL: EN 36		OPERATION: #00
ALL DIMENSIONS IN mms UNLESS OTHERWISE SPECIFIED. ALL DIMENSIONS ± 0.1 mm UNLESS OTHERWISE SPECIFIED.		DATE: 2011/10/05
THIS DRAWING AND ALL INFORMATION THERIN IS THE PROPERTY OF AND CONFIDENTIAL TO CFAM. IT MUST NOT BE MADE PUBLIC OR COPIED. IT IS LOANED SUBJECT TO RETURN UPON DEMAND. IT IS NOT TO BE USED DIRECTLY OR INDIRECTLY IN ANY WAY DETRIMENTAL TO OUR INTEREST. VIOLATION OF THE ABOVE WILL LEAD TO IMMEDIATE CIVIL AND CRIMINAL PROSECUTION!		REVISION: 1
		SCALE: 1:2
		SHEET: 2 / 3



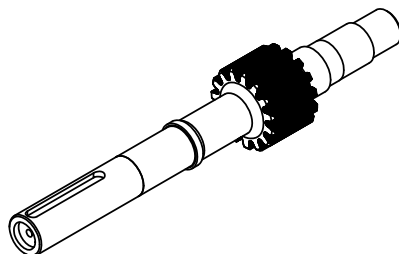
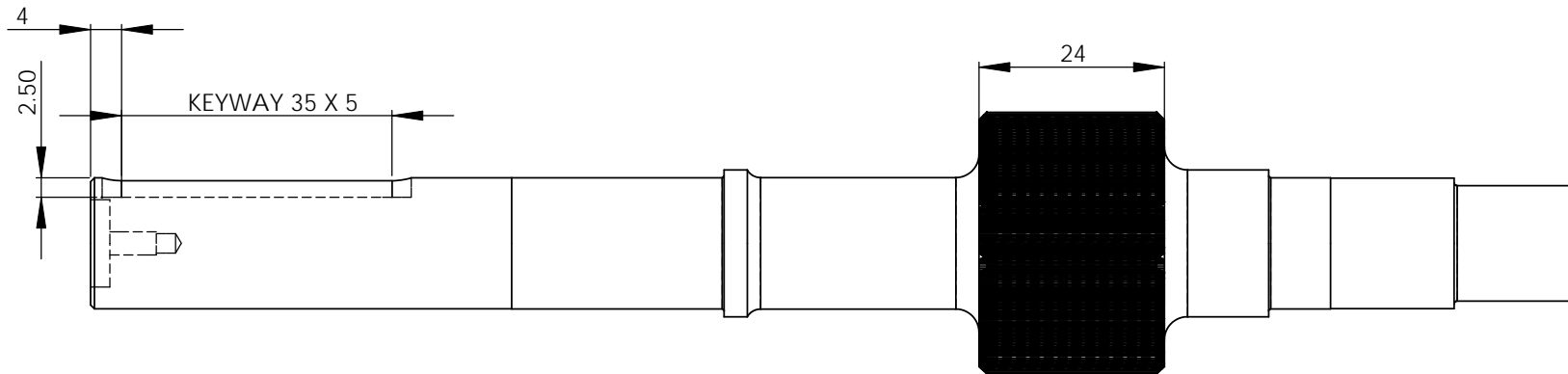
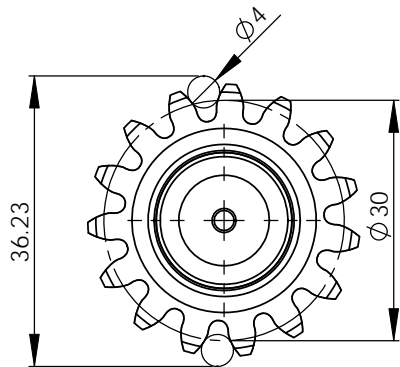
SECTION A-A
SCALE 1.5 : 1

NOTE: CORNER RADIUS VERY IMPORTANT

RAW MATERIAL:
EN 36

THIS DRAWING AND ALL INFORMATION THEREIN IS THE PROPERTY OF AND CONFIDENTIAL TO CFAM. IT MUST NOT BE MADE PUBLIC OR COPIED. IT IS LOANED SUBJECT TO RETURN UPON DEMAND. IT IS NOT TO BE USED DIRECTLY OR INDIRECTLY IN ANY WAY DETRIMENTAL TO OUR INTEREST. VIOLATION OF THE ABOVE WILL LEAD TO IMMEDIATE CIVIL AND CRIMINAL PROSECUTION!

DRAWING NUMBER: TX28P-0025-C4			QTY: 1
DESCRIPTION: LEFT OUTPUT SHAFT		DRAWN: JS OOSTHUIZEN	
ALL DIMENSIONS IN mm UNLESS OTHERWISE SPECIFIED. ALL DIMENSIONS ±0.1mm UNLESS OTHERWISE SPECIFIED.		OPERATION: #00	DATE: 2011/10/05
		CHECKED:	REVISION: 1
		SCALE: 1:2	SHEET: 1 / 3



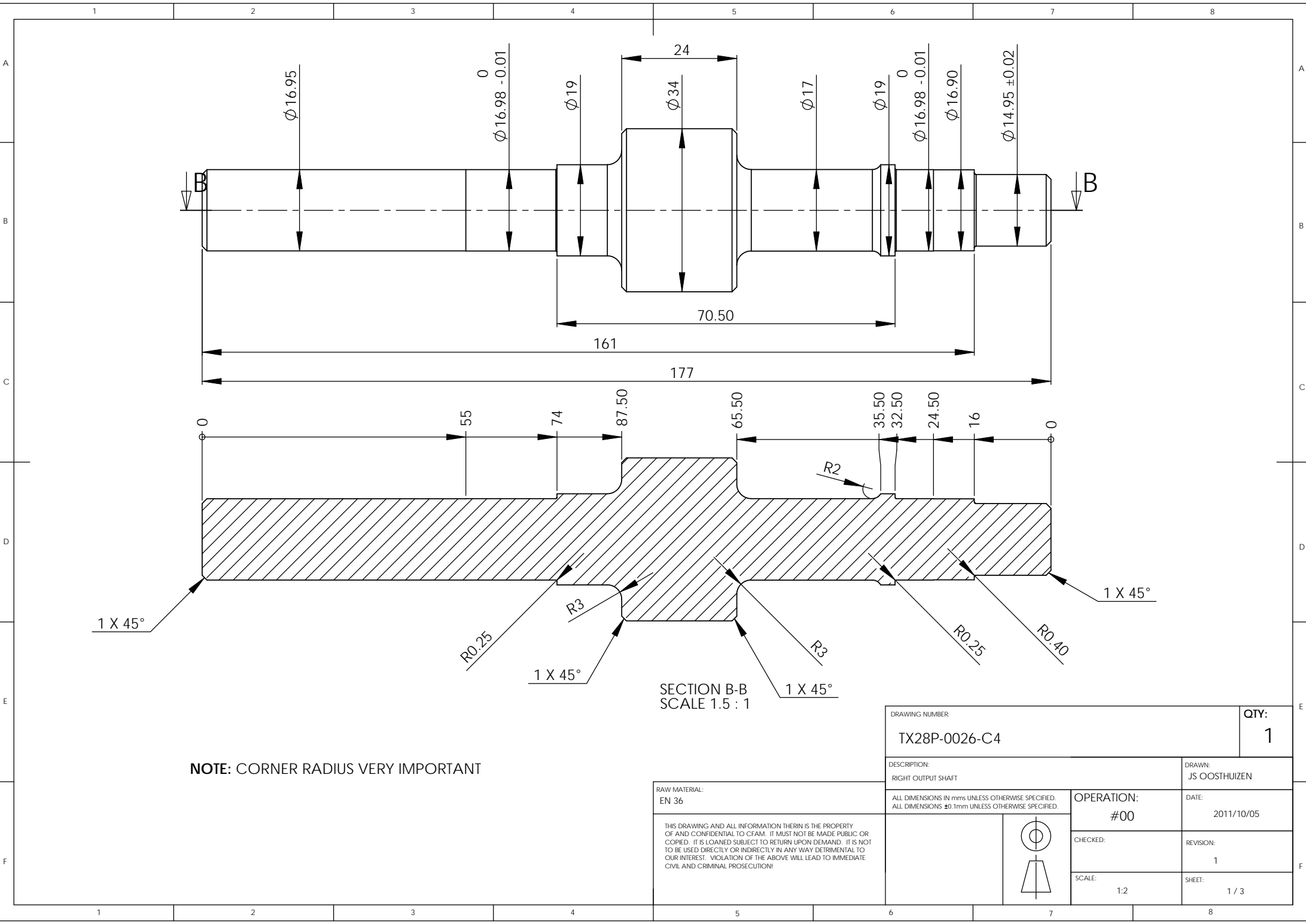
GEAR DATA	
NO OF TEETH	15
MODULE	2
PRESSURE ANGLE	20
HELIX ANGLE	0
FACE WIDTH	24

DRAWING NUMBER: TX28P-0025-C4		QTY: 1
DESCRIPTION: LEFT OUTPUT SHAFT		DRAWN: JS OOSTHUIZEN
OPERATION: #00	DATE: 2011/10/05	
	CHECKED:	REVISION: 1
	SCALE: 1:2	SHEET: 2 / 3

RAW MATERIAL:
EN 36

THIS DRAWING AND ALL INFORMATION THERIN IS THE PROPERTY OF AND CONFIDENTIAL TO CFAM. IT MUST NOT BE MADE PUBLIC OR COPIED. IT IS LOANED SUBJECT TO RETURN UPON DEMAND. IT IS NOT TO BE USED DIRECTLY OR INDIRECTLY IN ANY WAY DETRIMENTAL TO OUR INTEREST. VIOLATION OF THE ABOVE WILL LEAD TO IMMEDIATE CIVIL AND CRIMINAL PROSECUTION!

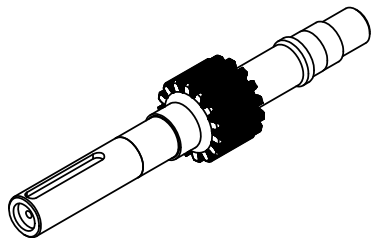
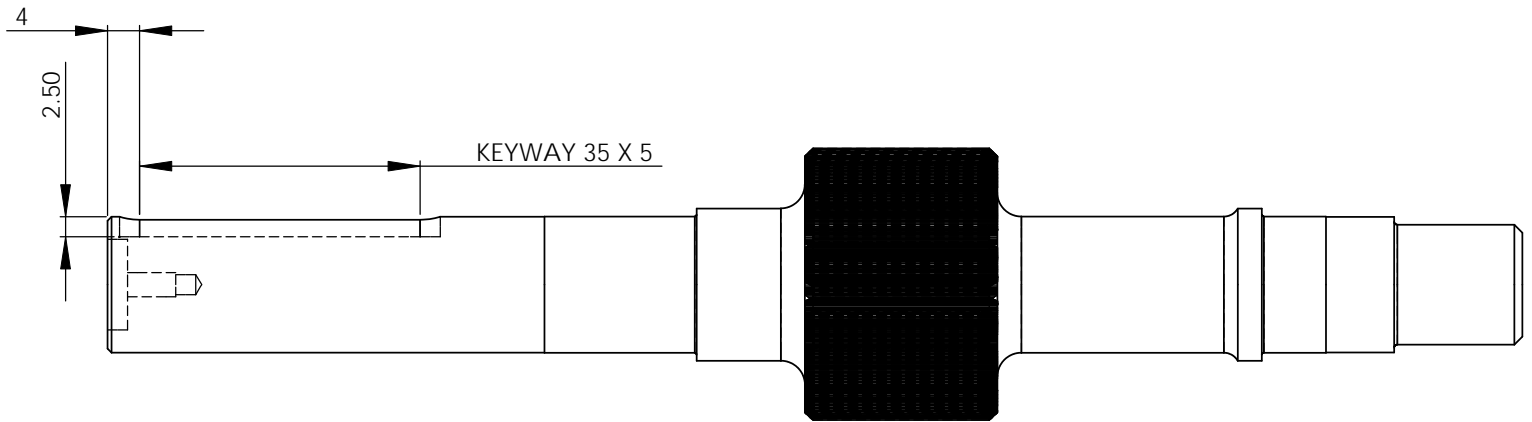
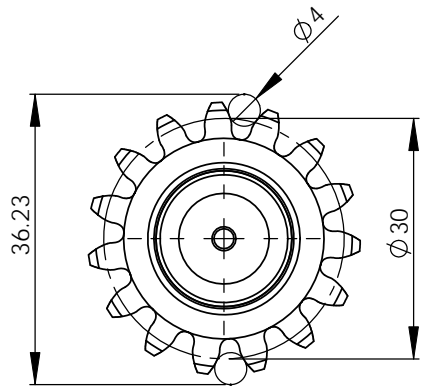




NOTE: CORNER RADIUS VERY IMPORTANT

SECTION B-B
SCALE 1.5 : 1

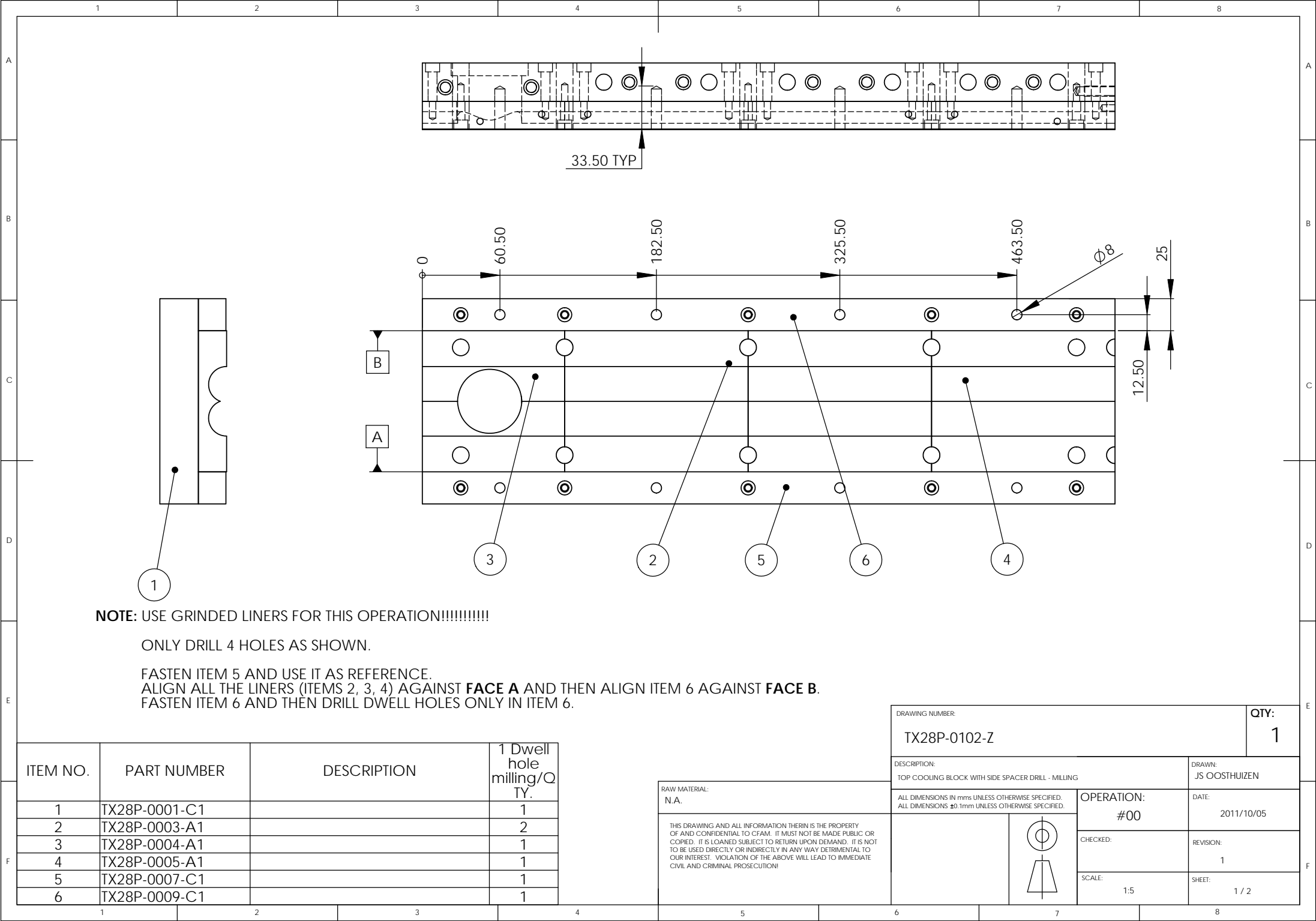
DRAWING NUMBER: TX28P-0026-C4			QTY: 1
DESCRIPTION: RIGHT OUTPUT SHAFT		DRAWN: JS OOSTHUIZEN	
ALL DIMENSIONS IN mms UNLESS OTHERWISE SPECIFIED. ALL DIMENSIONS $\pm 0.1\text{mm}$ UNLESS OTHERWISE SPECIFIED.		OPERATION: #00	DATE: 2011/10/05
<div>THIS DRAWING AND ALL INFORMATION THERIN IS THE PROPERTY OF AND CONFIDENTIAL TO CFAM. IT MUST NOT BE MADE PUBLIC OR COPIED. IT IS LOANED SUBJECT TO RETURN UPON DEMAND. IT IS NOT TO BE USED DIRECTLY OR INDIRECTLY IN ANY WAY DETRIMENTAL TO OUR INTEREST. VIOLATION OF THE ABOVE WILL LEAD TO IMMEDIATE CIVIL AND CRIMINAL PROSECUTION!</div> <div></div>		CHECKED:	REVISION: 1
		SCALE: 1:2	SHEET: 1 / 3

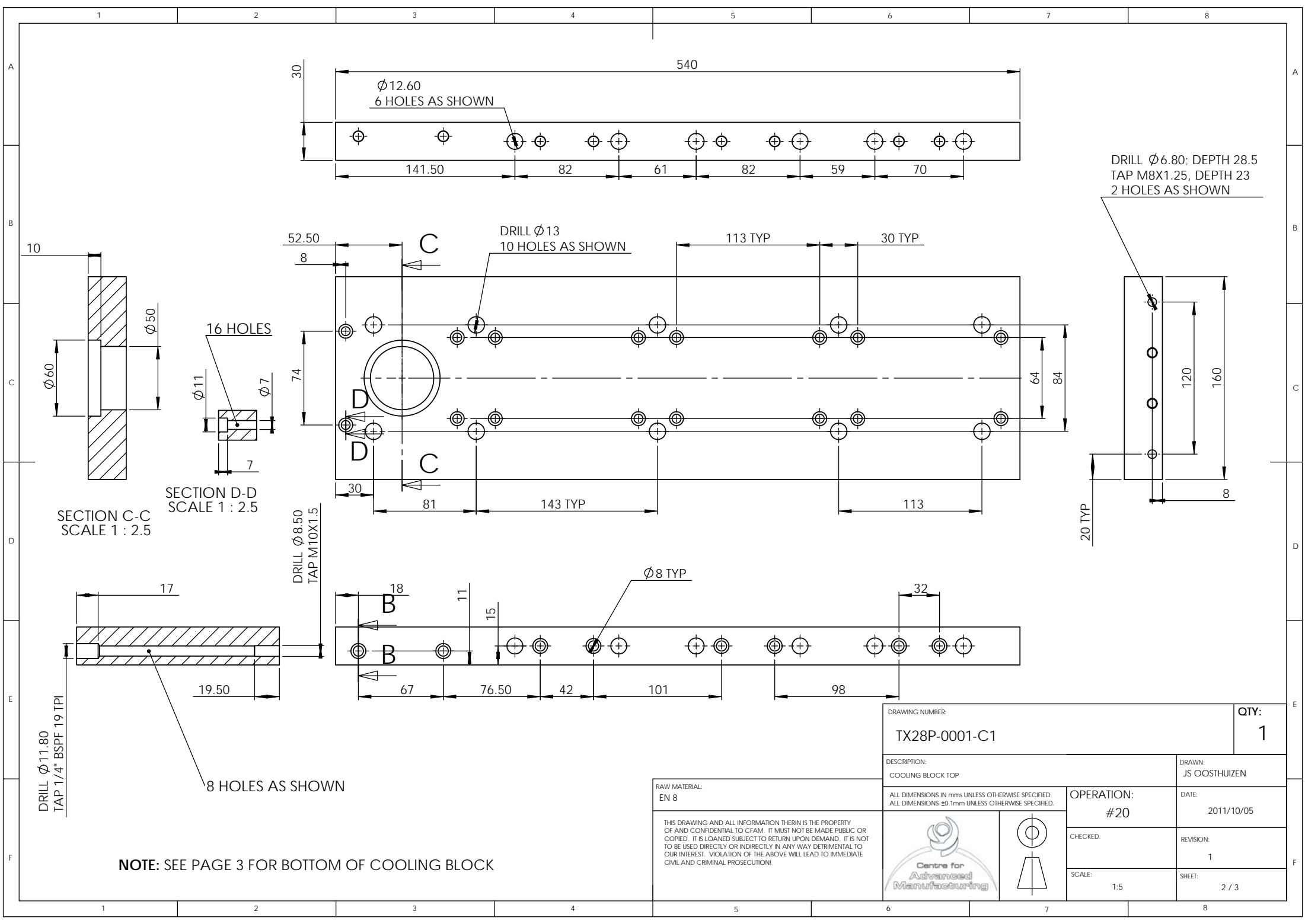


GEAR DATA	
NO OF TEETH	15
MODULE	2
PRESSURE ANGLE	20
HELIX ANGLE	0
FACE WIDTH	24

DRAWING NUMBER:		QTY:	
TX28P-0026-C4		1	
DESCRIPTION:		DRAWN:	
RIGHT OUTPUT SHAFT		JS OOSTHUIZEN	
RAW MATERIAL:		OPERATION:	
EN 36		#00	
ALL DIMENSIONS IN mms UNLESS OTHERWISE SPECIFIED. ALL DIMENSIONS ±0.1mm UNLESS OTHERWISE SPECIFIED.		DATE:	
THIS DRAWING AND ALL INFORMATION THERIN IS THE PROPERTY OF AND CONFIDENTIAL TO CFAM. IT MUST NOT BE MADE PUBLIC OR COPIED. IT IS LOANED SUBJECT TO RETURN UPON DEMAND. IT IS NOT TO BE USED DIRECTLY OR INDIRECTLY IN ANY WAY DETRIMENTAL TO OUR INTEREST. VIOLATION OF THE ABOVE WILL LEAD TO IMMEDIATE CIVIL AND CRIMINAL PROSECUTION!		2011/10/05	
		REVISION:	
		1	
		SHEET:	
		2 / 3	
		SCALE:	
		1:2	



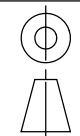


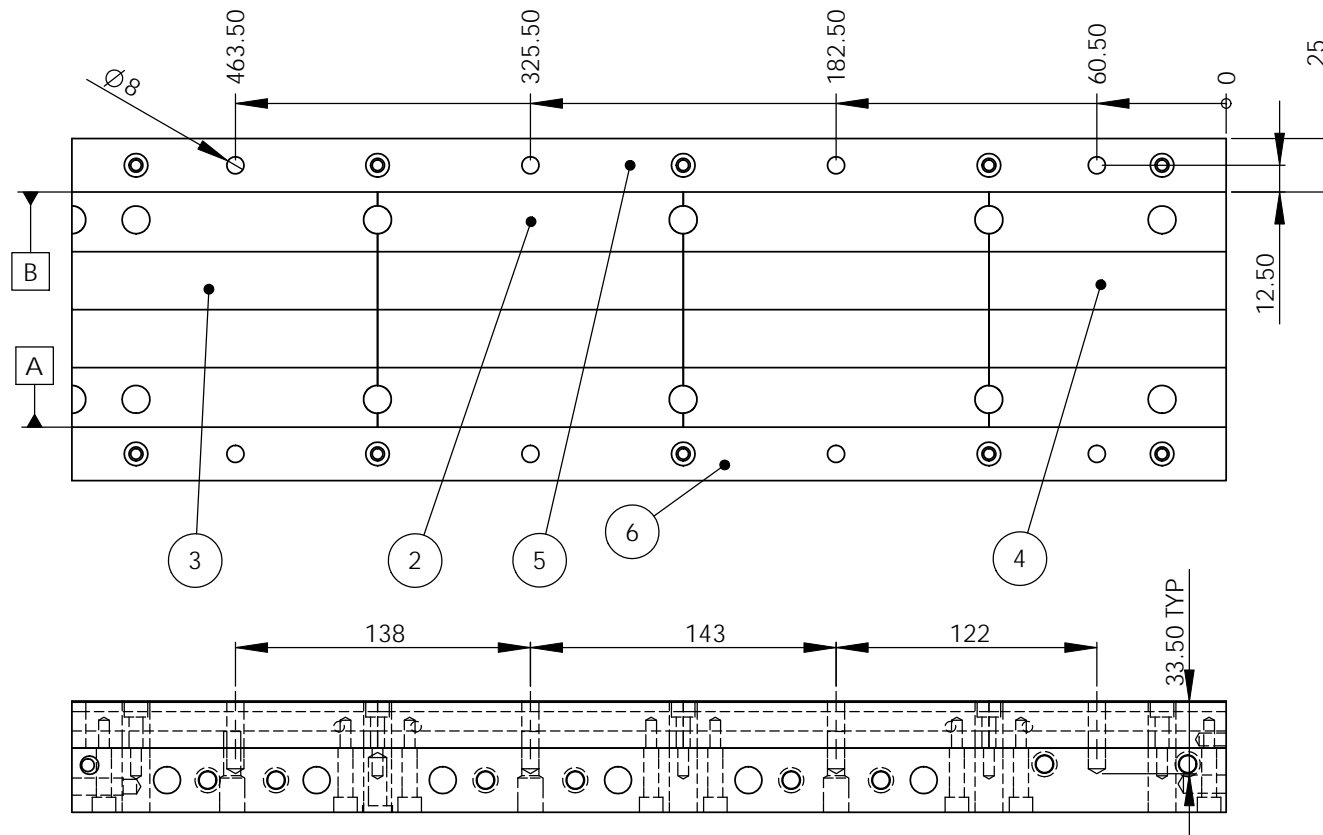


DRAWING NUMBER: TX28P-0001-C1		QTY: 1	
DESCRIPTION: COOLING BLOCK TOP		DRAWN: JS OOSTHUIZEN	
ALL DIMENSIONS IN mm UNLESS OTHERWISE SPECIFIED. ALL DIMENSIONS ± 0.1 mm UNLESS OTHERWISE SPECIFIED.		OPERATION: #20	DATE: 2011/10/05
CHECKED:		REVISION: 1	
SCALE: 1:5		SHEET: 2 / 3	

RAW MATERIAL:
EN 8

THIS DRAWING AND ALL INFORMATION THEREIN IS THE PROPERTY OF AND CONFIDENTIAL TO CFAM. IT MUST NOT BE MADE PUBLIC OR COPIED. IT IS LOANED SUBJECT TO RETURN UPON DEMAND. IT IS NOT TO BE USED DIRECTLY OR INDIRECTLY IN ANY WAY DETRIMENTAL TO OUR INTEREST. VIOLATION OF THE ABOVE WILL LEAD TO IMMEDIATE CIVIL AND CRIMINAL PROSECUTION!





NOTE: USE GRINDED LINERS FOR THIS OPERATION!!!!!!!!!!!!!!

ONLY DRILL 4 HOLES AS SHOWN.

FASTEN ITEM 6 AND USE IT AS REFERENCE.
ALIGN ALL THE LINERS (ITEMS 2, 3, 4) AGAINST **FACE A** AND THEN ALIGN ITEM 5 AGAINST **FACE B**.
FASTEN ITEM 5 AND THEN DRILL DWELL HOLES ONLY IN ITEM 5.

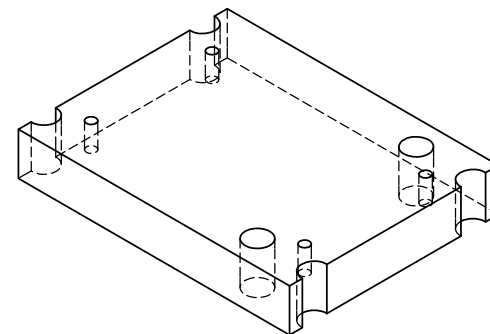
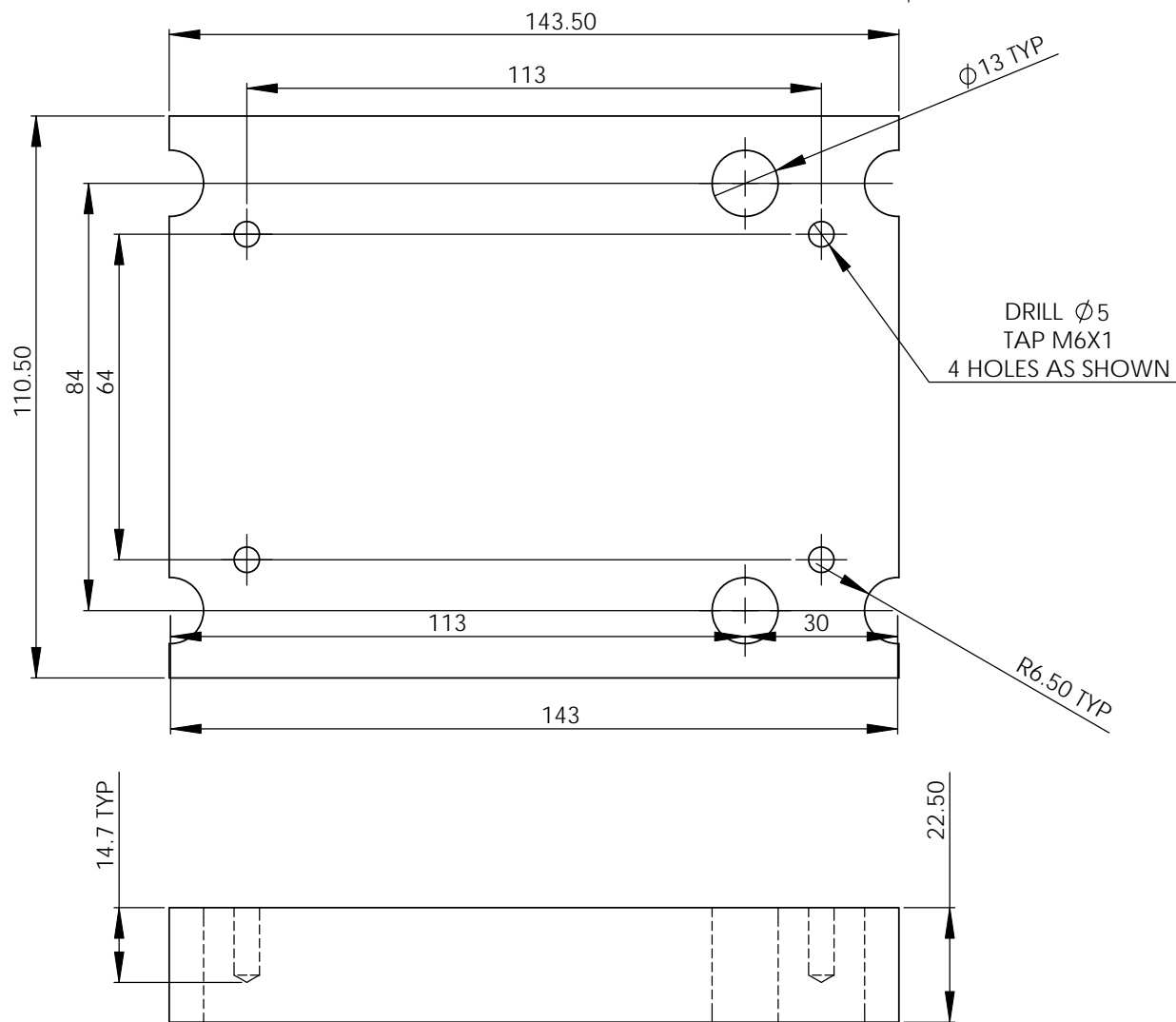
ITEM NO.	PART NUMBER	DESCRIPTION	1 dwell hole milling/Q TY.
1	TX28P-0002-C1		1
2	TX28P-0011-A1		2
3	TX28P-0012-A1		1
4	TX28P-0006-A1		1
5	TX28P-0013-C1		1
6	TX28P-0008-C1		1

RAW MATERIAL:
N.A.

THIS DRAWING AND ALL INFORMATION THERIN IS THE PROPERTY OF AND CONFIDENTIAL TO CFAM. IT MUST NOT BE MADE PUBLIC OR COPIED. IT IS LOANED SUBJECT TO RETURN UPON DEMAND. IT IS NOT TO BE USED DIRECTLY OR INDIRECTLY IN ANY WAY DETRIMENTAL TO OUR INTEREST. VIOLATION OF THE ABOVE WILL LEAD TO IMMEDIATE CIVIL AND CRIMINAL PROSECUTION!

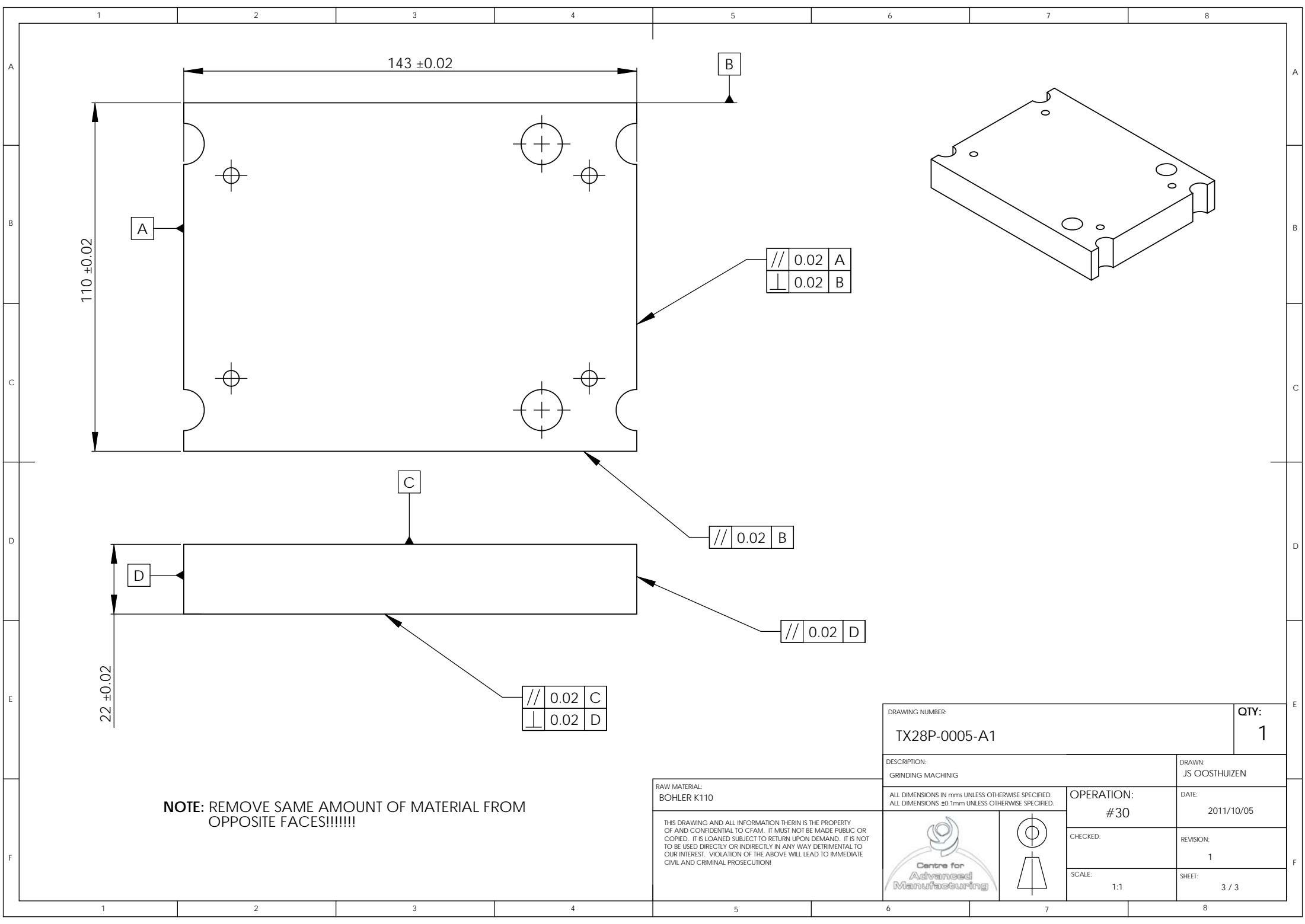


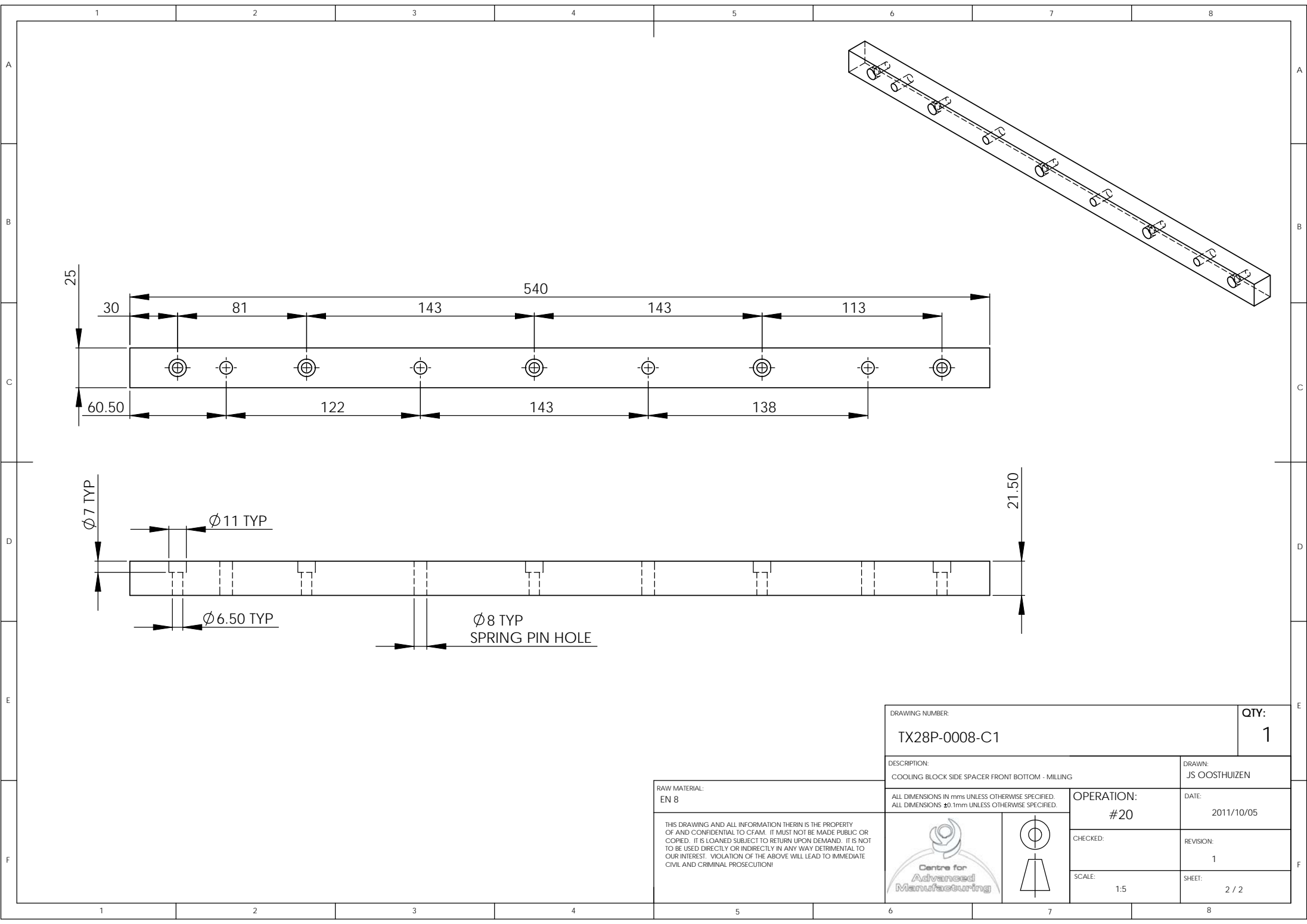
DRAWING NUMBER: TX28P-0101-Z		QTY: 1	
DESCRIPTION: BOTTOM COOLING BLOCK AND BACK SPACER - MILLING		DRAWN: JS OOSTHUIZEN	
ALL DIMENSIONS IN mms UNLESS OTHERWISE SPECIFIED. ALL DIMENSIONS ± 0.1 mm UNLESS OTHERWISE SPECIFIED.		OPERATION: #00	DATE: 2011/10/05
		CHECKED:	REVISION: 1
		SCALE: 1:5	SHEET: 1 / 2

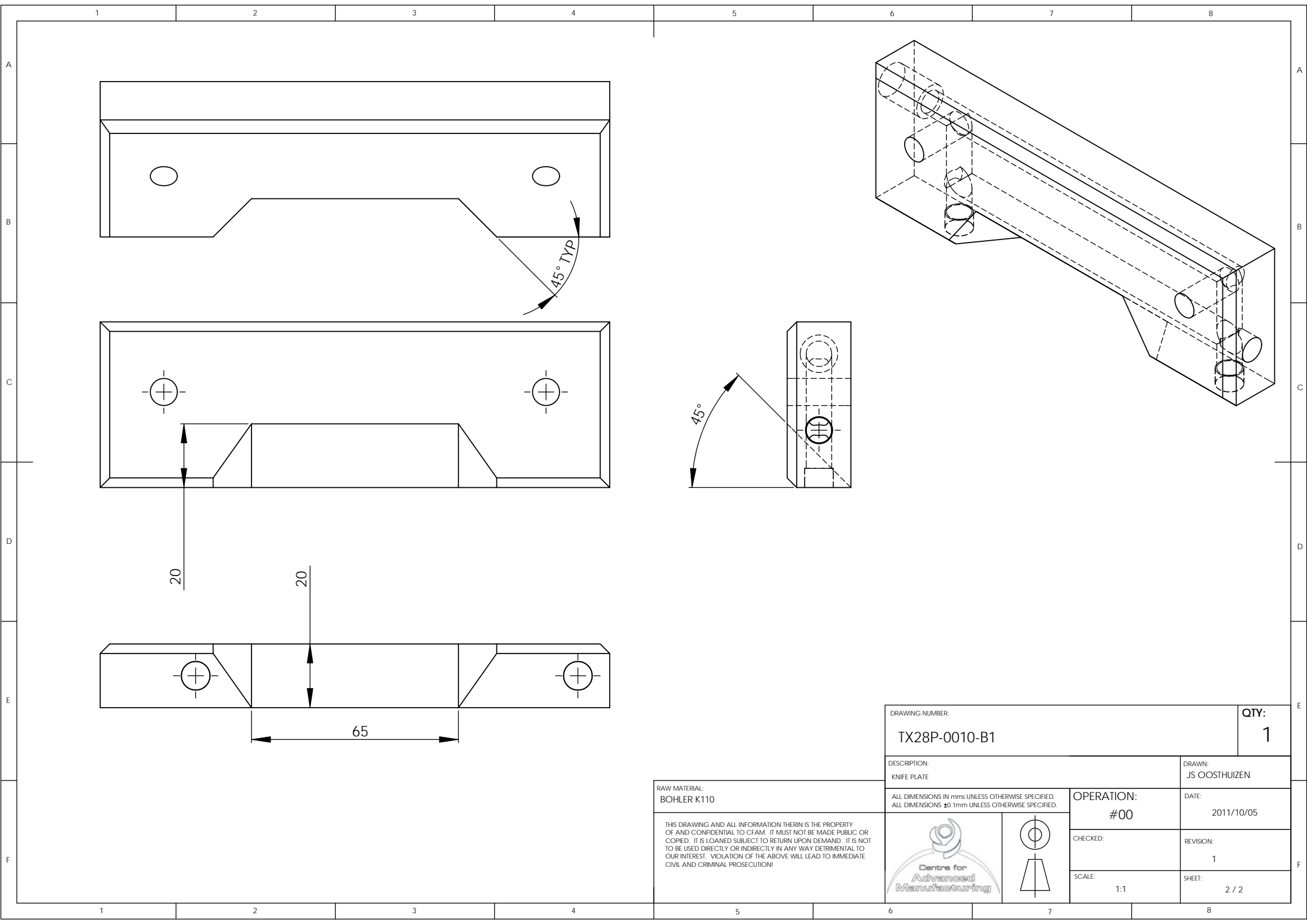



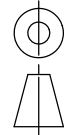
DRAWING NUMBER: TX28P-0005-A1			QTY: 1
DESCRIPTION: LINER FRONT TOP - MILLING		DRAWN: JS OOSTHUIZEN	
RAW MATERIAL: BOHLER K110		OPERATION: #20	DATE: 2011/10/05
ALL DIMENSIONS IN mms UNLESS OTHERWISE SPECIFIED. ALL DIMENSIONS ±0.1mm UNLESS OTHERWISE SPECIFIED.		CHECKED:	REVISION: 1
THIS DRAWING AND ALL INFORMATION THERIN IS THE PROPERTY OF AND CONFIDENTIAL TO CFAM. IT MUST NOT BE MADE PUBLIC OR COPIED. IT IS LOANED SUBJECT TO RETURN UPON DEMAND. IT IS NOT TO BE USED DIRECTLY OR INDIRECTLY IN ANY WAY DETRIMENTAL TO OUR INTEREST. VIOLATION OF THE ABOVE WILL LEAD TO IMMEDIATE CIVIL AND CRIMINAL PROSECUTION!		SCALE: 1:1	SHEET: 2 / 3





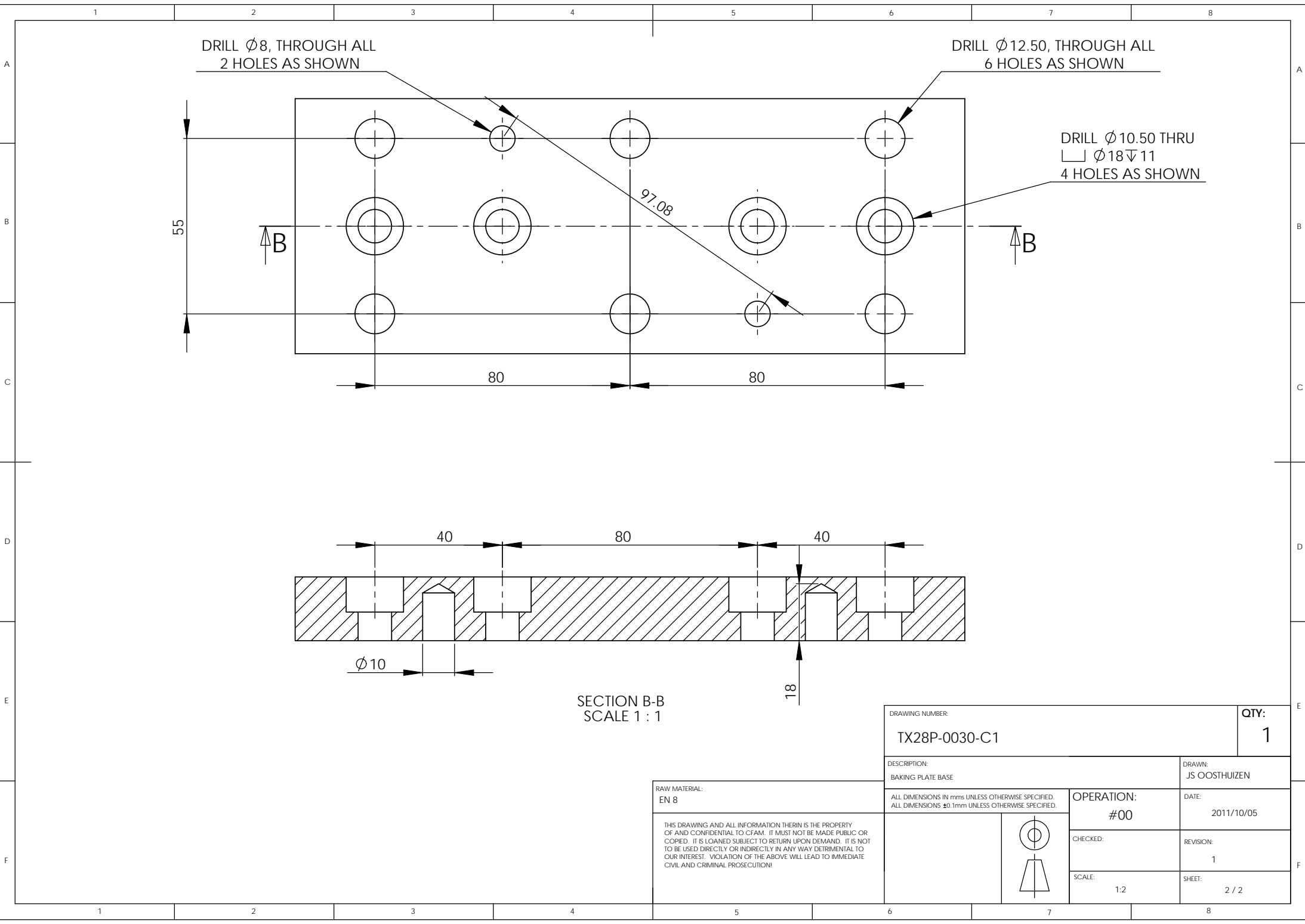




DRAWING NUMBER: TX28P-0010-B1			QTY: 1
DESCRIPTION: KNIFE PLATE		DRAWN: JS OOSTHUIZEN	
ALL DIMENSIONS IN mms UNLESS OTHERWISE SPECIFIED. ALL DIMENSIONS $\pm 0.1\text{mm}$ UNLESS OTHERWISE SPECIFIED.		OPERATION: #00	DATE: 2011/10/05
 		CHECKED:	REVISION: 1
		SCALE: 1:1	SHEET: 2 / 2

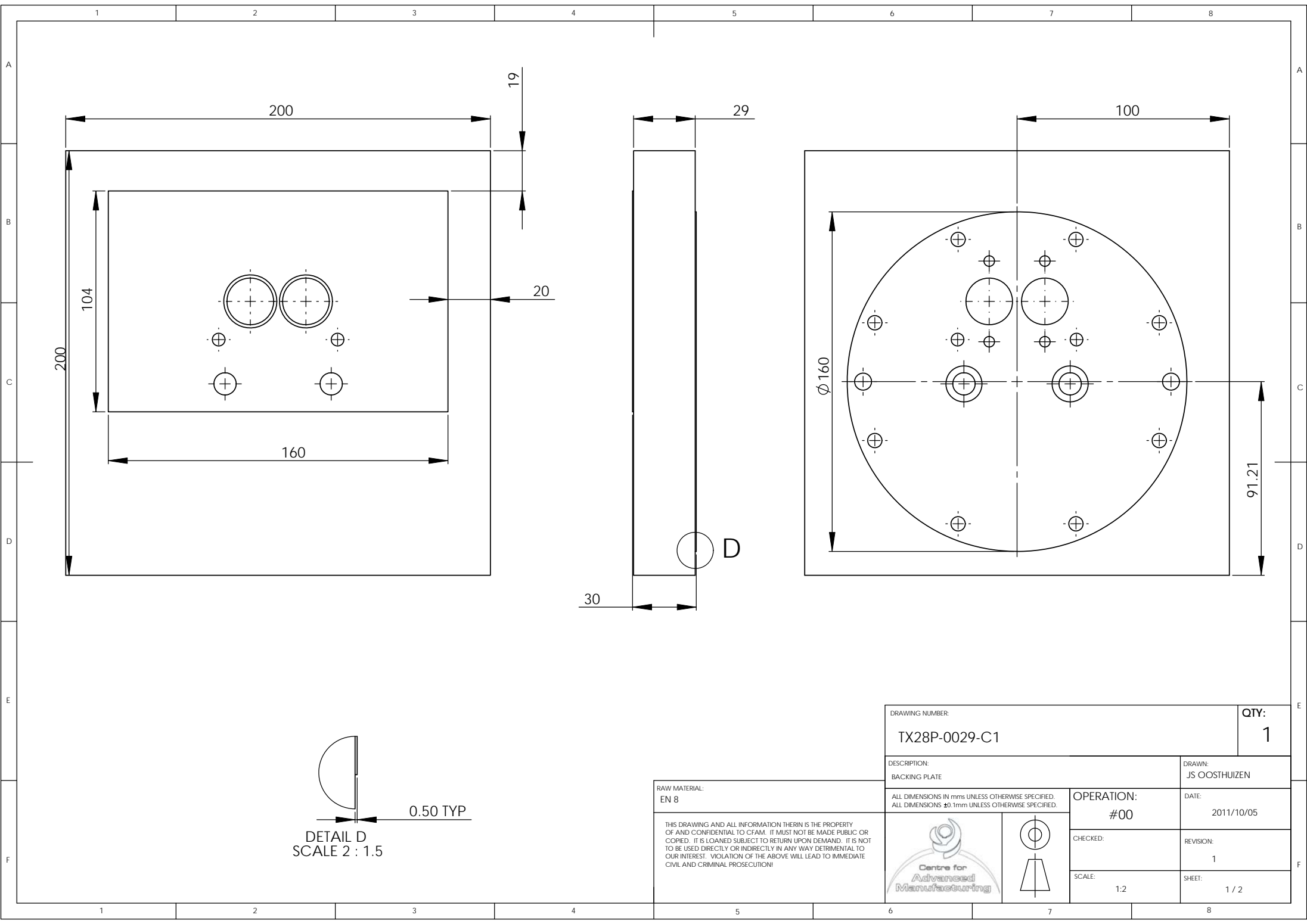
RAW MATERIAL:
BOHLER K110

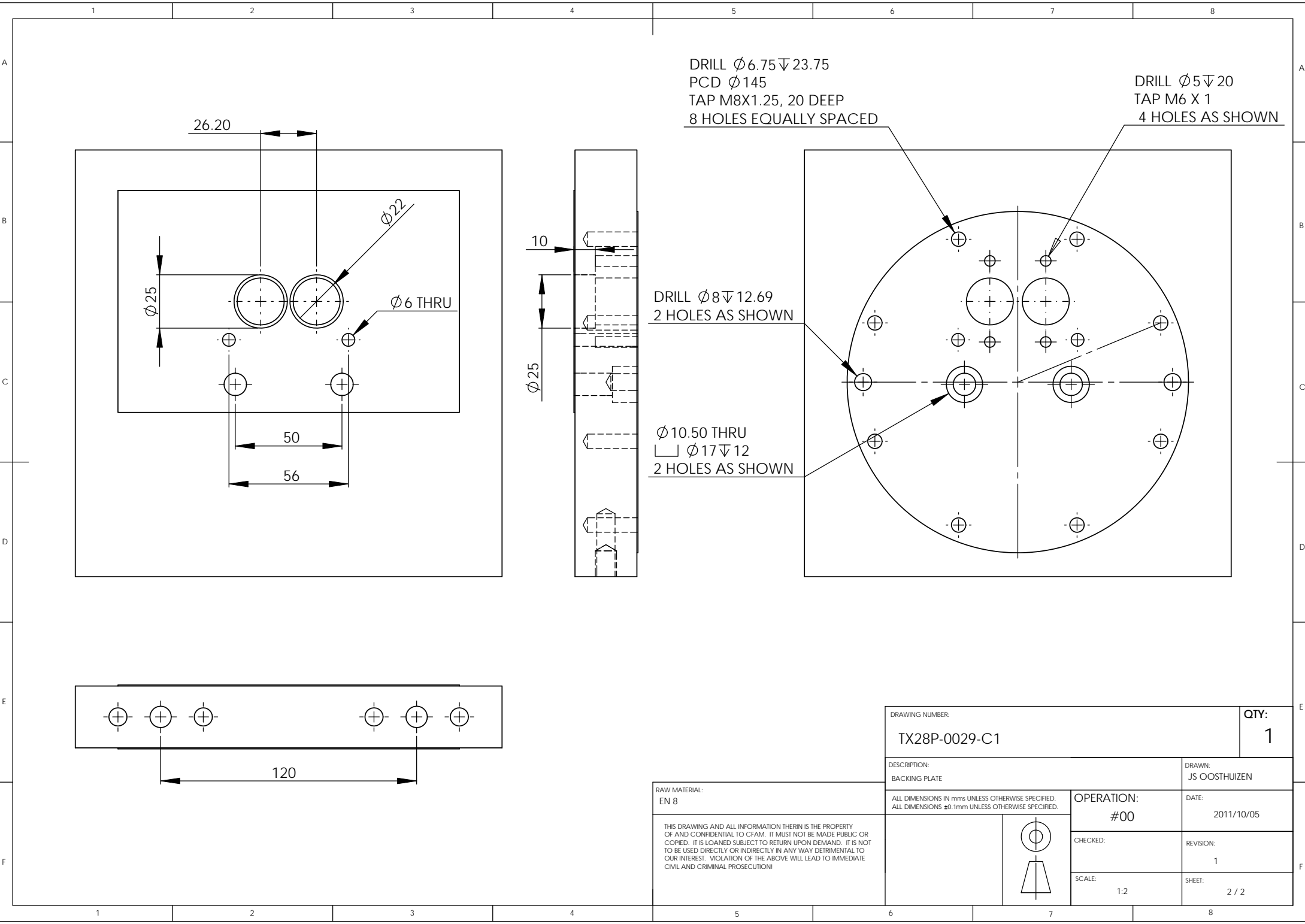
THIS DRAWING AND ALL INFORMATION THERIN IS THE PROPERTY OF AND CONFIDENTIAL TO CFAM. IT MUST NOT BE MADE PUBLIC OR COPIED. IT IS LOANED SUBJECT TO RETURN UPON DEMAND. IT IS NOT TO BE USED DIRECTLY OR INDIRECTLY IN ANY WAY DETRIMENTAL TO OUR INTEREST. VIOLATION OF THE ABOVE WILL LEAD TO IMMEDIATE CIVIL AND CRIMINAL PROSECUTION!



DRAWING NUMBER: TX28P-0030-C1			QTY: 1
DESCRIPTION: BAKING PLATE BASE		DRAWN: JS OOSTHUIZEN	
RAW MATERIAL: EN 8		OPERATION: #00	DATE: 2011/10/05
ALL DIMENSIONS IN mms UNLESS OTHERWISE SPECIFIED. ALL DIMENSIONS ± 0.1 mm UNLESS OTHERWISE SPECIFIED.		CHECKED:	REVISION: 1
THIS DRAWING AND ALL INFORMATION THERIN IS THE PROPERTY OF AND CONFIDENTIAL TO CFAM. IT MUST NOT BE MADE PUBLIC OR COPIED. IT IS LOANED SUBJECT TO RETURN UPON DEMAND. IT IS NOT TO BE USED DIRECTLY OR INDIRECTLY IN ANY WAY DETRIMENTAL TO OUR INTEREST. VIOLATION OF THE ABOVE WILL LEAD TO IMMEDIATE CIVIL AND CRIMINAL PROSECUTION!		SCALE: 1:2	SHEET: 2 / 2







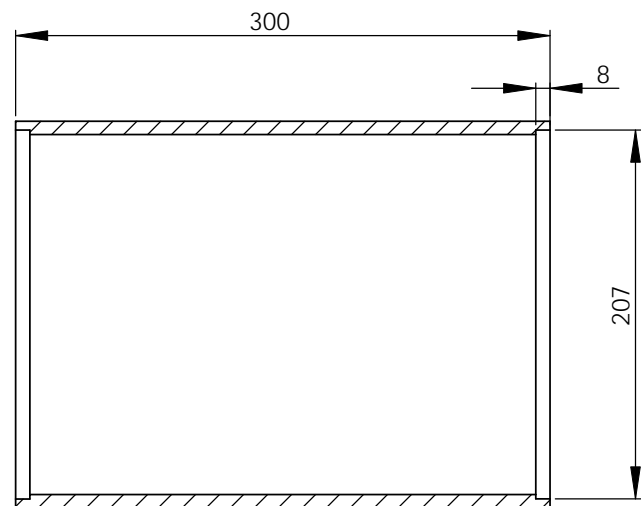
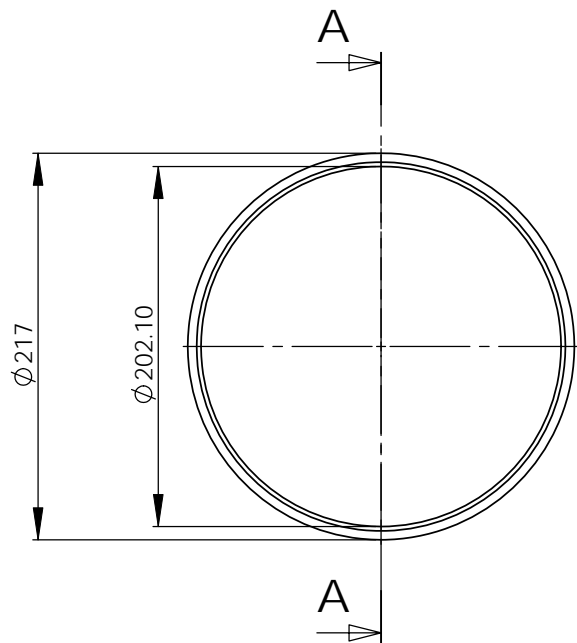
DRILL $\varnothing 6.75 \nabla 23.75$
PCD $\varnothing 145$
TAP M8X1.25, 20 DEEP
8 HOLES EQUALLY SPACED

DRILL $\varnothing 5 \nabla 20$
TAP M6 X 1
4 HOLES AS SHOWN

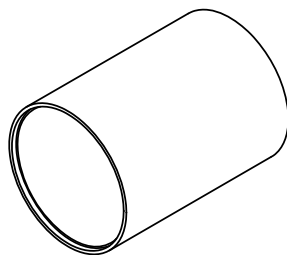
DRILL $\varnothing 8 \nabla 12.69$
2 HOLES AS SHOWN

$\varnothing 10.50$ THRU
 $\varnothing 17 \nabla 12$
2 HOLES AS SHOWN

DRAWING NUMBER: TX28P-0029-C1			QTY: 1
DESCRIPTION: BACKING PLATE		DRAWN: JS OOSTHUIZEN	
ALL DIMENSIONS IN mms UNLESS OTHERWISE SPECIFIED. ALL DIMENSIONS ± 0.1 mm UNLESS OTHERWISE SPECIFIED.		OPERATION: #00	DATE: 2011/10/05
<div>THIS DRAWING AND ALL INFORMATION THERIN IS THE PROPERTY OF AND CONFIDENTIAL TO CFAM. IT MUST NOT BE MADE PUBLIC OR COPIED. IT IS LOANED SUBJECT TO RETURN UPON DEMAND. IT IS NOT TO BE USED DIRECTLY OR INDIRECTLY IN ANY WAY DETRIMENTAL TO OUR INTEREST. VIOLATION OF THE ABOVE WILL LEAD TO IMMEDIATE CIVIL AND CRIMINAL PROSECUTION!</div> <div></div>		CHECKED:	REVISION: 1
		SCALE: 1:2	SHEET: 2 / 2



SECTION A-A
SCALE 1 : 3

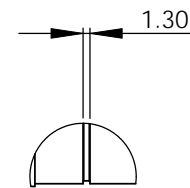
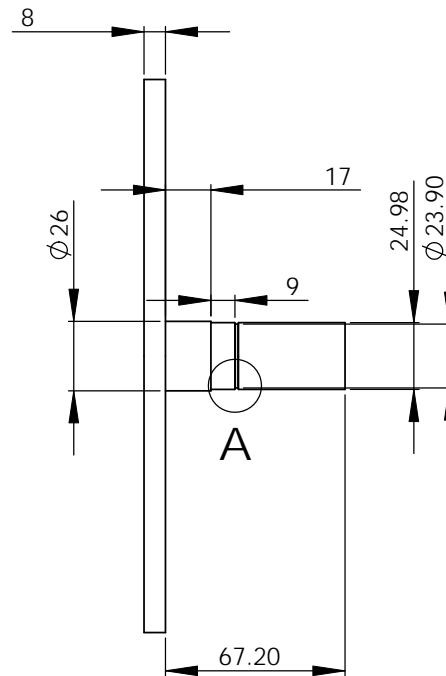
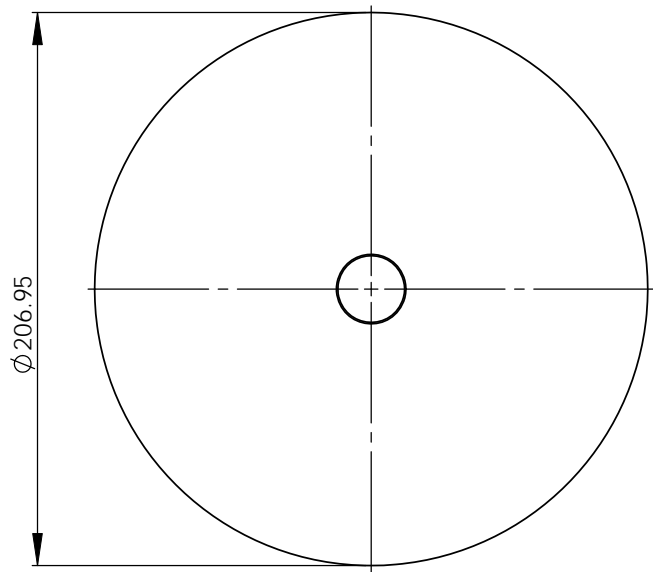


RAW MATERIAL:
EN8

THIS DRAWING AND ALL INFORMATION THERIN IS THE PROPERTY
OF AND CONFIDENTIAL TO CFAM. IT MUST NOT BE MADE PUBLIC OR
COPIED. IT IS LOANED SUBJECT TO RETURN UPON DEMAND. IT IS NOT
TO BE USED DIRECTLY OR INDIRECTLY IN ANY WAY DETRIMENTAL TO
OUR INTEREST. VIOLATION OF THE ABOVE WILL LEAD TO IMMEDIATE
CIVIL AND CRIMINAL PROSECUTION!

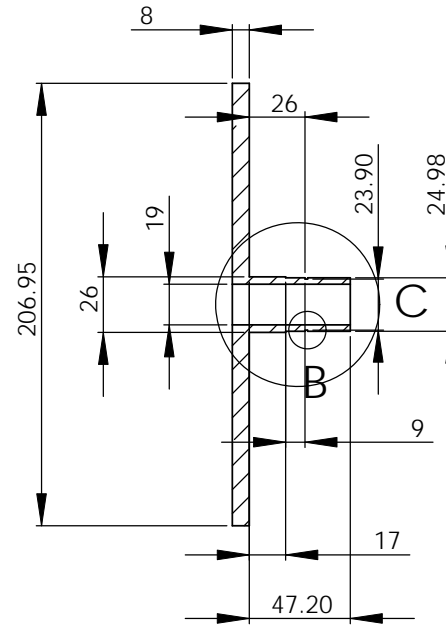
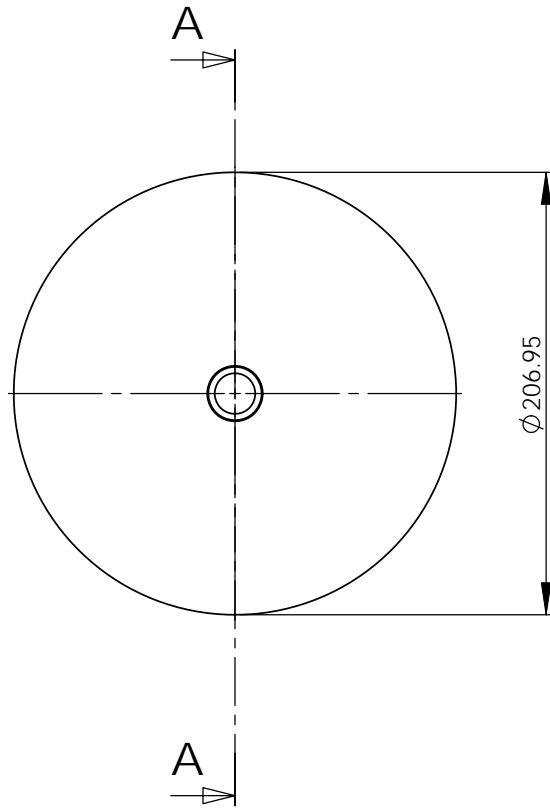


DRAWING NUMBER: CRU-LAB-0001-RL-2191-Z-C1-Z			QTY: 1
DESCRIPTION: Flange Union side		DRAWN: JS Oosthuizen	
ALL DIMENSIONS IN mms UNLESS OTHERWISE SPECIFIED. ALL DIMENSIONS $\pm 0.1\text{mm}$ UNLESS OTHERWISE SPECIFIED.		DIMENSIONED: JS Oosthuizen	DATE: 2011/10/23
		CHECKED:	REVISION: 1
		SCALE: 1:5	SHEET: 1 / 1

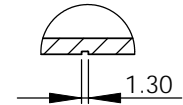


DETAIL A
SCALE 1 : 1

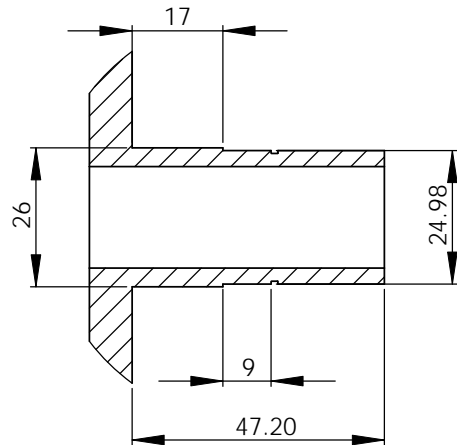
RAW MATERIAL: EN8		DRAWING NUMBER: CRU-LAB-0002-FL-26-Z-C1-Z		QTY: 1	
		DESCRIPTION: Roller Flange		DRAWN: JS OOSTHUIZEN	
THIS DRAWING AND ALL INFORMATION THERIN IS THE PROPERTY OF AND CONFIDENTIAL TO CFAM. IT MUST NOT BE MADE PUBLIC OR COPIED. IT IS LOANED SUBJECT TO RETURN UPON DEMAND. IT IS NOT TO BE USED DIRECTLY OR INDIRECTLY IN ANY WAY DETRIMENTAL TO OUR INTEREST. VIOLATION OF THE ABOVE WILL LEAD TO IMMEDIATE CIVIL AND CRIMINAL PROSECUTION!		ALL DIMENSIONS IN mms UNLESS OTHERWISE SPECIFIED. ALL DIMENSIONS ± 0.1 mm UNLESS OTHERWISE SPECIFIED.		DIMENSIONED: JS OOSTHUIZEN	
				DATE: 2011/10/23	
				REVISION: 1	
		SCALE: 1:5		SHEET: 1 / 1	



SECTION A-A
SCALE 1 : 2.5



DETAIL B
SCALE 1 : 1

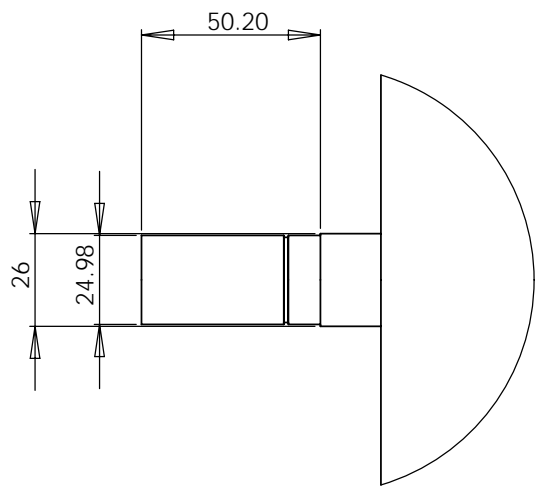
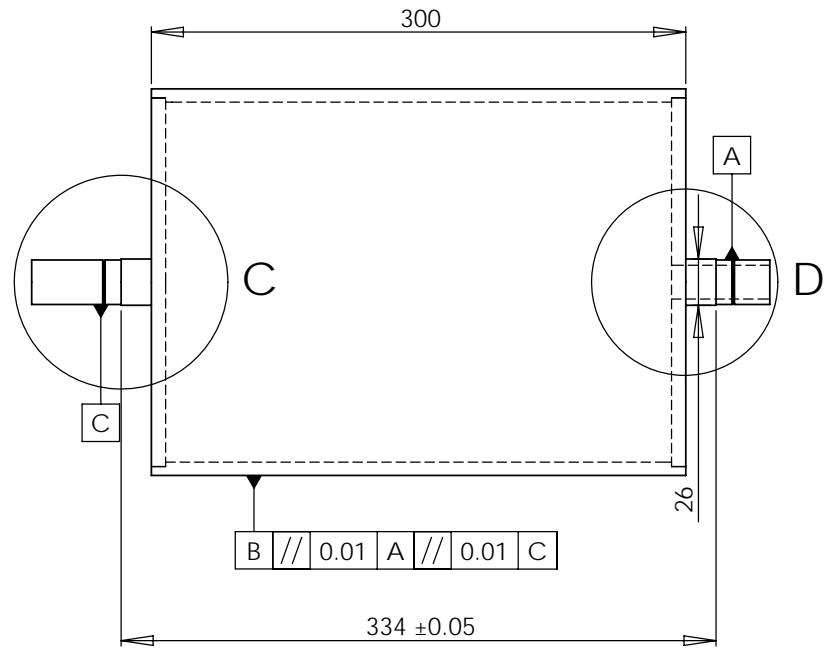
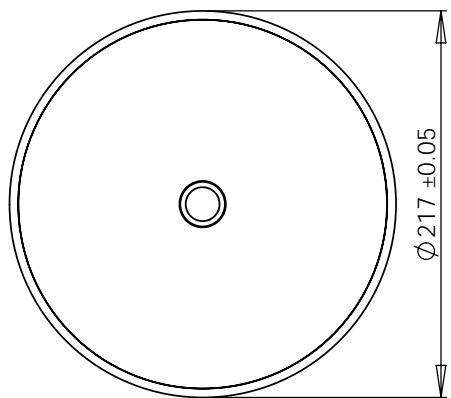


RAW MATERIAL:
EN8

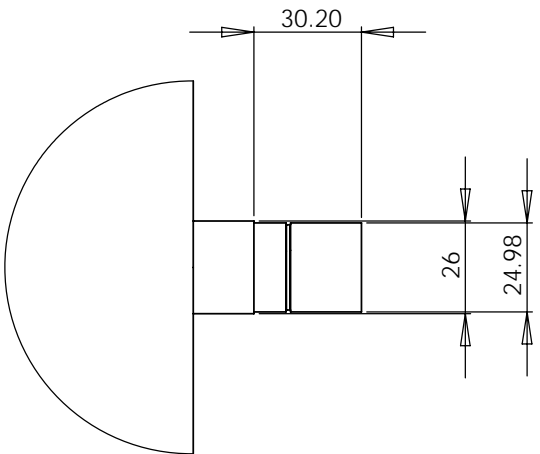
THIS DRAWING AND ALL INFORMATION THEREIN IS THE PROPERTY OF AND CONFIDENTIAL TO CFAM. IT MUST NOT BE MADE PUBLIC OR COPIED. IT IS LOANED SUBJECT TO RETURN UPON DEMAND. IT IS NOT TO BE USED DIRECTLY OR INDIRECTLY IN ANY WAY DETRIMENTAL TO OUR INTEREST. VIOLATION OF THE ABOVE WILL LEAD TO IMMEDIATE CIVIL AND CRIMINAL PROSECUTION!



DRAWING NUMBER: CRU-LAB-0003-FL-26-Z-C1-Z		QTY: 1	
DESCRIPTION: Flange Union side		DRAWN: JS Oosthuizen	
ALL DIMENSIONS IN mm UNLESS OTHERWISE SPECIFIED. ALL DIMENSIONS ± 0.1 mm UNLESS OTHERWISE SPECIFIED.		DIMENSIONED: JS Oosthuizen	DATE: 2011/10/23
		CHECKED:	REVISION: 1
		SCALE: 1:5	SHEET: 1 / 1



DETAIL C
SCALE 2 : 3



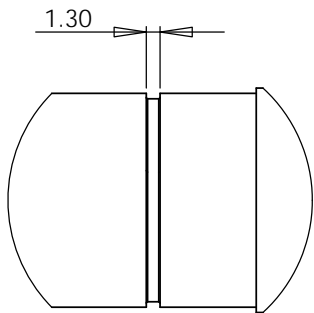
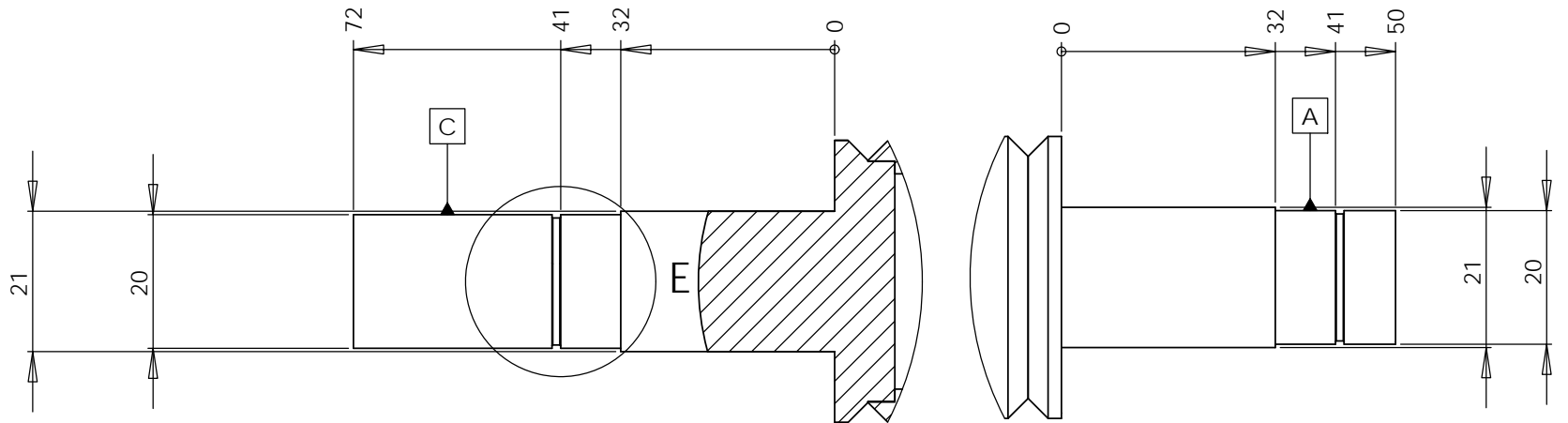
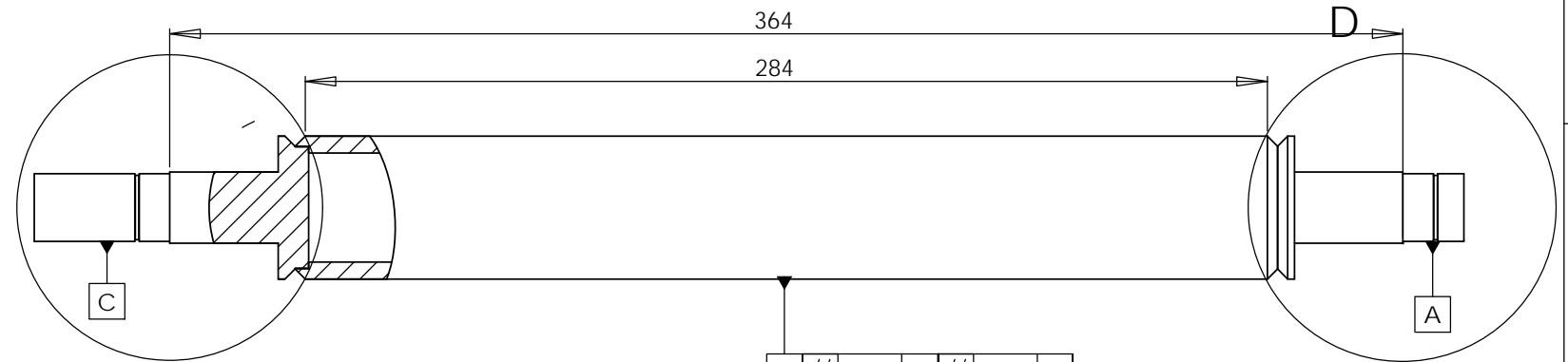
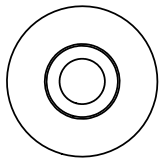
DETAIL D
SCALE 2 : 3

1. Pre-Grind Faces A, B and C
2. Flash Crome the whole part
3. Crome Face B to a thickness of 0.25 mm
4. Grind face B to final size.

RAW MATERIAL:
EN 8

THIS DRAWING AND ALL INFORMATION THERIN IS THE PROPERTY OF AND CONFIDENTIAL TO CFAM. IT MUST NOT BE MADE PUBLIC OR COPIED. IT IS LOANED SUBJECT TO RETURN UPON DEMAND. IT IS NOT TO BE USED DIRECTLY OR INDIRECTLY IN ANY WAY DETRIMENTAL TO OUR INTEREST. VIOLATION OF THE ABOVE WILL LEAD TO IMMEDIATE CIVIL AND CRIMINAL PROSECUTION!

DRAWING NUMBER: CRU-LAB-0101-ASM-ZZ-ZZ-ZZ-ZZ			QTY: 1
DESCRIPTION: Grinding		DRAWN: JS OOSTHUIZEN	
ALL DIMENSIONS IN mms UNLESS OTHERWISE SPECIFIED. ALL DIMENSIONS ±0.1mm UNLESS OTHERWISE SPECIFIED.		DIMENSIONED: JS OOSTHUIZEN	DATE: 3/3/2008
		CHECKED:	REVISION: 1
		SCALE: 1:3	SHEET: 2 / 2

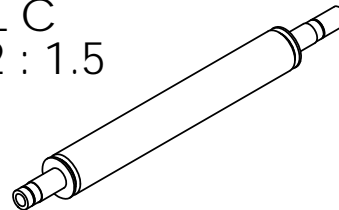


DETAIL E
SCALE 2 : 1

DETAIL C
SCALE 2 : 1.5

DETAIL D
SCALE 2 : 1.5

1. Pre-Grind Faces A, B and C
2. Flash Crome the whole part
3. Crome Face B to a thickness of 0.5 mm
4. Grind face B to final size.

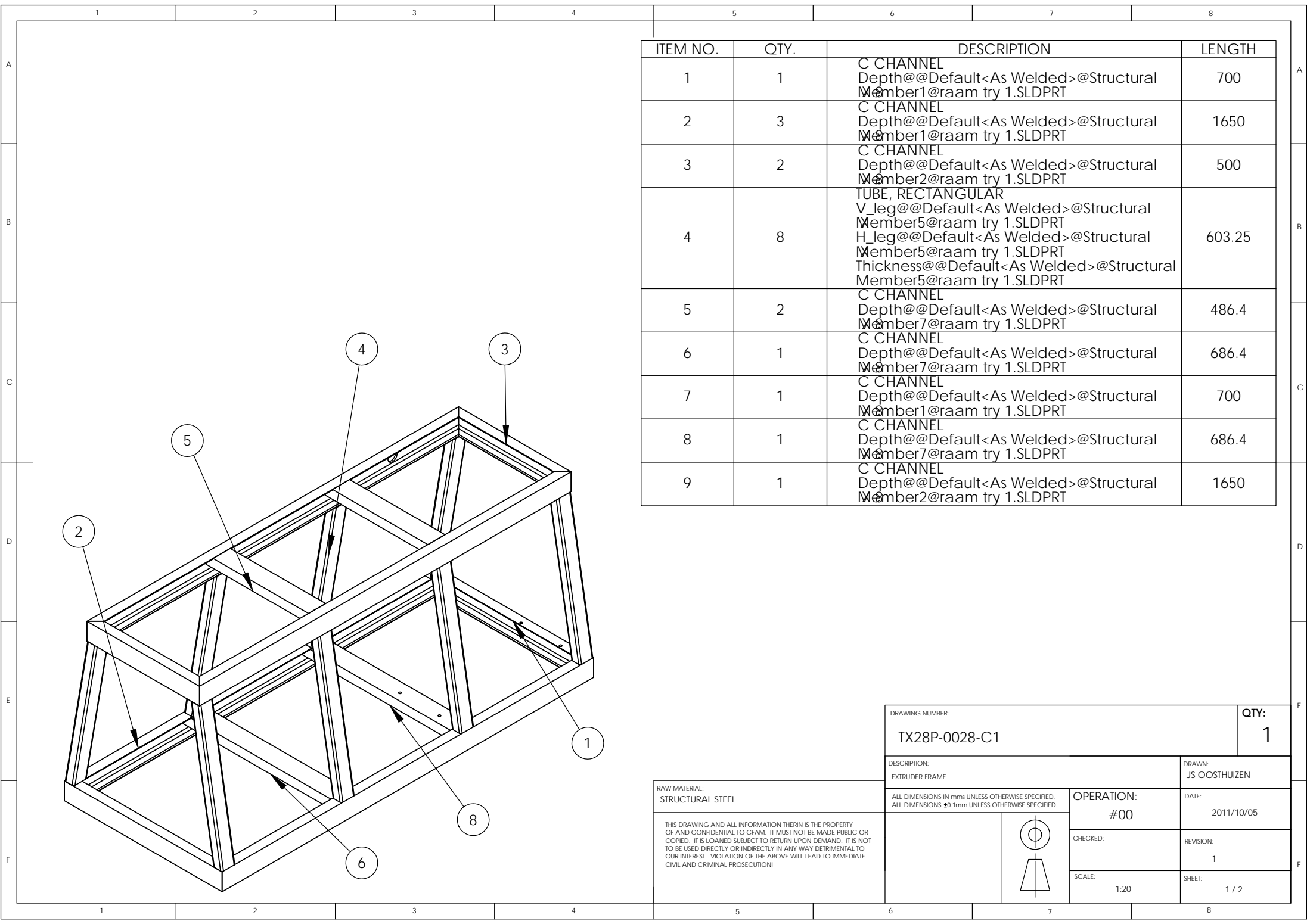


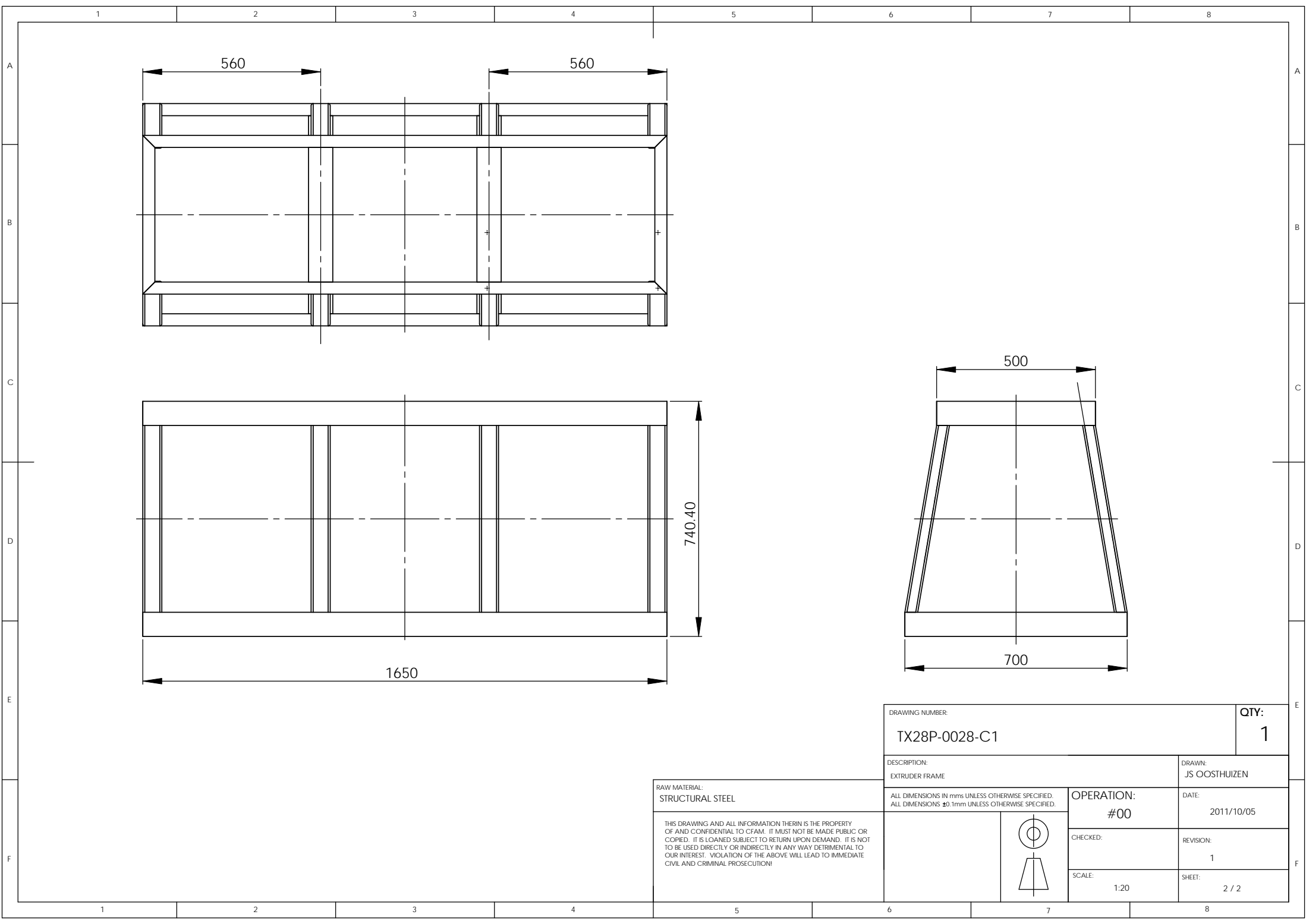
RAW MATERIAL:
EN8

THIS DRAWING AND ALL INFORMATION THERIN IS THE PROPERTY OF AND CONFIDENTIAL TO CFAM. IT MUST NOT BE MADE PUBLIC OR COPIED. IT IS LOANED SUBJECT TO RETURN UPON DEMAND. IT IS NOT TO BE USED DIRECTLY OR INDIRECTLY IN ANY WAY DETRIMENTAL TO OUR INTEREST. VIOLATION OF THE ABOVE WILL LEAD TO IMMEDIATE CIVIL AND CRIMINAL PROSECUTION!



DRAWING NUMBER: CRU-LAB-0103-ASM-ZZ-ZZ-ZZ-ZZ			QTY: 1
DESCRIPTION: Flange Union side		DRAWN: JS Oosthuizen	
ALL DIMENSIONS IN mms UNLESS OTHERWISE SPECIFIED. ALL DIMENSIONS ± 0.1 mm UNLESS OTHERWISE SPECIFIED.		DIMENSIONED: JS Oosthuizen	DATE: 2011/10/23
		CHECKED:	REVISION: 1
		SCALE: 1:5	SHEET: 2 / 2





ANNEXURE B

Annexure B contains photos taken during the energy consumption tests. The APV 2050 extruder as well as all the auxiliary and measuring equipment, is visible in the photos.



ANNEXURE C

Annexure C contains the design calculations of all the factors for the AGMA tooth strength calculations, as well as the factors for the shaft calculations.

Bending Strength

Overload Factor K_o

The overload factor is intended to make allowance for all external applied loads in excess of the nominal tangential load W^t in a particular application. The table provides values for the overload factor according to the driving machine and the shock load conditions on the driven machines. In case of extrusion the overload factor can be chosen as 1, where the driving machine is an electrical motor which provides a uniform input torque and the extruder operates at a uniform torque (SHIGLEY, J E et al., 2004).

Table of Overload Factors, K_o

Driven Machine			
Power source	Uniform	Moderate shock	Heavy shock
Uniform	1.00	1.25	1.75
Light shock	1.25	1.50	2.00
Medium shock	1.50	1.75	2.25

Dynamic Factor K_v

The dynamic factor is calculated by:

$$K_v = \left(\frac{A + \sqrt{200V}}{A} \right)^B$$

$$A = 50 + 56(1 - B)$$

$$B = 0.25(12 - Q_v)^{2/3}$$

Annexure C

Q_v is the quality number which defines the tolerances the gears of various sizes are manufactured to. Classes 8 to 12 are of precision gears. Using a quality number of 8 the dynamic factor becomes:

$$B = 0.25(12 - 8)^{2/3}$$

$$= 0.63$$

$$A = 50 + 56(1 - 0.63)$$

$$= 70.7$$

Pitch line velocity (V_t) is calculated as follows:

$$V_t = \omega \times r = \frac{2\pi N}{60} \frac{PCD}{2} = \frac{500 \times \pi \times 0.03}{60} = 0.79 \text{ m/s}$$

$$K_v = \left(\frac{70.7 + \sqrt{200 \times 0.79}}{70.7} \right)^{0.63}$$

$$K_v = 1.1$$

Load distribution factor K_H (SHIGLEY, J E et al., 2004, pp.747, 748)

$$K_H = 1 + C_{mc}(C_{pf}C_{pm} + C_{ma}C_e)$$

$$C_{mc} = 1 \text{ - for uncrowned gears}$$

$$C_{pf} = \frac{F}{10d} - 0.025$$

$$F = 24 \text{ mm} \text{ - face width of gear teeth}$$

$$d = 30 \text{ mm} \text{ - PCD of gear}$$

$$C_{pf} = \frac{24}{10 \times 30} - 0.025$$

$$= 0.055$$

$$C_{pm} = 1$$

$$C_e = 1$$

$$C_{ma} = A + BF + CF^2$$

Annexure C

$$= 0.0675 + 0.0128 \times .024 + (-0.926 \times 10^{-4} \times .024^2)$$

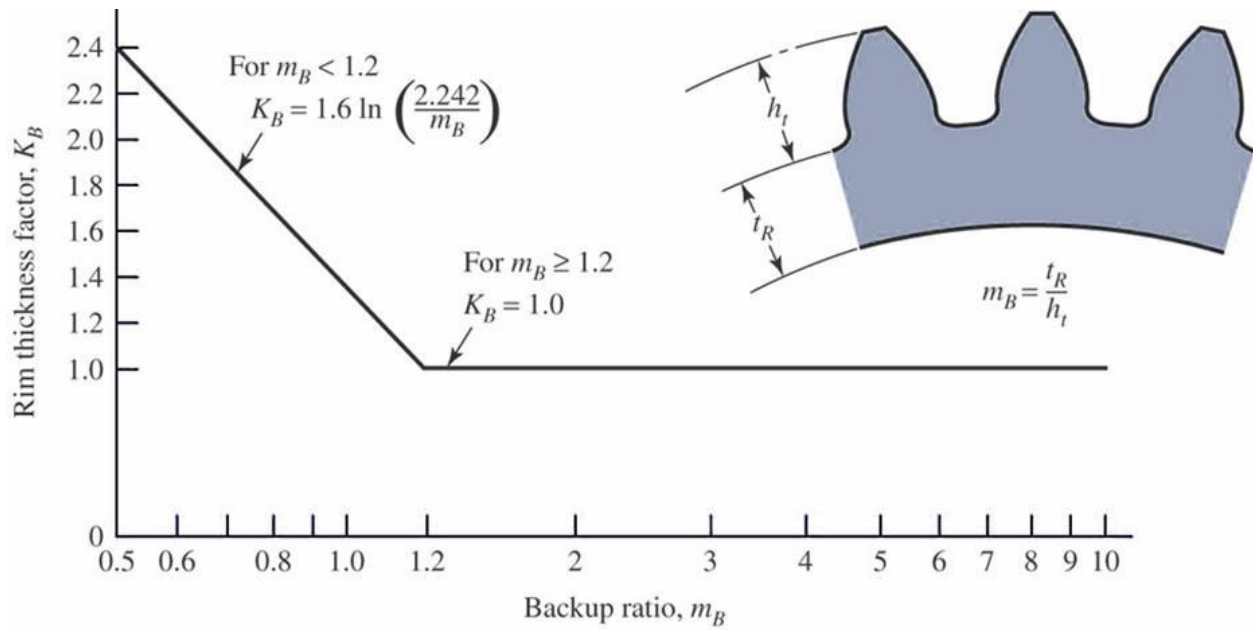
$$= 0.068$$

$$K_H = 1 + 1(0.055 + 0.068)$$

$$= 1.123$$

Rim thickness factor K_B

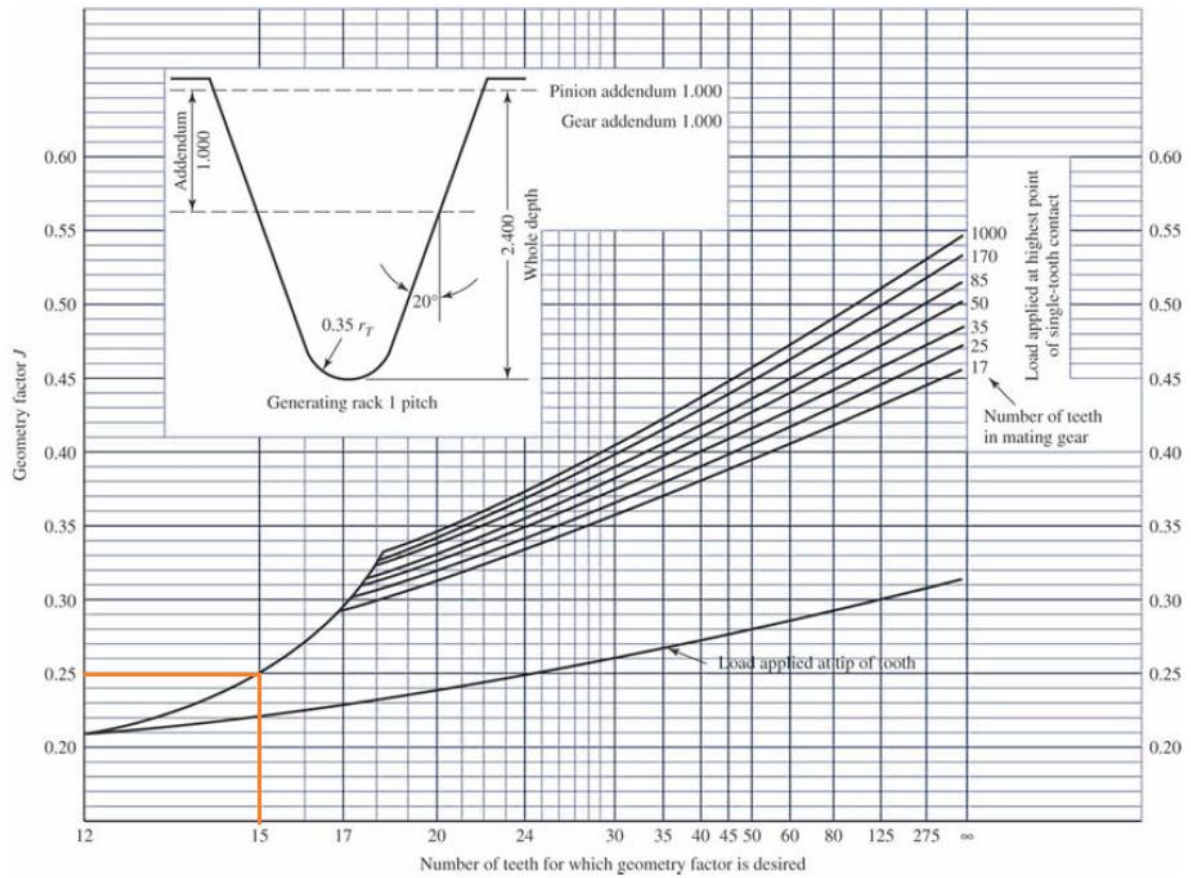
The pinion as well as the gear is integrated gear on the shaft, thus is there no rim thickness and $K_B = 1$ (AMERICAN GEAR MANUFACTURING ASSOCIATION, 1988).



Annexure C

Geometry factor Y_J

(AMERICAN GEAR MANUFACTURING ASSOCIATION, 1988)



Pinion number of teeth: 25

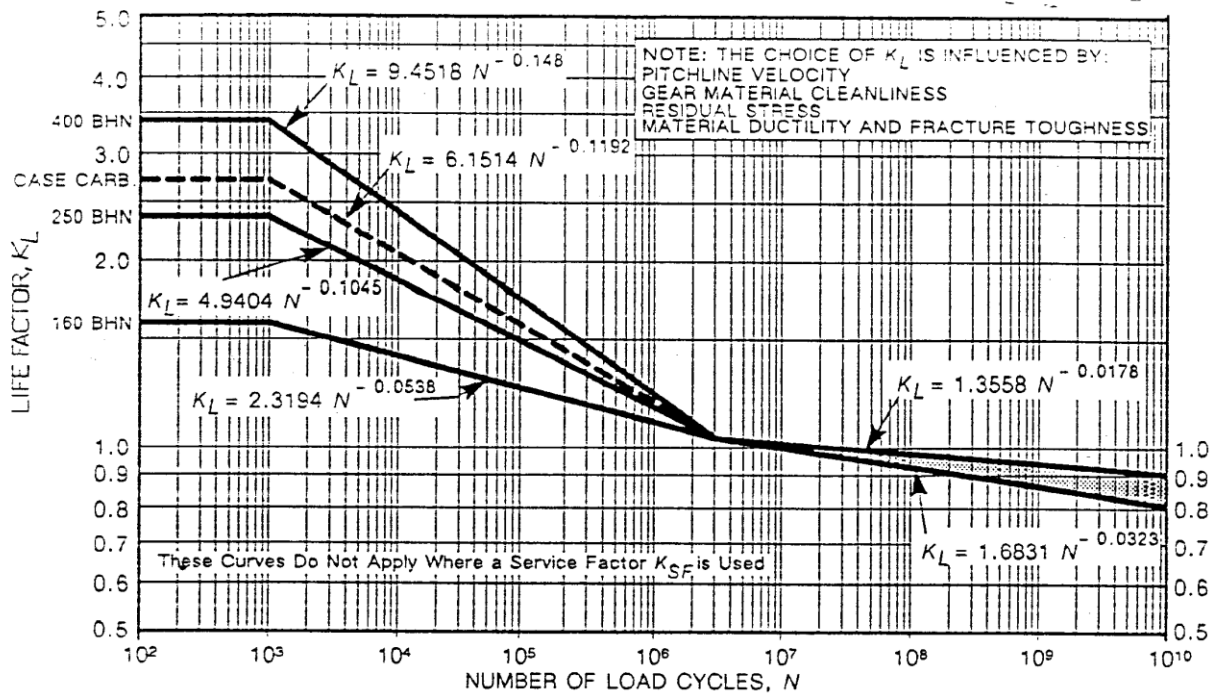
Gear number of teeth: 15

$Y_J = 0.25$

Annexure C

Stress cycle factor Y_N

(AMERICAN GEAR MANUFACTURING ASSOCIATION, 1988)



From the design specifications, the design life must be for 1×10^6 cycles. For case hardened material the life factor $Y_N = 6.1514N^{-0.1192}$ applies. The value for Y_N is thus.

$$Y_N = 6.1514(1 \times 10^6)^{-0.1192} = 1.185$$

Temperature factor Y_θ

For temperatures less than 120°C $Y_\theta = 1$

(SHIGLEY, J E et al., 2004, p.752)

Reliability factor Y_Z

For a reliability of 99%, $Y_Z = 1$

(SHIGLEY, J E et al., 2004, p.752)

Contact strength

Elastic coefficient Z_E (SHIGLEY, J E et al., 2004, p.745)

$$Z_E = 191 \text{ MPa}$$

Surface condition factor Z_R (SHIGLEY, J E et al., 2004, p.746)

$$Z_R = 1$$

Geometry factor Z_I (SHIGLEY, J E et al., 2004, p.743)

The geometry factor can be calculated by the following expression:

$$Z_I = \frac{\sin \alpha \cos \alpha}{2} \frac{m_G}{m_G + 1}$$

and

$$m_G = \frac{d_G}{d_P}$$

$$= \frac{50}{30} = 1.66$$

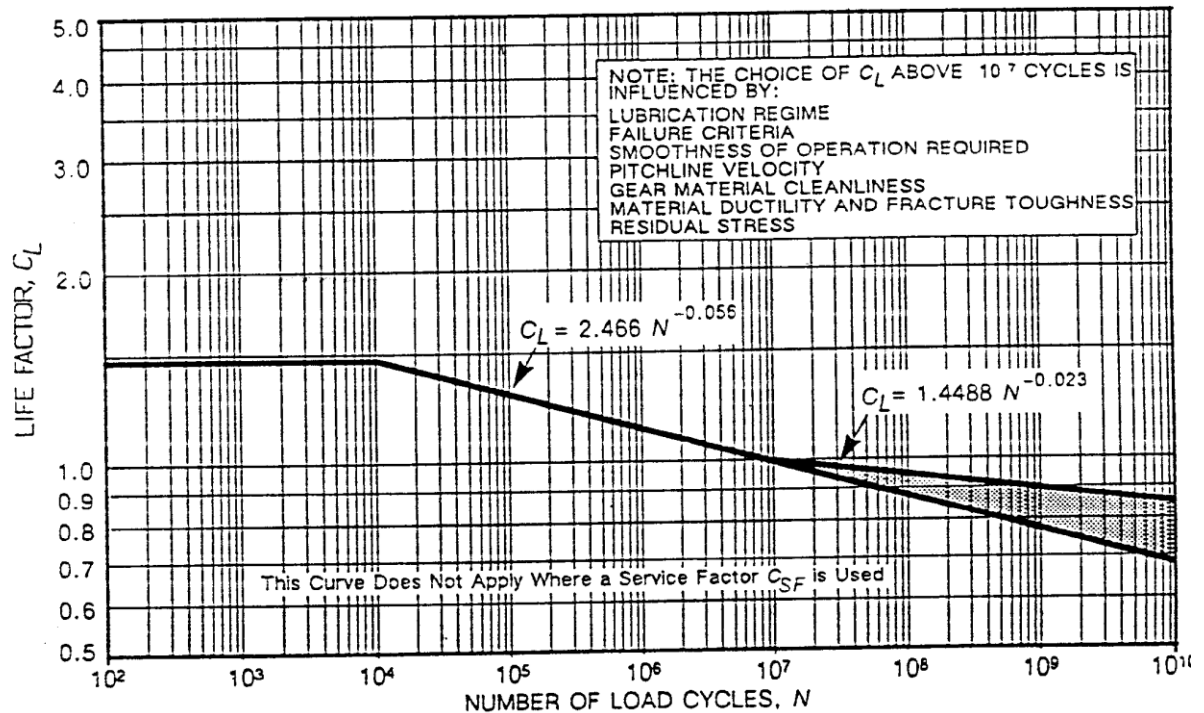
$$\therefore Z_I = \frac{\sin 20 \cos 20}{2} \frac{1.66}{1.66 + 1}$$

$$= 0.1$$

Annexure C

Stress cycle life factor Z_N

(AMERICAN GEAR MANUFACTURING ASSOCIATION, 1988)



From the design specifications, the design life must be for 1×10^6 cycles. For case hardened material the life factor $Y_N = 2.466N^{-0.056}$ applies. The value for Y_N is thus.

$$Y_N = 2.466(1 \times 10^6)^{-0.056} = 1.14$$

Hardness ratio factor Z_W

The default value of $Z_W = 1$

(AMERICAN GEAR MANUFACTURING ASSOCIATION, 1988)

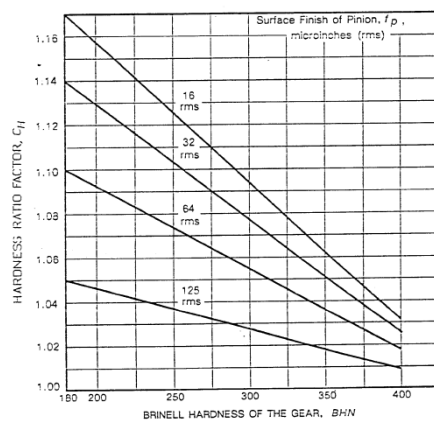


Fig 15-2 Hardness Ratio Factor, C_H (Surface Hardened Pinions)

Shaft Design

Material specifications

(EN 36B)

$$S_{ut} = 880 \text{ MPa}$$

$$S_y = 765 \text{ MPa}$$

Endurance limit

$$S'_e = 0.504 \times S_{ut}$$

$$0.504 \times 880$$

$$= 443.5 \text{ MPa}$$

Surface factor k_a :

$$k_a = a \times S_{ut}^b$$

for machined $a = 4.51$ and $b = -0.265$

$$k_a = 0.748$$

Size factor k_b :

$$k_b = 1.24 \times d^{-0.107}$$

$$k_b = 1.24 \times 17^{-0.107}$$

$$= 0.916$$

Reliability factor k_e :

for 99%

$$k_e = 0.814$$

Endurance limit at the critical location on the shaft (115 mm from front of shaft) is calculated as:

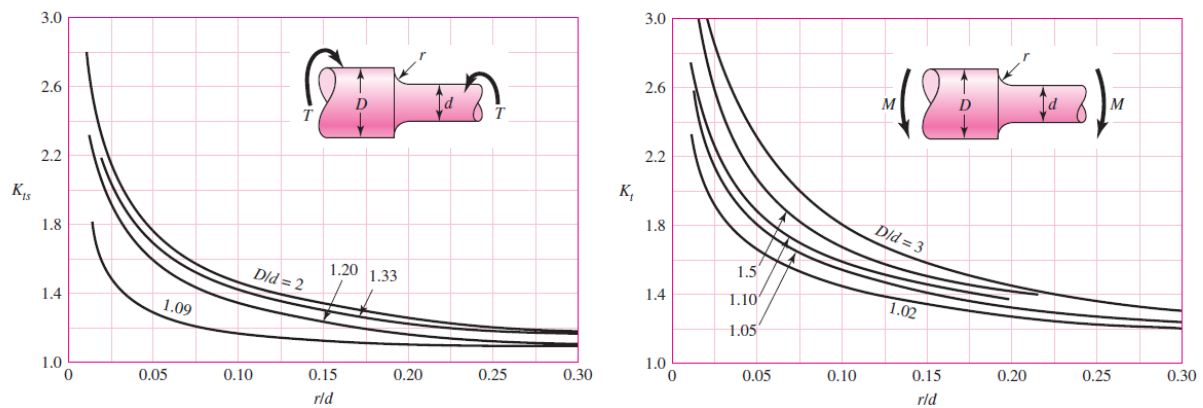
$$S_e = S'_e \cdot k_a \cdot k_b \cdot k_e$$

$$= 443.5 \times 0.748 \times 0.916 \times 0.814 = 247 \text{ MPa}$$

Annexure C

Stress concentration factors

(SHIGLEY, J E et al., 2004, p.984)



Stress concentration for bending K_t :

$$D = 25 \text{ mm}$$

$$d = 17 \text{ mm}$$

$$r = 3 \text{ mm}$$

$$D/d = 25/17 = 1.47$$

$$r/d = 3/17 = 0.18$$

$$K_t = 1.4$$

$$K_f = \frac{K_t}{1 + \frac{2(K_t-1)}{K_t} \times \frac{\sqrt{a}}{\sqrt{r}}}$$

$$\text{for a shoulder } \sqrt{a} = \frac{139}{s_{ut}} = 0.16$$

$$K_f = \frac{1.4}{1 + \frac{2(1.4-1)}{1.4} \times \frac{0.16}{\sqrt{3}}}$$

$$= 1.3$$

Annexure C

Stress concentration for torsion K_{ts} :

$$K_{ts} = 1.3$$

$$K_{fs} = \frac{K_t}{1 + \frac{2(K_t-1)}{K_t} \times \frac{\sqrt{a}}{\sqrt{r}}}$$

$$\text{for a shoulder } \sqrt{a} = \frac{139}{S_{ut}} = 0.16$$

$$\begin{aligned} K_{fs} &= \frac{1.3}{1 + \frac{2(1.3-1)}{1.3} \times \frac{0.16}{\sqrt{3}}} \\ &= 1.25 \end{aligned}$$

Material Specification

Material specification for EN 36B (Special steels, 2011)

Product Information:
EN36B - 655M13



EN36B - 655M13 Black (As rolled or forged) (ALLOY STEEL) (Case hardening) (3% Nickel/Chromium)			
Equivalents: BS970 Part 1 1983, 655M13 BS970 of 1955 EN36B German W. Stoff No. 1.5752 American AISI 9315			
Chemical: <u>Composition %</u>			
Carbon	= 0,12 - 0,16	Sulphur	= 0,040 max
Silicon	= 0,10 - 0,35	Phosphorus	= 0,035 max
Manganese	= 0,35 - 0,60		
Nickel	= 3,00 - 3,75		
Chromium	= 0,70 - 1,00		
Characteristics: <ul style="list-style-type: none">• A 6% allowance should always be made for removal of surface defects during machining• Machinability good• Required hardness can be achieved by case hardening the outer surface by means of one of the following methods:<ul style="list-style-type: none">i. Carburising, Carbonitriding, Nitriding, Nitrocarburising, Tuftriding			
Typical Applications: Auto and heavy vehicle transmission components Engineering machinery gearbox parts Aircraft gears Mining steering worms Chuck jaws Track pins Gadgeon pins Mining gearbox gears Pinions and cogs			

Mechanical Properties

TENSILE STRENGTH		A min on 5,65 √So	IMPACT		Test Bar mm DIA
Tons/Sq inch	RM MPA		IZOD FT.Lb	KCV Joules	
65	1000	9	30	35	19

Tel: + 27 (0)11 865 4939. Fax: + 27 (0)11 902 8995. e-mail: sales@specialsteels.co.za

Annexure C

Allowable bending and contact stress number for case hardened gears (AMERICAN GEAR MANUFACTURING ASSOCIATION, 1988).

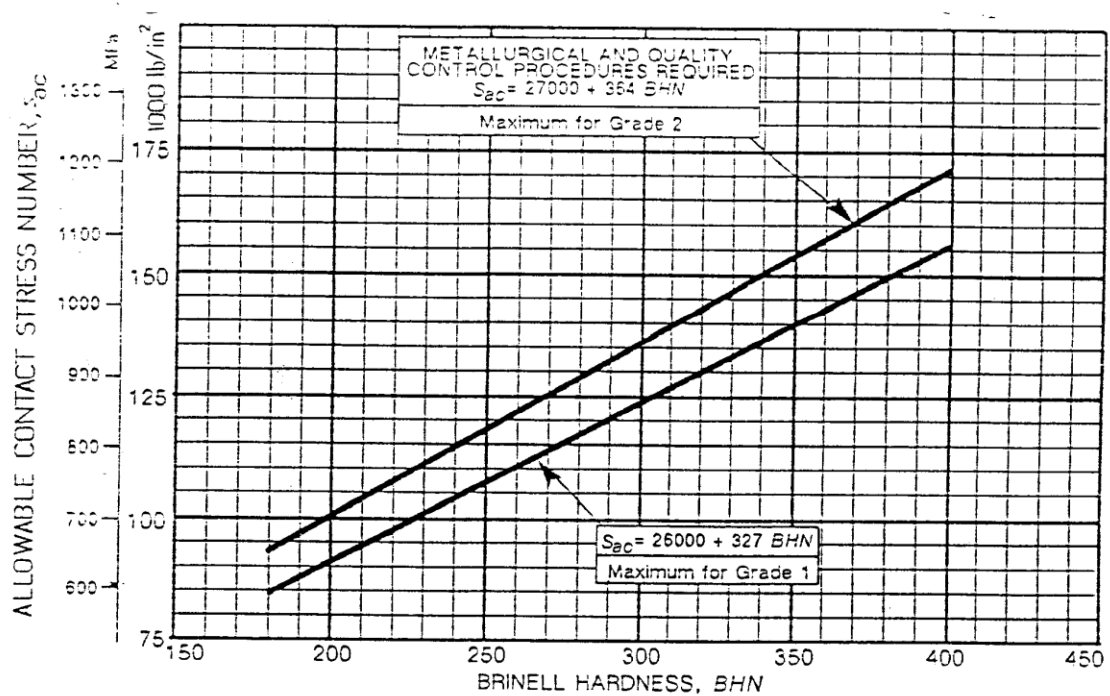


Fig 14-1 Allowable Contact Stress Number for Steel Gears, s_{ac}

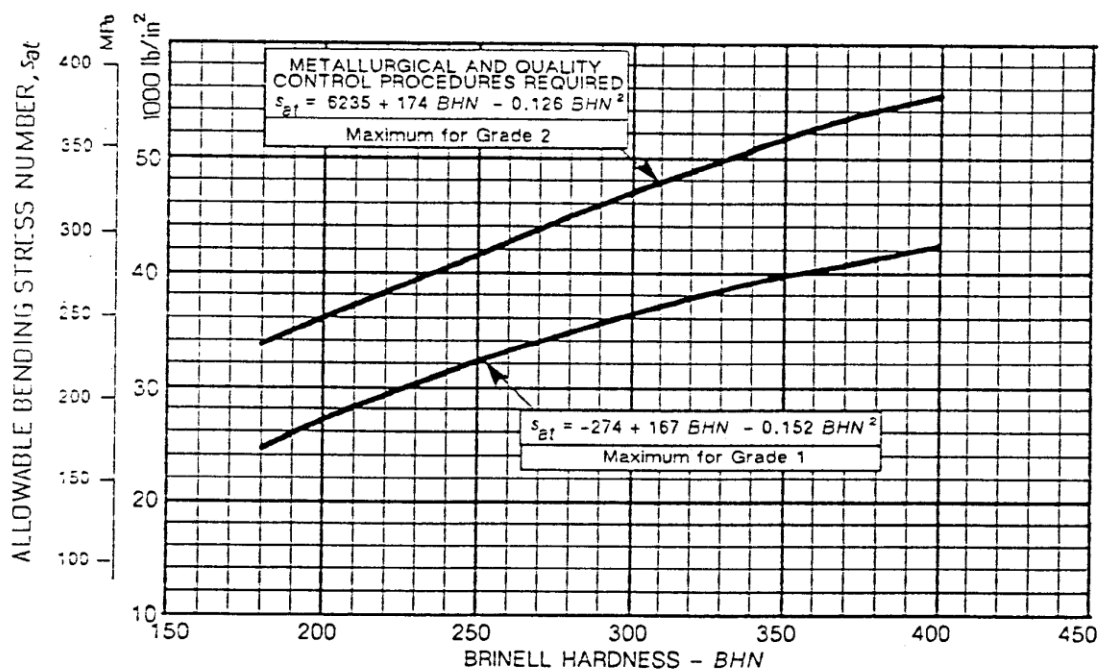


Fig 14-2 Allowable Bending Stress Number for Steel Gears, s_{at}

Annexure C

Allowable contact stress numbers for steel gears (AMERICAN GEAR MANUFACTURING ASSOCIATION, 1988).

Table 14-1
Allowable Contact Stress Number, s_{ac} , for Steel Gears

Material Designation	Heat Treatment	Minimum Hardness at Surface ¹	Allowable Contact Stress Number, s_{ac} lb/in ² (MPa)		
			Grade 1 ²	Grade 2 ²	Grade 3 ²
Steel	Through Hardened ³	180 BHN & less	85 000 (590)	95 000 (660)	
		240 BHN	105 000 (720)	115 000 (790)	
		300 BHN	120 000 (830)	135 000 (930)	
		360 BHN	145 000 (1000)	160 000 (1100)	
		400 BHN	155 000 (1050)	170 000 (1160)	
	Flame ⁴ or Induction Hardened ⁴	50 HRC	170 000 (1150)	190 000 (1300)	
		54 HRC	175 000 (1200)	195 000 (1350)	
	Carburized & Case Hardened ⁴	see Table 14-5	180 000 (1250)	225 000 (1550)	275 000 (1900)
AISI 4140	Nitrided ⁴	84.5 15N	155 000 (1050)	180 000 (1250)	
AISI 4340	Nitrided ⁴	83.5 15N	150 000 (1050)	175 000 (1200)	
Nitralloy 135M	Nitrided ⁴	90.0 15N	170 000 (1150)	195 000 (1350)	
Nitralloy N	Nitrided ⁴	90.0 15N	195 000 (1350)	205 000 (1400)	
2.5% Chrome	Nitrided ⁴	87.5 15N	155 000 (1050)	172 000 (1100)	
2.5% Chrome	Nitrided ⁴	90.0 15N	192 000 (1300)	216 000 (1500)	

1 Hardness to be equivalent to that at the start of active profile in the center of the face width.

2 See Tables 14-3 through 14-6 for metallurgical factors for each stress grade of steel gears.

3 These materials must be annealed or normalized as a minimum.

4 The allowable stress numbers indicated may be used with the case depths prescribed in 14.2.

Annexure C

Surface hardness of carburized and hardened steel gears (AMERICAN GEAR MANUFACTURING ASSOCIATION, 1988).

Table 14-5
Major Metallurgical Factors Affecting the Contact Stress Number, s_{ac} , of
Carburized and Hardened Steel Gears^{*1,2,3}

METALLURGICAL FACTOR ^{4,5}	GRADE 1	GRADE 2	GRADE 3
Surface Hardness (HRC or equivalent on representative surface)	55-64	58-64	58-64 ⁶
Case Hardness (at 0.003 inch depth on gear tooth test coupon with microhardness tester) ⁴	55-64 HRC or equivalent	58-64 HRC or equivalent	58-64 HRC or equivalent ⁶
Limit of Carbides in Case	Semi-continuous	Acceptable per AGMA 246	Acceptable per light discontinuous micro per AGMA 246
Tempering	Recommended	Required	Required
Grinding Burns (per AGMA 230 with swab technique permitted)	Class C	Class B	Class B
Cleanliness ⁷	Not specified	AMS 2301 or ASTM A534 for wrought steel (certification not required); castings are permissible which have primarily Type 1(round) sulphide inclusions.	AMS 2300 or ASTM A535 (certification required)
Ultrasonic Inspection (UT)	Not specified	Specified for wrought per ASTM A388, using either the back reflection or reference block 8-0400, 8/64 inch FBH per ASTM E428, techniques(described in Part 1 of AGMA 6033) Inspection is from the O.D. to mid-radius and a 360 degree scan is required. A distance amplitude correction curve(single point DAC) is not intended. Other UT specifications which insure the same quality level are permitted. Specified for castings per ASTM A609 Level 1 in Zone 1 (OD to 1.0 inch below roots)and level 2 in Zone 2 (remainder of rim) using 8/64 inch FBH; or approved equivalent using back reflection technique (Described in Part 1 of AGMA 6033).	Specified for wrought per ASTM A388, using either the back reflection or reference block 3-0400, 3/64 inch FBH per ASTM E428, techniques(described in Part 1 of AGMA 6033) Inspection is from the O.D. to mid-radius and a 360 degree scan is required. A distance amplitude correction curve(single point DAC) is not intended. Other UT specifications which insure the same quality level are permitted.

* See notes following table.